ANTICONVULSANT AND NEUROPROTECTIVE ROLES OF SGK1.1

Doctoral thesis

ELVA MARTIN BATISTA

Supervisors:

Dra. Teresa Giráldez Fernández

Dr. Diego Álvarez de la Rosa

Universidad de La Laguna

Facultad de Medicina-Área de Fisiología

Tenerife-Spain

24th of September 2021

Universidad de La Laguna

Teresa Giráldez Fernández, Profesora Titular de Fisiología de la Universidad de La Laguna y Diego Álvarez de la Rosa Rodríguez, Catedrático de Fisiología de la Universidad de La Laguna.

Certifican:

Que Elva Martín Batista ha realizado bajo su supervisión la tesis titulada: *Anticonvulsant and neuroprotective roles of SGK1.1*, que presenta para optar al grado de Doctora con mención internacional por la Universidad de La Laguna.

Para que conste y surta los efectos oportunos, firmamos el presente certificado en La Laguna a 19 de Julio 2021.

Dra. Teresa Giráldez Fernández Dr. Diego Álvarez de la Rosa Rodríguez

2

Este trabajo ha sido financiado por el Ministerio de Ciencia, Innovación y Universidades (BFU2015-66490-R, BES-2016-077337).

4

"La naturaleza es sabia, así han de ser quienes la estudian"

Hilario José Martín Francisco

6

AGRADECIMIENTOS

AKNOWLEDGMENTS

En primer lugar, a mis supervisores, Teresa y Diego, por permitirme formar parte de su equipo y confiar en mí desde el primer momento. Gracias por la dedicación con la que me han ayudado a crecer como científica y a estar aquí hoy.

In the first place, to my supervisors, Teresa and Diego, for letting me be part of the group and trust me from the very first moment. Thank you for your dedication, that has helped me to grow as a scientist and to be here today.

Gracias a mi familia. A los que están, a los que se han ido y a los que considero recién llegados. Porque son mi gran apoyo y la razón principal por la que lucho día a día por superarme.

Thanks to my family. To those that are here, those that left and those that I consider recently incorporated. Because they are my greatest support and the main reason why I do my best everyday.

En especial a mis padres y a mi hermana. Porque juntos somos insuperables y porque sé que cuento con ellos de forma incondicional, siempre.

Specially to my parents and sister. Because together we are unbeatable and because I know I can count on them unconditionally, always.

Gracias a Geoffrey Abbott y Rian Manville por todo lo aprendido durante mi estancia en la Universidad de California, Irvine.

Thanks to Geoffrey Abbott and Rian Manville for everything I learnt during my stay at the University of California, Irvine.

A todos mis compañeros del laboratorio porque al final nos hemos convertido en familia. Todos me han enseñado algo que me llevaré conmigo para siempre.

To all my lab mates because we ended up being a family. Each of you has taught me something that I will take with me forever.

A Laura Maglio y Natalia Armas porque ellas fueron mis mentoras en mis comienzos y nadie lo podría haber hecho mejor. Mil gracias

To Laura Maglio and Natalia Armas because they were my mentors at the beginning and no one could have done it better. Thank you very much

Y por último gracias a toda la comunidad científica por el esfuerzo conjunto que todos hacemos y gracias al cual contamos hoy en día con el conocimiento y los avances que mejoran la calidad de vida de millones de personas.

And finally, I would like to take advantage of this opportunity to thank all the scientific community. Because together we create the knowledge and advances that improve the quality of life of millions of people.

10

INDEX

1. INTRODUCTION 27

1.1 Epilepsy. Classification, Etiology and Facts. 27

Antiepileptic treatments 31

1.2 Status epilepticus in epileptogenesis 33

Neuronal apoptosis in the framework of status epilepticus 34

Animal models of status epilepticus and epilepsy 35

1.3 Ion channels and epilepsy 41

Voltage-gated K^+ channels (Kv) 42

1.4 Serum and glucocorticoids-regulated kinase 1 (SGK1) 45

1.5 SGK1.1 is a new modulator of M-channels 49

1.6 SGK1.1 as a neuroprotective factor 54

2. HYPOTHESIS AND AIMS OF THE STUDY 56

3. MATERIAL AND METHODS 58

3.1 Statistical analysis 58

3.2 Animals 58

Transgenic mouse model (B6/FVB.Tg.sgk1) 58

Genotyping 59

3.3 Epileptic paradigm and behavioral evaluation 60

Kainic acid administration and seizure behaviour evaluation 60

Pilocarpine administration and seizure behaviour evaluation 61

3.4 Electrophysiology in brain slices 62

3.5 Western blot 63

3.6 Antibodies 63

Generation of a specific SGK1.1 antibody 64

Denaturing immunoprecipitation 66

3.7 Brain damage analysis by histological procedures 66

Neurodegeneration analysis by Fluoro-Jade C 66

Gliosis evaluation by GFAP and IBA-1 immunohistochemistry 68

3.8 Cell lines and transfection 68

3.9 Terminal deoxynucleotidyl transferase dUTP nick end labeling (TUNEL) Assay 68

3.10 Neurogenesis quantification by bromodeoxyuridine immunohistochemistry 69

3.11 CRISPR/Cas9 70

3.12 Immunocytochemistry 71

3.13 Proximity Ligation Assay (PLA) 71

3.14 Two Electrode Voltage Clamp (TEVC) 72

Channel subunit cRNA preparation and Xenopus laevis oocyte injection 72

4. RESULTS 75

SECTION 1: SEIZURE BEHAVIOUR 75

4.1 Tg.sgk1 mice show reduced seizure severity and lower lethality during acute KA-induced SE 75

4.1.1 Inhibition of SGK1.1 by EMD638683 abolishes the protective effect of SGK1.1 after KA 75

4.1.2 Reduced seizure severity in B6.Tg.sgk1 mice depends on M-current activation 76

4.1.3 SGK1.1-dependent protection against seizures is retained in FVB/NJ genetic background 79

4.2 B6.Tg.sgk1 CA1 pyramidal neurons show unaltered basal synaptic transmission 81

4.3 Phosphorylation of Nedd4-2 by SGK1.1: a proposed mechanism for M-current up-regulation 83

SECTION 2: NEUROPROTECTION 86

4.4 SGK1.1 protects mice from KA-induced neuronal cell death 86

4.5 Activation of SGK1.1 reduces levels of reactive gliosis after status epilepticus 90

4.6 SGK1.1-mediated protection against neuronal death and gliosis is independent of mouse strain 92

4.7 SGK1.1 is mainly expressed in pyramidal neurons 95

4.8 SGK1.1 exerts an antiapoptotic role comparable to AKT 97

4.9 Activation of SGK1.1 reduces levels of pro-apoptotic mediator Bim and up-regulates Bcl-X_L 99

4.10 Activation of SGK1.1 does not alter neurogenesis processes in hippocampus 100

SECTION 3: REGULATION OF KV7 CHANNEL FAMILY AND KV7.2 EPILEPSY-INDUCING MUTANTS BY SGK1.1 102

4.11 SGK1.1 DOES NOT AFFECT HOMOMERIC Kv7.4 AND Kv7.5 CURRENTS, BUT UP-REGULATES HETEROMERIC Kv7.3/5 CHANNELS 103

4.12 SGK1.1 DOES NOT AFFECT THE MAJOR REPOLARIZING CARDIAC CURRENT Kv7.1/KCNE1 (I_{KS}) 106

4.13 ACTIVATED SGK1.1 UP-REGULATES Kv7.2 EPILEPSY MUTATIONS R207W AND A306T IN HETEROMERIC ASSEMBLY WITH Kv7.3 106

4.14 SGK1.1 IS IN CLOSE PROXIMITY TO Kv7.2/3 CHANNELS 109

5. DISCUSSION 116

5.1 M-CURRENT UP-REGULATION IS THE KEY MECHANISM UNDERLYING SGK1.1 MEDIATED PROTECTION AGAINST SEIZURES 116

5.2 SGK1.1 ACTIVATION LEADS TO A SIGNIFICANT PROTECTION AGAINST SE-INDUCED BRAIN DAMAGE 119

5.3 SGK1.1 ACTIVATION UP-REGULATES M-CHANNEL IN PRESENCE OF EPILEPSY MUTATIONS 123

5.4 SUMMARY, LIMITATIONS, AND FUTURE PERSPECTIVES 128

6. CONCLUSIONS 132

7.REFERENCES 135

ABSTRACT

Epilepsy is a neurological disease that affects more than 50 million people around the world. It is characterized by recurrent seizures, the most extreme form of synchronous brain activity. In the nervous system, Kv7 channels are responsible for the M-current, which is important to regulate neuronal excitability. Our laboratory has previously described a new modulator of Kv7.2/3 channels, the neuronal isoform of SGK1 kinase, SGK1.1, which up-regulates channel activity and counteracts hyperexcitability. Using a kainic acid-induced model of temporal lobe epilepsy with transgenic mice expressing a constitutively active form of SGK1.1, we have demonstrated that this kinase is a potent anticonvulsant factor, shortening seizure severity and duration independently of age, sex and genetic background. Furthermore, we show that SGK1.1 drastically reduces seizure-induced neuronal death and associated gliosis through M current-dependent and -independent mechanisms. In addition, our results demonstrate that constitutively active SGK1.1 is able to up-regulate Kv7 channels harboring epilepsy-causing mutations. Altogether, our results establish SGK1.1 as a new potential therapeutic target for epilepsy treatment.

RESUMEN

La epilepsia es una enfermedad neurológica que afecta a más de 50 millones de personas en el mundo y está caracterizada por la aparición recurrente de convulsiones, la forma más extrema de actividad cerebral sincronizada. En el sistema nervioso, los canales Kv7 constituyen la base molecular de la corriente M, importante para regular la excitabilidad neuronal. El trabajo previo de nuestro laboratorio había descrito un nuevo modulador de los canales Kv7.2/3, la isoforma neuronal de la quinasa SGK1, SGK1.1, capaz de incrementar la actividad del canal y contrarrestar así estados de hiperexcitabilidad. En esta Tesis Doctoral hemos utilizado un modelo de epilepsia de lóbulo temporal inducida por acido kaínico en un ratón transgénico con expresión de SGK1.1 constitutivamente activa para demostrar que esta quinasa tiene un potente efecto anticonvulsivo, disminuyendo tanto la intensidad como la duración de las crisis, independientemente de la edad, género y fondo genético. Además, hemos probado que SGK1.1 produce una drástica disminución de la muerte neuronal inducida por convulsiones, así como la gliosis asociada a la misma, a través de mecanismos dependientes e independientes de la corriente M. Finalmente, nuestros resultados demuestran que la activación constitutiva de SGK1.1 es capaz de activar canales Kv7 alterados por mutaciones causantes de epilepsia. En su conjunto, nuestros datos establecen que SGK1.1 podría constituir una nueva diana terapéutica para el tratamiento de la epilepsia.

ABBREVATIONS

AEDs Antiepileptic Drugs

APS 3-Aminopropyltriethoxysilane

BAC Bacterial Artificial Chromosome

BAC Bicinchoninic Acid

Bcl-x_L B-cell lymphoma-extra large

BFNE Benign Familial Neonatal Epilepsy

Bim Bcl-2-like protein

BrdU Bromodeoxyuridine

BSA Bovine Serum Albumin

CNQX 7-nitro-2,3-dioxo-1,4-dihydroquinoxaline-6-carbonitrile

CNS Central Nervous System

DAG Diacylglycerol

DCX Doublecortin

DFNA2 dominant progressive hearing loss

DG Dentate gyrus

DMSO Dimethyl Sulfoxide

DNA Deoxyribonucleic Acid

DPX Dibutylphthalate Polystyrene Xylene

FA Formaldehyde

FBS Fetal Bovine Serum

FJC Fluoro-Jade C

FoxO Forkhead transcription factor of the O class

FoxO3 Forkhead box O3

GFAP Glial Fibrillary Acidic Protein

GSK-3 Glycogen synthase kinase 3

GST Glutathione-S-Transferase

HEK-293T Human Embryonic Kidney cells

HeLa cervical cancer cells derived from Henrietta Lacks

H_2O_2 Hydrogen peroxide

IBA-1 Ionized calcium-Binding Adaptor molecular 1

ILAE International League Against Epilepsy

Ins(1,4,5)P3 Inositol triphosphate

IPTG isopropyl ß-D-1-thiogalactopyranoside

IR Insulin Receptor

IRS Insulin Receptor Substrate

JLNS Jervill and Lange-Nielsen Syndrome

KA Kainic Acid

MAP 2 Major microtubule associated protein 2

mEPSC Miniature Excitatory Post-Synaptic Currents

mIPSC Miniature Inhibitory Post-Synaptic Currents

mTORC2 mammalian Target Of Rapamycin Complex 2

NEE Neonatal Epileptic Encephalopathy

NOS Nitrous Oxygen Systems

N2a Neuro2A cells from mouse neuroblastoma

OHC outer hair cell

PAGE Polyacrylamide gel electrophoresis

PAM Protospacer Adjacent Motif

PBS Phosphate -Buffered Saline

PDK1 Phosphoinositide-Dependent protein Kinase 1

PFA Paraformaldehyde

PI Pilocarpine

PtdIns(4,5)P2/PIP_2 Phosphatidylinositol biphosphate

PI3K Phosphatidylinositol 3-kinase

PKA Protein Kinase A

PKB/AKT Protein Kinase B

PKC Protein Kinase C

PLA Proximity Ligation Assay

PLC Phospholipase C

PN Pyramidal neurons

PTZ Pentylenetetrazol

Puma P53-up-regulated mediator of apoptosis

RMP Resting Membrane Potential

RNA Ribonucleic Acid

ROS Reactive Oxygen Species

RWS Romano–Ward Syndrome

SCG Superior Cervical Ganglion

SDS Sodium Dodecyl Sulfate

SE Status Epilepticus

SGK1 Serum and Glucocorticoids-regulated Kinase

SGK1.1 Serum and Glucocorticoids-regulated Kinase isoform 1

SRSs Spontaneous Recurrent Seizures

TBI Trauma Brain Insult

TEVC Two Electrode Voltage Clamp

TLE Temporal Lobe Epilepsy

TdT terminal deoxynucleotidyl transferase enzyme

TUNEL Terminal deoxynucleotidyl transferase dUTP Nick-End Labeling

WHO World Health Organization

20

TABLES & FIGURES APPENDIX

Figure 1. Framework for classification of the epilepsies 28

Figure 2. Cellular events occurring during epileptogenesis 30

Figure 3. Schematic representation of the two operational dimensions of status epilepticus according to ILAE 33

Figure 4. Schematic representation of cellular events following KA-receptors activation 39

Figure 5. Schematic representation of M1 muscarinic pathway-Kv7 channels 41

Figure 6. Tissue distribution of Kv7 subunits 44

Figure 7. Sgk1 gene illustration 46

Figure 8. SGK1 regulation at transcriptional and post-transcriptional levels 48

Figure 9. SGK1.1 increases Kv7.2/3 currents in heterologous expression systems 50

Figure 10. SCG neurons isolated from B6.Tg.sgk1 mice show a significant increase in M-current 51

Figure 11. B6.Tg.sgk1 mice show reduced seizure severity and lower lethality after systemic administration of kainic acid 52

Figure 12. Reduced excitability in CA1 pyramidal neurons with increased SGK1.1 activity 53

Figure 13. Schematic representation of the 3' end of Tg.sgk1 mRNA isoforms 58

Figure 14. Genotyping 59

Figure 15. Seizure stages according to a modified Racine scale 60

Figure 16. Schematic representation of pilocarpine model procedure 62

Figure 17. Design and production of anti-SGK1.1 antibody 65

Figure 18. Coronal sections used for FJC analysis 67

Figure 19. Schematic representation of the mechanism underlying TUNEL Assay 69

Figure 20. *Sgk1*-KO N2a cells generation by CRISPR/Cas9 71

Figure 21. Inhibition of SGK1.1 with EMD638683 equalizes the seizure behaviour between genotypes 76

Figure 22. Tg.sgk1 mice show reduced seizure severity and mortality after systemic KA administration via M-current activation 77

Figure 23. Different doses of pilocarpine (275-480 mg/kg) were evaluated according to the seizure severity score 78

Figure 24. Activation of muscarinic pathway by pilocarpine abolishes the SGK1.1-mediated resistance to KA-induced seizures 79

Figure 25. SGK1.1 protective role against KA-induced seizures is independent of genetic background 81

Figure 26. Basal synaptic transmission is not altered in B6.Tg.sgk1 mice 82

Figure 27. SGK1.1 enhances phosphorylation levels of Nedd4-2 and GSK-3-β in heterologous expression systems 84

Figure 28. SGK1.1 phosphorylates Nedd4-2 in mouse hippocampus 85

Figure 29. FJC staining reveals significant differences in neuronal death between B6.WT and B6.Tg.sgk1 87

Figure 30. SGK1.1- induced neuroprotection depends on kinase activity 88

Figure 31. FJC staining on KA + XE991 treated B6 mice demonstrates SGK1.1 activity-dependent neuroprotection includes M-current dependent and independent mechanisms 89

Figure 32. Astrogliosis in hippocampi and cortex from KA-injected B6.WT and B6.Tg.sgk1 mice 90

Figure 33. Microgliosis analysis in B6.WT and B6.Tg.sgk1 demonstrates increased IBA-1 levels in wild type mice after KA treatment 91

Figure 34. FJC staining demonstrates SGK1.1-mediated protection against neurodegeneration is independent of strain 93

Figure 35. Astrogliosis in hippocampus and cortex of KA-injected FVB.WT and FVB.Tg.sgk1 mice 94

Figure 36. Reactive microglia in hippocampus and cortex of KA-injected FVB.WT and FVB.Tg.sgk1 mice 95

Figure 37. Characterization of a new rabbit polyclonal anti-SGK1.1 antibody 96

Figure 38. SGK1.1 is selectively expressed at the soma and processes of pyramidal neurons 97

Figure 39. SGK1.1 activation leads to significant anti-apoptotic effect similarly to AKT 98

Figure 40. Bim levels are significantly reduced in Tg.sgk1 mice after status epilepticus 99

Figure 41. Bcl-x_L levels are significantly lower in B6.WT after status epilepticus 100

Figure 42. Activation of SGK1.1 does not alter neurogenesis processes in hippocampus 101

Figure 43. Wild type and constitutively active (S515D) SGK1.1 increases heteromeric Kv7.2/3 currents at similar levels, supporting previously obtained results 103

Figure 44. SGK1.1 fails to increase homomeric Kv7.4 and Kv7.5 currents, similarly to previously reported results for homomeric Kv7.2/3 104

Figure 45. SGK1.1 increases heteromeric Kv7.3/5 currents like heteromeric Kv7.2/3, supporting the need for heteromeric channel assembly to observe SGK1.1 effects 105

Figure 46. SGK1.1 does not affect the major repolarizing cardiac current Kv7.1/KCNE1 (I_{KS}) 106

Figure 47. Constitutively active form of SGK1.1(S515D) up-regulates Kv7.2 epilepsy mutation R207W in heteromeric assembly with Kv7.3 while WT SGK1.1 fails to 107

Figure 48. Constitutively active form of SGK1.1(S515D) up-regulates Kv7.2 epilepsy mutation A306T in heteromeric assembly with Kv7.3(A315T) 108

Figure 49. Representative confocal images showing expression of Kv7.2/3, SGK1.1 and Nedd4-2 110

Figure 50. Association between activated SGK1.1 and heteromeric channel Kv7.2/3 is reduced in presence of epilepsy mutant Kv7.2(R207W) but not Kv7.2(A306T) 112

Figure 51. Kv7.2/3 heteromeric channel associates with Nedd4-2 and this association weakens in presence of activated SGK1.1 113

Table 1. Approved antiepileptic drugs and their main mechanisms of action 32

Table 2. Main rodent models in epilepsy research 37

Table 3. Genes and proteins mutated in idiopathic epilepsies encephalopathies 43

Table 4. Kv7 subunits: location, channel function and channelopathy 45

Table 5. Oligonucleotides used throughout this work and their sequences 59

INTRODUCTION

1. INTRODUCTION

1.1 Epilepsy. Classification, Etiology and Facts.

The study of the brain continues to expand at a rapid stride, shedding light on the basic mechanisms underlying nervous system diseases (Sontheimer 2015). Among the myriad list of neurological conditions, epilepsy is a non-communicable chronic disease characterized by an enduring predisposition to generate seizures. Recurrent and unpredictable seizures are caused by highly synchronized hyperactivity in one or several areas of the brain (Fisher et al. 2005). A single episode of abnormal electrical discharge in the brain, accompanied by alterations in behaviour and consciousness, is considered a seizure event (Fisher et al. 2005). Recently, the International League Against Epilepsy (ILAE) defined epilepsy based on at least one of the following conditions: (1) at least two unprovoked seizures occurring more than 24 hours apart; (2) one unprovoked seizure and a probability of further seizures similar to the general recurrence risk after two unprovoked seizures, occurring over the next ten years; (3) diagnosis of an epilepsy syndrome (Fisher et al. 2014). Although it has been traditionally referred to as a disorder, the ILAE agreed that epilepsy is best considered to be a disease in order to avoid underestimating the seriousness of the condition (Fisher et al. 2014).

According to the World Health Organization (WHO) (World Health Organization 2019), around 50 million people worldwide suffer from epilepsy, making it one of the most common neurological conditions globally. Further, it is estimated that up to 70% of people with epilepsy live in low-and middle-income countries, which increases the risk of not having access to proper treatment.

Classification of epilepsies is as diverse as their etiology. Different etiologic groups have been described to facilitate treatment. These groups are based on mechanism: genetic, structural, infectious, metabolic, immune or unknown. The new classification of epilepsies by ILAE is based on 3 key features: seizure type, epilepsy type and epilepsy syndrome (Scheffer et al. 2017) (**Figure 1**) whose diagnosis strongly depends on the resources available to the clinician.

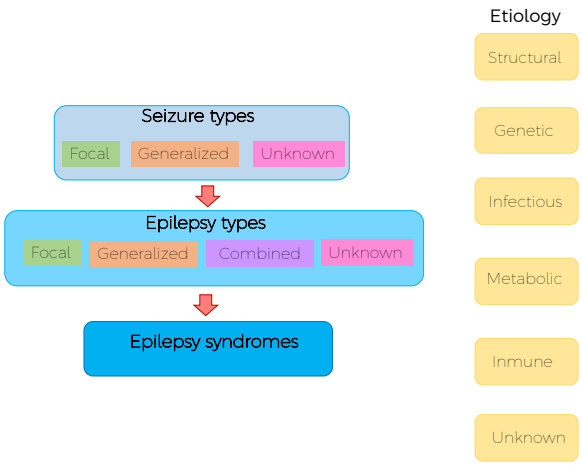

Figure 1. Framework for classification of the epilepsies. There are three levels of diagnosis in epilepsy including seizure type, epilepsy type and epilepsy syndrome. Each of them requires a series of resources and techniques that might limit their determination by a clinician. Focal seizures lead to involuntary movement of parts of the body and are originated in a specific brain area while generalized seizures involve the entire body, affecting the whole brain (Fisher et al. 2017). Focal epilepsies include unifocal and multifocal disorders as well as seizures involving one hemisphere whereas combined epilepsies refer to those cases with both focal and generalized seizures. For a diagnosis of generalized epilepsy, the patient would typically have a range of seizure types including absence, myoclonic, atonic, tonic and tonic-clonic seizures. The term "unknown" is used to denote where it is understood that the patient has epilepsy but it is difficult to determine if the epilepsy type is focal or generalized (Fisher et al. 2014). The third level of diagnosis is Epilepsy Syndrome, which includes a cluster of features regarding seizure type, EEG and imaging profiles. After the first seizure, efforts should be made to determine the etiology of the patient's epilepsy. Modified from Scheffer et al 2017.

Other than its complex classification, it is estimated that approximately 30% of diagnosed people will not gain total seizure control from medication (Löscher and Schmidt 2011). Also, according to the WHO, the risk of premature death in people with epilepsy is up to three times higher than the general population and in many parts of the world, people with epilepsy and their families suffer from stigma and discrimination (World Health Organization 2019). These facts, along with the significant proportion of world's disease burden that this disease accounts for, makes epilepsy research one of the most ambitious goals in neuroscience today.

The gradual transformation from a previously healthy brain into one inundated by spontaneous and recurrent seizures (SRSs) is known as epileptogenesis and it is generally divided into three stages. First, an initial insult, such as an uncontrolled seizure

with long-term consequences, also known as status epilepticus (SE), initiates cellular and molecular changes in the affected brain areas. Second, a latent period free of seizures starts and lasts until chronic, unprovoked seizures occur. Third, after the manifestation of SRSs, molecular and cellular changes continue to exacerbate the severity of the disease (Jacobs et al. 2009; Patel et al. 2019). Importantly, the process of epileptogenesis does not always require an initial insult, as in the case of genetically based epilepsies. According to the new terminology, “epileptogenesis” no longer refers only to the time period between the epileptogenic event and diagnosis of epilepsy; rather, the term epileptogenesis now includes the mechanisms of progression that can last even after the diagnosis of epilepsy (Pitkänen et al. 2014).

The profuse list of pathophysiological processes occurring during epileptogenesis includes neurodegeneration (Dingledine et al. 2014), reactive gliosis and uncontrolled inflammation (Vezzani et al. 2011; Sofroniew 2014), ectopic neurogenesis (Jessberger and Parent 2015), brain-blood barrier breakdown (Van Vliet et al. 2007), changes in neural circuits and expression and functional changes in receptors, ion channels, transporters and enzymes involved in excitatory and inhibitory neurotransmission (Goldberg and Coulter 2013). The effects of such events create a vicious circle that contributes to the generation of new seizures, development of epilepsy and/or diverse comorbidities (Pitkänen and Lukasiuk 2009) (Figure 2).

Epilepsy can be the result of an inciting acute event that disrupts the normal function of the brain, giving rise to seizures (acquired epilepsy). Nevertheless, it can also occur in idiopathic forms, which are mainly of genetic origin as a result of congenital abnormalities (genetic epilepsy) or it can be part of a neurological disorder. Importantly, the rate and risk of epileptogenesis does not only depend on the initial insult but also on genetic factors, microbiome and environmental influence (Hesdorffer et al. 1998; Miller et al. 2010; Wagner et al. 2010; Graham et al. 2013; Henshall et al. 2014; Kobow and Blümcke 2014; Peng et al. 2018; Kyyriäinen et al. 2019). In fact, it has been getting more and more clear that there is not a consistent division between acquired and genetic epilepsies (Steinlein 2008). The major part of epilepsies are considered acquired, and temporal lobe epilepsy (TLE) is the most common among them (Allen Hauser and Annegers 1996; Wieser 2004; Goldberg and Coulter 2013).

However, there are also familial forms of TLE. Key features of TLE are: implication of limbic structures (hippocampus, amygdala and entorhinal cortex) (Bartolomei et al. 2005); frequently, a precipitating event that precedes the manifestation of TLE (Mathern et al. 2002); a latent period free of seizures; and a high rate of mesial sclerosis caused by neuronal loss and gliosis (Mathern et al. 1997; Goldberg and Coulter 2013). Gliosis is the process by which glial cells react to CNS damage, such as seizures. Reactive astrocytes and microglia have been found in the resected hippocampi of TLE patients (Crespel et al. 2002; Aronica et al. 2007; Van Gassen et al. 2008; Ravizza et al. 2008).

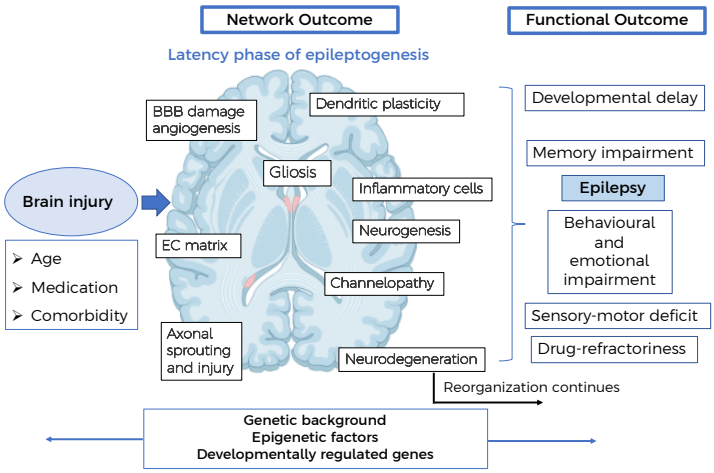

Figure 2. Cellular events occurring during epileptogenesis. Brain insults such as SE, trauma brain insult (TBI) and stroke can trigger the process. Alterations might lead to several functional impairments as well as epilepsy per se. During the epileptogenic process, these alterations might be modulated by genetic background and epigenetic factors. Modified from Pitkänen and Lukasiuk 2009.

Although it is known that glial cells have an essential role in maintaining brain homeostasis, different inflammatory mediators can be produced by glial cells and contribute to the generation of new seizures. There is, indeed, a growing sum of evidence supporting the hypothesis of inflammation being a consequence as well as a cause of epilepsy (Marchi et al. 2009; Vezzani et al. 2011).

Multiple factors may incite TLE including SE, febrile seizures or TBI (Nirwan et al. 2018). The study of TLE implicates the use of animal models reproducing the stages involved in the development of the syndrome.

Antiepileptic treatments

Currently, available treatments include the administration of antiepileptic drugs (AEDs), surgical removal of the affected brain area (Wiebe et al. 2001; Yasuda et al. 2006; Vale et al. 2015), vagal nerve or deep brain stimulation (Schachter 2002; Fisher et al. 2010; Fisher et al. 2015) and cell transplantation therapy (Noebels et al. 2012). Efforts in epilepsy research are yielding new advances in the development of AEDs and knowledge about their mechanisms of action. Available antiepileptic drugs interact with diverse molecular targets and, normally, one drug can act on several targets, commonly producing side effects. Future research should be directed to determine the exact mechanisms of drug action and reduce side effects (Potschka 2013). Approved AEDs are shown in Table 1 (Gunthorpe et al. 2012; Abou-Khalil 2019), classified into those decreasing excitability and those increasing inhibition. In the last years, brivaracetam, cannabidiol and stiripentol have been approved by the US Food and Drug Administration (FDA) and retigabine has been discontinued due to adverse side effects. Both monotherapies and adjunctive therapies can be used to treat epilepsy, although combinations should avoid unfavorable pharmacokinetic interactions.

Despite the great advances in the development of AEDs, 20-30% of the patients are resistant to treatments with eventual remission episodes (Sillanpää and Schmidt 2006; Brodie et al. 2012). Moreover, marketed drugs have demonstrated their ability to suppress seizures once they occur, but they neither prevent progression of the disease nor the effect of SE-induced neurotoxicity, which has been recognized as a risk for progressive structural and cognitive impairments (Temkin 2009; Schmidt 2012; Henshall et al. 2013).

AEDs are unable to treat comorbidities related to epilepsy such as anxiety (Tellez-Zenteno et al. 2007; Kanner et al. 2010), depression (Lambert, Michelle V; Robertson 1999; Kobau et al. 2006), heart disorders (Elliott et al. 2009) and even mortality (Devinsky et al. 2016; Chamorro-Muñoz et al. 2017). Altogether, considerable efforts should be made to translate the existing knowledge into effective

pharmacological and clinical actions that improve the efficacy of current treatments and overcome the neurotoxic effects after the precipitating event. The latent period after the inciting event constitutes an opportunity for counteracting the effects of epileptogenesis, prevent seizures, modify the severity or even cure (Löscher 2012; Pitkänen et al. 2014; White and Löscher 2014). Thus, treatments should be applied in patients after epileptogenic brain insults like TBI, stroke, febrile seizures, or SE.

Table 1. Approved antiepileptic drugs and their main mechanisms of action. (Modified from Gunthorpe et al 2012 and Abou-Khalil 2019).

AED	REDUCE EXCITATION				INCREASE INHIBITION	
	Na^+	Ca^{2+}	SV2A	Glutamate	Cl^-(GABA)	K^+(KCNQ)
Benzodiazepines					✦	
Brivaracetam			✦			
Carbamazepine	✦					
Cannabidiol					✦?	
Ethozuximide		✦				
Eslicarbazepine acetate	✦					
Felbamate	✦			✦	✦	
Gabapentin		✦				
Lacosamide	✦					
Lamotrigine	✦					
Levetiracetam			✦			
Oxcarbazepine	✦					
Phenobarbital		✦		✦	✦	
Phenytoin	✦					
Pregabalin		✦				
Perampanel				✦		
Rufinamide	✦					
Tiagabine					✦	
Topiramate	✦			✦	✦	
Valproate	✦	✦			✦	
Vigabatrin					✦	
Zonisamide	✦	✦				
Retigabine						✦*
Flupirtine						✦*

*Treatment with these drugs have been suspended due to side effects; ? Mechanism is not clear

1.2 Status epilepticus in epileptogenesis

Definition of SE has been in constant change over the last decades due to imprecise terms regarding timeframes. The special report from the ILAE (Trinka et al. 2015) clarifies the term. Traditionally, it was defined as a "seizure that persists for a sufficient length of time or is repeated frequently enough to produce a fixed and enduring condition". With the new definition provided by the ILAE it is now considered that "SE is a condition resulting either from the failure of the mechanisms responsible for seizure termination or from the initiation of mechanisms which lead to abnormally prolonged seizures (after time point t_1). It is a condition that can have long-term consequences (after time point t_2) including neuronal death, neuronal injury, and alteration of neuronal networks, depending on the type and duration of seizures". The first time point (t_1) refers to length of the seizure and the moment at which the seizure should be regarded as an "abnormally prolonged seizure". The second time point (t_2) is the time of ongoing seizure activity beyond which there is a risk of long-term consequences.

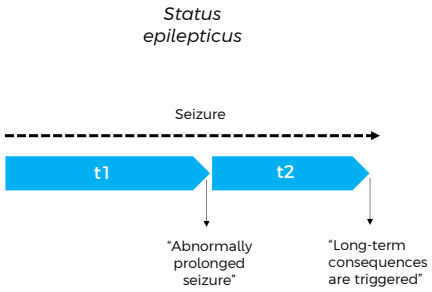

Figure 3. Schematic representation of the two operational dimensions of status epilepticus according to ILAE.

Mechanisms underlying the manifestation of SE are diverse and involve excessive neuronal excitability through increased activity of NMDA receptors and/or aberrant function of inhibitory neurons that exhibit inadequate GABAergic activity (Kapur et al. 1989; Kapur and Lothman 1989; Kapur and Macdonald 1997). Long-term outcomes of SE include subsequent epilepsy and risk of premature death both in adults and children (Towne et al. 1994; Raspall-Chaure, M; Chin, RFM; Neville, BG; Scott

2006; Devinsky et al. 2016; Sculier et al. 2018). Epidemiologic studies show that in populations of adults and children, subsequent epilepsy after SE may occur in 22%-41% (Hesdorffer et al. 1998; Cooper et al. 2009; Sculier et al. 2018). Moreover, long-term mortality after SE is a very serious concern seen in up to 20% of children and 55% of adults. Early treatment of seizures with first line treatments (benzodiazepines) along with neuroprotective approaches constitutes a key factor to control or prevent long-term outcomes (Legriel et al. 2010), as it has been demonstrated that the prognosis of SE worsens with increasing event duration (Towne et al. 1994; DeLorenzo et al. 1999).

However, some forms of SE, referred as refractory SE, are pharmacoresistant and do not respond to first, second or third-line therapies (Novy et al. 2010). Therefore, clinical and experimental studies should be performed if we want to find new and efficient therapies that terminate SE and overcome the associated neuronal damage. Animal models of epilepsy have considerably improved our knowledge in the field and still constitute a very useful tool to study both acquired and idiopathic epilepsy (Pitkänen, Asla; Schwartzkroin, Philip; Moshé 2005; White and Löscher 2014).

Neuronal apoptosis in the framework of *status epilepticus*

Experimental and clinical studies have confirmed that SE results in neuronal damage or death that might contribute to epileptogenesis and impairments in cognitive function. Although it has been well described that SE-induced neuronal death relies on necrotic events following excessive glutamate release (Fujikawa 2005), apoptotic cell death mechanisms have also been evidenced in experimental models. Apoptosis is a physiologic process for killing cells by a highly organized molecular cascade that is usually energy-dependent and might involve new gene transcription. In contrast to the main features of necrosis that include mitochondrial matrix swelling, dilatation of endoplasmic reticulum and breakup of intracellular membranes, apoptosis is characterized by aggregation of chromatin altering the nuclear membrane, conservation of intracellular organelle integrity and later dispersion of cell contents (Wyllie et al. 1980).

Different studies have demonstrated that seizures can cause mitochondrial dysfunction activating intrinsic pathway components like caspases 3 and 9 and Bcl-2 family members. Moreover, experimental seizures and clinical data have shown that the

extrinsic, death-receptor-dependent pathway is also triggered after seizures (for an illuminating review, see Henshall 2007). Several reports have related different apoptotic factors to seizure-induced neuronal damage. For example, it is known that transcription factor p53 accumulates upon SE leading to up-regulation of p53-up-regulated mediator of apoptosis (Puma) and to hippocampal damage. Further, pharmacological inhibition of p53 led to a reduction in hippocampal damage and in the occurrence of spontaneous seizures (Engel et al. 2010). This result suggests a potential role of anti-apoptotic approaches in preventing epileptogenesis.

Other studies addressing the molecular changes after SE have shown that SE decreases the levels of AKT activity and its binding to FoxO3a while increasing the levels of Bim and cleaved caspase-3 in the hippocampus (Kim et al. 2014). Recently, one study has demonstrated that targeting the miR-15a-5p/NR3B/ERK1/2 route, which is involved in cellular maintenance, inhibits apoptosis in hippocampal neurons in SE (Liu et al. 2020). Following SE, mitochondrial dysfunction can result in oxidative stress that also plays an important role in SE-induced neuronal death as several studies demonstrate. For instance, it has been proven that upregulation of nitric oxide synthase II contributes to apoptotic cell death in CA3 region of hippocampus after SE (Chuang et al. 2007). Although more studies need to be performed to further elucidate the molecular pathways involved in neuronal death, the evidence available supports the idea of apoptosis being an important feature of SE-induce neuronal death in different experimental models. Therefore, pharmacological approaches targeting apoptosis might constitute a useful strategy to diminish some of the negative impacts following SE as well as to prevent epileptogenesis. Specific patterns of apoptosis found in the KA model of SE will be presented in more detail on section Kainic acid model of epilepsy.

Animal models of status epilepticus and epilepsy

Animal models of epilepsy have been a highly valuable source of knowledge since 1937, when Tracy Putnam and Houston Merritt discovered the properties of phenytoin in a seizure model in cats (Putnam, TJ; Merritt 1937; Löscher 2017). A broad variety of animal models have been developed since then to reproduce chronic epilepsy and acute seizures induced by chemoconvulsants, TBI and electrical or sound stimuli. Table 2 summarizes the main experimental models used in epilepsy research.

The classification generally depends on the epilepsy syndrome reproduced and the long-term outcomes to study. Thus, acute models include SE and the consequent neuronal damage produced, whereas chronic models can mimic diverse epileptic syndromes (Reddy and Kuruba 2013; Kandratavicius et al. 2014). Several drugs inducing SE in rodent species have been widely used to characterize pathophysiological mechanisms or to address new therapies. Chemoconvulsants enhancing glutamatergic transmission or blocking GABAergic inhibition are commonly used to trigger seizures. Also, chemicals activating cholinergic neurotransmission can induce SE. Accordingly, Kainic acid (KA) induces seizures by activating KA-type glutamate receptors, Pentylenetetrazol (PTZ) does it through inhibition of $GABA_A$ receptors and Pilocarpine (PI) through activation of muscarinic receptors (Lévesque et al. 2016).

An important group of epilepsy paradigms are post-SE models of TLE, where chemical or electrical induction of acute seizures in rodents is used for testing the efficacy of novel treatments (Löscher 2017). As mentioned above, some of the most important in this category are the PI and the KA models, which reproduce the typical histopathological alterations and spontaneous chronic seizures seen in epileptic patients (Lévesque et al. 2016). Importantly, it has been described that the effect of chemoconvulsants might differ with genetic background, age, gender and environment (animal facility, handling, diet, etc.) (Binder, Devin K.; Scharfman 1997; Montagutelli 2000; McKhann et al. 2003; McLin and Steward 2006; Lévesque et al. 2016; Li and Liu 2019). For instance, the C57BL6/J mouse strain has been reported to show low sensitivity to various convulsants and little KA-induced neurodegeneration compared to FVB/NJ strain, which is more susceptible to seizure disorders (Royle et al. 1999; Kasugai et al. 2007). These factors should be considered when deciding the most appropriate model and breeding conditions if we are to obtain reliable results.

Table 2. Main rodent models in epilepsy research. Chemoconvulsants can be administered by intraperitoneal (ip), subcutaneous (sc) or intracranial (ic) injection in mice and rats. Genetic modifications can be used to generate predisposed or resistant strains that can be useful for AEDs screening or to elucidate epileptogenesis and its mechanisms. In vitro models commonly require rodent brain slices to study electrophysiological features. (Modified from Reddy and Kuruba 2013 and Kandratavicius et al. 2014).

MODEL	CHARACTERISTICS	MANIFESTATION	USE
Chemoconvulsants			
Kainic acid (KA)	AMPA/KA receptors agonist	SE and/or SRSs	Acute model or TLE
Pilocarpine (PI)	Acetylcholine receptors	SE and/or SRSs	Acute model or TLE
Pentylentetrazol (PTZ)	$GABA_A$ receptors antagonist	SE	Acute model
Electrical stimulation			
Electroshock	Whole brain stimulation protocols	Generalized tonic-clonic seizures	Acute model
Afterdischarges	Focal electrical stimulation	Partial and myoclonic seizures	Seizure spread patterns
Kindling	Repeated focal afterdischarge induction	Partial-generalized seizures/ SRSs	Epileptogenic processes in TLE
Genetics			
Genetic modified mice (i.e.KCNQ2, NaV, Gabrg2 KO)	Transgenic, "knock-out" or "knock-in" mice with gain or lost of function of relevant genes	More susceptibility to seizures and/or SRSs	Relevant epileptic genes
Spontaneous models (i.e.GAERS, WAG/Rjj and models of absence seizures)	Rodents with spontaneous seizures	Inherited epilepsies, SRSs	Hereditary epilepsies
In vitro			
Acute hippocampal slice In low Mg^{2+} In high K^+ In kainic acid	Epileptic-like activity depelopment after bath or in vivo treatment	Electrophysiological seizures	Acute models
Organotipic hippocampal slice cultures			Brain damage

Kainic acid model of epilepsy

The KA model is a very well described animal model, widely accepted for the study of TLE, the associated pathophysiological changes and pharmacology (Ben-Ari and Cossart 2000). KA is a cyclic analog of L-glutamate that acts as an agonist of the ionotropic AMPA and KA receptors. Thus, it leads to depolarization of neurons by allowing cationic currents through the cell and provoking progressive excitotoxic effects (Vincent and Mulle 2009). Its ability to produce neuronal damage was first described

by Nadler et al. in 1978 (Nadler et al. 1978) and its first use as a model of excitation-induced TLE was proposed by Ben-Ari and Lagowska the same year (Ben-Ari and Lagowska 1978). Since then, numerous studies have demonstrated the ability of KA to induce SE in rodents and reproduce neuropathological lesions similar to those occurring in some patients with epilepsy (Ben-Ari et al. 1979; Lothman et al. 1981; Scerrati et al. 1986; Willoughby et al. 1997). Systemic or intraperitoneal injection at a single dose of 20-30 mg/kg usually produces behavioral signs within 5 minutes whereas generalized convulsions might start after 30-60 minutes (Sperk 1994; Willoughby et al. 1997) with SE-induced lethality rates of around 20% (McLin and Steward 2006). Intra-cerebral injection leads to epileptiform discharges starting in limbic structures and is associated with lower mortality rates (Carriero et al. 2012). Systemic administration produces consistent seizures, mossy fiber sprouting and SRSs and it is associated with higher mortality rates that can be reduced by multiple dosing (Sharma et al. 2007). The behavioral symptoms upon KA and PI treatments are usually scored using the Racine scale (Racine 1972), which assigns numeric values to the different observed stages depending on seizure severity. It has been proven that the EEG of animal models treated with KA shows increased beta (20-30 Hz) and gamma (30-100 Hz) bands during the acute phase in hippocampus and neocortex (Lothman et al. 1981; Medvedev et al. 2000). Decreases and increases in these waves are usually related to pathologic conditions including brain abscess, stroke, dysplasia or epilepsy (Marcuse et al. 2016; Malik and Amin 2017).

Treatment with KA commonly yields recurrent seizures with variable frequency and remarkable brain damage (Nadler et al. 1978; Cavalheiro et al. 1982). It has been shown that epileptiform seizures after KA are generated in the CA3 region of hippocampus and then progress to other limbic structures, leading to a characterized pattern of neuronal loss, mossy fiber sprouting and glial activation. The rapid effect of KA in hippocampal formation might be easily explained if we consider the high expression of kainate receptors (GluR5-7/KA1-2) in hippocampal neurons (Paternain et al. 2000). Upon KA receptors activation, a cascade of cellular events starts (**Figure 4**), including a massive influx of Ca^{2+} (Arundine and Tymianski 2003; Wang et al. 2005) and consequent production of reactive oxygen species (ROS) and nitrous oxide systems

(NOS) (Cheng and Sun 1994; Gluck et al. 2000; Candelario-Jalil et al. 2001; Milatovic et al. 2002). In turn, these conditions induce DNA damage, changes in mitochondrial function, cell death and activation of glial cells (Ben-Ari 1985a; Ben-Ari and Cossart 2000; Chen et al. 2005; Galluzzi et al. 2009). Moreover, apoptotic pathways are activated during seizures, involving the Bcl-2 family of proteins, cytochrome c and caspases 9 and 3 (Franklin 2011; Almeida 2013; Auladell et al. 2017). Neurodegeneration appears within 8 to 24 hours after KA and has a vigorous impact on CA3, CA1 and dentate gyrus (DG) cells, although it also affects extrahippocampal regions like entorhinal cortex, thalamus and amygdalar complex (Nadler et al. 1978; Schwob et al. 1980; Ben-Ari et al. 1981; Ben-Ari 1985b; Ben-Ari and Cossart 2000; Schoenebeck et al. 2005; Drexel et al. 2012).

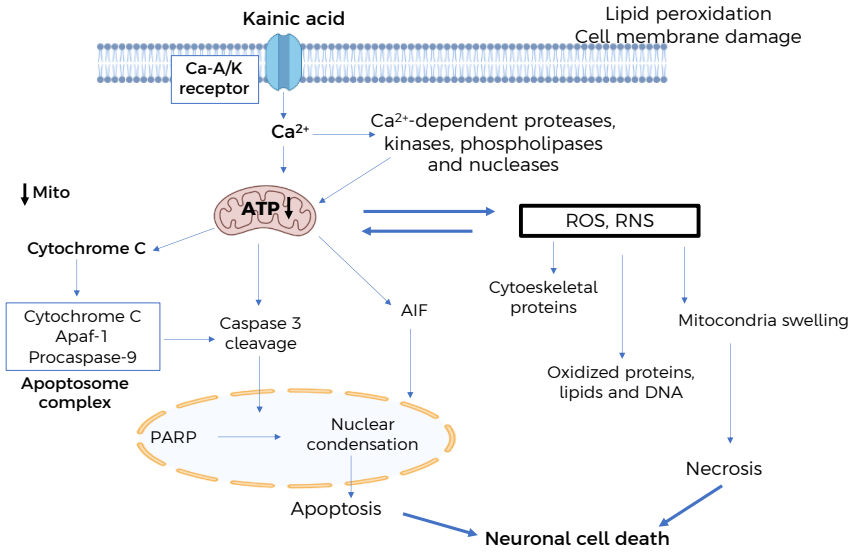

Figure 4. Schematic representation of cellular events following KA-receptors activation. KA stimulates the Ca^{2+}-A/K (AMPA and KA receptors), leading to rapid Ca^{2+} entry and generation of ROS and reactive nitrogen species (RNS), which leads to damage of intracellular membranes and activation of apoptotic pathways that will end up in neuronal cell death. Alternatively, Ca^{2+} overload can lead to direct mitochondrial damage causing neuronal necrosis. Modified from Wang et al. 2005.

During KA-induced brain damage, non-neuronal cells like astrocytes and microglia are also disturbed. These cells have significant influence on the survival and post-injury repair of neurons (Chen et al. 2005) and their activation, also called gliosis,

involves a variety of physicochemical and physiological changes that arise in response to CNS insults and diseases (Sofroniew 2014). Gliosis indicators include hypertrophy of cell bodies, upregulated expression of different proteins, cellular proliferation and generation of a gliotic scar rich in extracellular matrix molecules (Silver and Miller 2004). Some of the most frequently used markers are glial fibrillary acidic protein (GFAP) to detect astrogliosis and ionized calcium-binding adaptor molecular 1 (IBA-1) to detect microgliosis.

Pilocarpine model of epilepsy

PI is a muscarinic acetylcholine receptor agonist that, after systemic or intracerebral injection, provokes SE. This model has been extensively used for the evaluation of AEDs since its first description in 1983 (Turski et al. 1983). Reasons to use it include the rapid effect after systemic administration, the presence of a latent period preceding SRSs (Leite et al. 1990; Cavalheiro et al. 1991), manifestation of brain damage with lesions found in TLE patients (Mello et al. 1993; Wieser 2004) and the fact that, similarly to some refractory epilepsies, AEDs poorly control seizures in PI-treated rodents (Glien et al. 2002; Chakir et al. 2006). Similarly to KA, treatment with PI also leads to neuronal death and gliosis events within hours or weeks after SE depending on the area (do Nascimento et al. 2012). PI can cause lesions in neocortical areas (Bonilha et al. 2010) making the model useful to study extrahippocampal damage in TLE (Sharma et al. 2007). The mechanism of action relies on the activation of M1 subtype muscarinic receptors that, in the CNS, modulate the M-current. This modulation is totally lost in M1 knock-out mice that are highly resistant to seizures induced by PI (Hamilton et al. 1997). M-current is a voltage-dependent K^+ current that controls neuronal excitability and receives its name after its well-known inhibition by muscarinic pathway activation (Brown and Adams 1980; Brown 1987; Delmas and Brown 2005) (Figure 5). Although SE induction occurs through M1 receptors, considerable evidence suggest that seizure maintenance depends on NMDA receptors (Nagao, T; Alonso, A; Avoli 1996; Smolders et al. 1997).

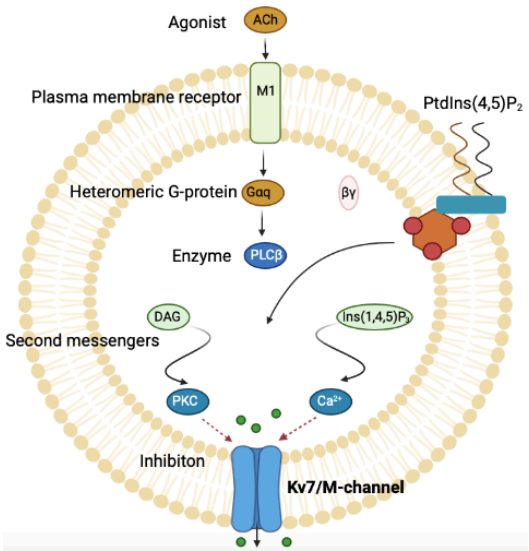

Figure 5. Schematic representation of M1 muscarinic pathway-Kv7 channels. Binding of acetylcholine to M1 receptors triggers the activation of the G family protein Gq and consequent activation of membrane-associated phospholipase-Cβ (PLCβ), whose activity leads to the disruption of phosphatidylinositol-4.5-biphosphate (PtdIns(4,5)P_2) into diacylglycerol (DAG) and inositol-1,4,4-triphosphate (Ins(1,4,5)P_3). Substantial evidence suggest that PtdIns(4,5)P_2 might be a crucial determinant of modulation as its binding to M-channel keeps it opened. Release of Ca^{2+} and activation of protein kinase C (PKC) by DAG might modify the interaction of the channel with PtdIns(4,5)P_2. Modified from Delmas and Brown 2005.

In adult animals, the systemic administration of a single ip dose (360-400 mg/kg) can trigger SE within 1 hour and mortality rates range around 30-40% (Curia et al. 2008). Different pretreatments have been used by combining PI with other drugs including lithium, N-methylscopolamine or diazepam. Lithium, usually administered 24 h prior to PI, allows the use of lower doses of chemoconvulsant to induce SE (Honchar et al. 1983). Antimuscarinic drug N-methylscopolamine minimizes the peripheric effects of PI by blocking muscarinic receptors outside of the CNS (Clifford et al. 1987). Use of diazepam prevents the development of behavioral and EEG alterations and reduce the duration of seizures induced by PI (Turski et al. 1984).

1.3 Ion channels and epilepsy

Common to other neurological diseases, inherited defects in neuronal ion channels genes controlling neuronal excitability have been associated to epilepsy

(Lamas 2005; Ryan and Ptáček 2010). Ion channels are pore-forming proteins that allow the flux of ions –mainly potassium (K^+), sodium (Na^+), chloride (Cl^-) and calcium (Ca^{2+})– across plasma and organelle membranes generating and modulating electrical signals in living cells of excitable tissues. They respond to various stimuli including membrane voltage and ligand binding (Hille 2001; Alexander et al. 2010). Thus, in the nervous system, they are responsible for action potentials and cell-to-cell communication by synaptic transmission. Genetic mutations in ion channels affecting their functionality have been associated to different types of inherited epilepsy. Genetic-caused dysfunction of ion channels (also known as channelopathies) can be due to mutations in encoding genes of diverse ion channels including Na^+, K^+, Ca^{2+} and Cl^- channels (Lerche et al. 2001; Lerche et al. 2013). Table 3 summarizes the list of genes and the corresponding proteins mutated in some idiopathic epilepsies and epileptic encephalopathies.

Voltage-gated K^+ channels (Kv)

K^+ channels conform the largest and most diverse family of ion channels and show a high heterogenicity of functions as well as regulation of intrinsic electrical properties of cells. Among voltage-gated K^+ channels (Kv), Kv7 channels are encoded by the *KCNQ* genes and comprise five members (Kv7.1-5) with major roles in cardiac muscle (Kv7.1), inner ear (Kv7.4) and neuronal function (Kv7.2, Kv7.3 and Kv7.5) (Figure 6). Kv7 channels conduct an outwardly directed current, whose function is associated to hyperpolarization and stabilization of the membrane potential. Mutations in their encoding genes are related to different diseases as shown in Table 4.

Structurally, all members share the same organization consisting of tetramers of alpha subunits. Each of these subunits contains six transmembrane segments (S1-S6). The regions S1-S4 constitute the voltage-sensor domain whereas S5-S6 forms the ion-selective pore (Brown 2008; Soldovieri et al. 2011). Importantly, accessory ß subunits are found in some physiological structures including Kv7.1/KCNE1, a very well described combination that gives place to the characteristic slow Kv7.1 opening in the cardiac muscle (Barhanin et al. 1996). Mutations in this subunit or inadequate interactions are related to heart disease (Olesen et al. 2012; Rothenberg et al. 2016).

Table 3. Genes and proteins mutated in idiopathic epilepsies encephalopathies. Modified from Lerche et al. 2013 (see full references therein).

	Abbreviation	Gene	Protein	References
Idiopathic focal epilepsies				
Bening familial neonatal seizures	BFNS1/EBN1	KCNQ2	Kv7.2 (K^+ channel)	Biervert et al. 1998 Singh et al. 1998
Bening familial neonatal-infantile seizures	BFNS2/EBN2 BFNIS	KCNQ3 SCN2A	Kv7.3 (K^+ channel) Nav1.2 (Na^+ channel)	Charlier et al. 1998 Heron et al. 2002 Berkovic et al. 2004
Autosomal dominant nocturnal frontal lobe epilepsy	ADNFLE	CHRNA4 CHRNB2 CHRNA2	α_4 subunit (nACh) receptor β_2 subunit (nACh) receptor α_2 subunit (nACh) receptor	Steinlein et al. 1995 De Fusco et al. 2000 Aridon et al. 2006
Idiopathic generalized epilepsies and associated syndromes				
Childhood absence epilepsy with febrile seizures	CAE+FS	GABRG2	γ_2 subunit ($GABA_A$ receptor)	Wallace et al. 2001
Absence epilepsy and episodic ataxia	CAE+EA2	CACNA1A	$Ca_v2.1$ (Ca^{2+} channel)	Jouvenceau et al. 2001; Imbrici et al. 2004
Juvenile myoclonic epilepsy	JME	GABRA1	α_1 subunit ($GABA_A$ receptor)	Cossette et al. 2002
Genetic (generalized epilepsy with febrile seizures plus (GEFS+)	GEFS+	EFHC1 SCN1A SCN1B GABRG2	EF hand motif protein Nav1.1 (Na^+ channel) β_1 subunit (nACh receptor) γ_2 subunit ($GABA_A$) receptor	Suzuki et al. 2004 Escayg et al. 2000 Wallace et al. 1998 Baulac et al. 2001
Generalized epilepsy and paroxismal dyskinaesia	GEPD	KCNMA1	$K_{Ca}1.1$ (K^+ channel)	Du et al. 2005
Epileptic encephalopathies				
Dravet síndrome (severe myoclonic epilepsy of infancy)	SMEI	SCNA1	$Na_v1.1$ (Na^+ channel)	Claes et al. 2001
Other syndromes				
Focal epilepsy and episodic ataxia	EA1+FE	KCNA1	Kv1.1 (K^+ channel)	Zuberi et al. 1999

In CNS, Kv7.2 and Kv7.3 subunits co-assemble to form a tetramer that underlies the M-current (Brown and Adams 1980; Wang et al. 1998). Kv7.4 and Kv7.5 are also associated with the M-current, although to a lesser extent (Kubisch et al. 1999; Lerche et al. 2000; Schroeder et al. 2000; Shah et al. 2002). M-channels are active at subthreshold membrane potentials (near -60 mV). Their activation is slow and therefore they do not contribute to the repolarization of individual action potentials. Also, they do not inactivate, therefore generating a steady voltage-dependent outward current that

leads to the stabilization of the membrane potential, contributing to the resting membrane potential (RMP). Thus, M-current plays a critical role in regulating the electrical excitability of neurons, determining their firing properties and responsiveness to synaptic input (Brown and Adams 1980; Wang et al. 1998; Brown and Passmore 2009). The relevance of their functionality is demonstrated by the negative effects of mutations on their encoding genes. Mutations in *KCNQ2* and *KCNQ3* (Table 3) have been associated to a long list of hyperexcitability phenotypes including benign familial neonatal epilepsy (BFNE) and neonatal epileptic encephalopathy (NEE) (Singh et al. 1998; Singh et al. 2003; Soldovieri et al. 2014; Nappi et al. 2020). BNFE is a dominantly inherited condition affecting newborns and characterized by the occurrence of focal, multifocal, or generalized seizures. Risk of later acquired epilepsy is around 15%, which is clearly higher than that for the general population (Ronen et al. 1993; Plouin, P; Anderson 2005). In NEE, encephalopathy is present from birth and persists during a period when seizures are uncontrolled leading to developmental impairment. Cessation of seizures generally occurs between age nine months and four years (Miceli et al. 2010).

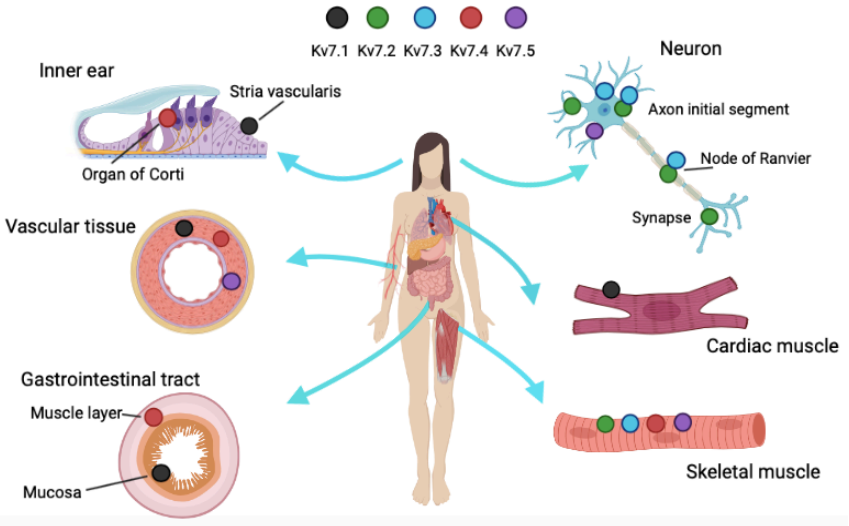

Figure 6. Tissue distribution of Kv7 subunits. The different panels in the figure report the principal sites of expression of each Kv7 channel subunit. Modified from Soldovieri et al. 2011.

Modulation of M-current constitutes a potential target to treat epilepsy and other diseases driven by neuronal hyperexcitability, such as neuropathic pain, ischemia and schizophrenia (Wulff et al. 2009). In fact, a number of pharmacological tools have been identified which modulate M-current. Among them, retigabine and flupirtine prevent convulsant activity both in animal models and clinical trials (Wickenden et al. 2004). However, due to drug-induced liver injury by flupirtine and alterations in tissue pigmentation, including the retina, by retigabine, both drugs have been recently discontinued from therapeutic use (Michel et al. 2012; Clark et al. 2015; Surur et al. 2019). Since adverse effects are not related to the mechanism of action, it seems promising to continue studying the potential role of Kv7.2/3 as effective targets for new anticonvulsant treatments (Surur et al. 2019). In line with this idea, our group has described a new M-channel modulator, the neuronal kinase SGK1.1 (Miranda et al. 2013), which is the protagonist of this thesis.

Table 4. Kv7 subunits: location, channel function and channelopathy. Modified from Brown 2008.

SUBUNIT	MAIN LOCATION	CHANNEL/CURRENT	FUNCTION(S)	DISEASE MUTATION
Kv7.1	Heart	Delayed rectifier I_{Ks}	Repolarizes action potential	Long QT-syndrome (RWS)
	Cochlea		Potassium transport	Congenital deafness (JLNS)
Kv7.2	Brain, ganglia	M-current $I_{K(M)}$	Controls excitability	Epilepsy (BFNE)
Kv7.3	Brain, ganglia	M-current $I_{K(M)}$	Controls excitability	Epilepsy (BFNE)
Kv7.4	Cochlea Smooth muscle	OHC K^+ current I_{Ks}	Potassium transport RMP	Deafness (DFNA2)
Kv7.5	Brain Skeletal and smooth muscle	M-current Vascular muscle K^+ current	Controls excitability RMP	None

BFNE, Benign Familial Neonatal Epilepsy; DFNA2, dominant progressive hearing loss; JLNS, Jervill and Lange-Nielsen Syndrome; OHC, outer hair cell; RWS, Romano-Ward Syndrome; RMP, Resting membrane potential

1.4 Serum and glucocorticoids-regulated kinase 1 (SGK1)

SGK1 was originally described as a serine/threonine kinase induced by serum and glucocorticoids in mouse breast cancer cells (Webster et al. 1993). The *Sgk1* gene spans around 118 kb with exons 1-16 yielding three different transcripts designated as SGK1, SGK1.1 and SGK1.2 (Figure 7). They all share identical catalytic domain and

COOH-terminal hydrophobic motif (exons 6-16) and differ in their NH_2-terminal domain (Arteaga et al. 2008), generated by alternative splicing and different transcription start sites from independent promotors that respond to different stimuli. For instance, the presence of a glucocorticoid-responsive element (GRE) in intron 4 controls the transcription of the canonical SGK1 isoform, whose mRNA levels are upregulated by glucocorticoids (Itani et al. 2002). Thus, alternative transcription sites and alternative splicing producing differential NH_2-termini confer specific properties to each splice isoform, including tissue-specific expression, different transcriptional regulation and different subcellular localization and protein stability.

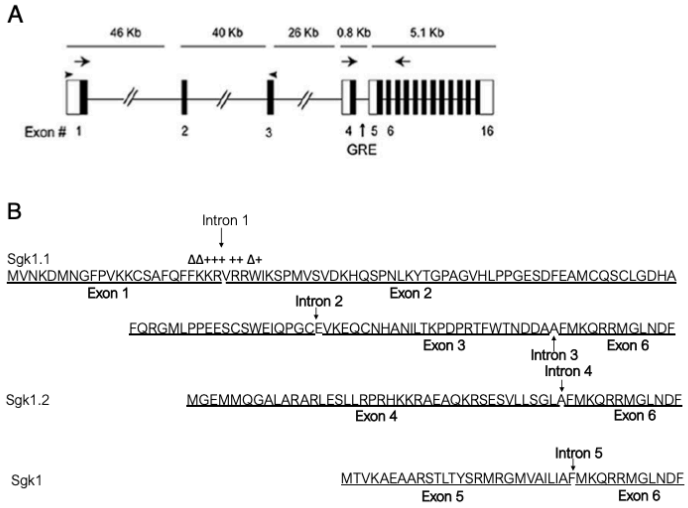

Figure 7. Sgk1 gene illustration. (A) The *Sgk1* genes spans approximately 118 kb; white and black boxes indicate 5' and 3' untranslated regions and exons and lines represent introns. The gene produces at least three splice isoforms with corresponding promotors located upstream of exon 1, intron 3 and intron 4 for transcription of SGK1.1, SGK1.2 and SGK1 respectively. Arrows and arrowheads indicate sites of qPCR primers and the in-situ hybridization probe specific for the SGK1.1 isoform. (B) Amino acid sequence of the three isoforms showing the N-termini. Intron-exon boundaries are indicated with arrows. Polybasic motif (+) with large hydrophobic residues (Δ) is shown above SGK1.1 protein. Modified from Arteaga et al 2008.

Sgk1 protein products belong to the AGC family of kinases that also include protein kinase A (PKA) and protein kinase B (PKB/AKT). Their catalytic domain shares high homology (45-55%) to AKT, $p70^{S6K}$ and protein kinase C (PKC) (Kobayashi et al. 1999). The shortest isoform, known as SGK1, is ubiquitous, and exerts diverse functions

including the control of membrane protein trafficking and cell survival. One of its best characterized roles takes place in the kidney, where SGK1 modulates transepithelial Na^+ reabsorption and thus blood pressure by regulating membrane abundance of epithelial Na^+ channel (ENaC) (Alvarez de la Rosa et al. 1999). The underlying mechanism involves SGK1-dependent phosphorylation and subsequent inactivation of the ubiquitin-ligase Nedd4-2, which in normal conditions ubiquitinates the channel by interacting with PY motifs, targeting it for degradation (Alvarez de la Rosa et al. 1999; Debonneville et al. 2001; Kamynina and Staub 2002). The SGK1/Nedd4-2 pathway regulates the endocytosis of other channels including ClC2 (Palmada et al. 2004), Kv1.3 (Palmada et al. 2004), Kv7.2/3 (Schuetz et al. 2008) and Kv7.1 (Andersen et al. 2013). Other downstream targets of SGK1 include GSK3β and FoxO proteins. This last pathway results in the inactivation of FoxO3a and therefore confers SGK1 an important role in promoting cell survival and reducing apoptosis (Brunet et al. 2001; Ferrelli et al. 2015). Furthermore, it has been suggested that SGK1 participates in diverse brain pathologies, mainly based on its overexpression under certain circumstances, including ischemia (Zhang et al. 2014), Parkinson's disease, amyotrophic lateral sclerosis (Schoenebeck et al. 2005) and Rett syndrome (Nuber et al. 2005). Altogether, this data suggests important roles for SGK1 in the control of brain function although further studies should be performed to determine its implications.

SGK1 is tightly regulated by a variety of stimuli, including steroid hormones, stress conditions, growth factors and glucose, inducing its rapid transcription in a tissue specific manner (Firestone et al. 2003). At the post-translational level, SGK1 is sequentially activated by phosphorylation on residues S422 and T253 by mammalian target of rapamycin 2 (mTORC2) and phosphatidylinositol-3-phosphate dependent kinase 1 (PDK1) (Kobayashi et al. 1999) (Figure 8).

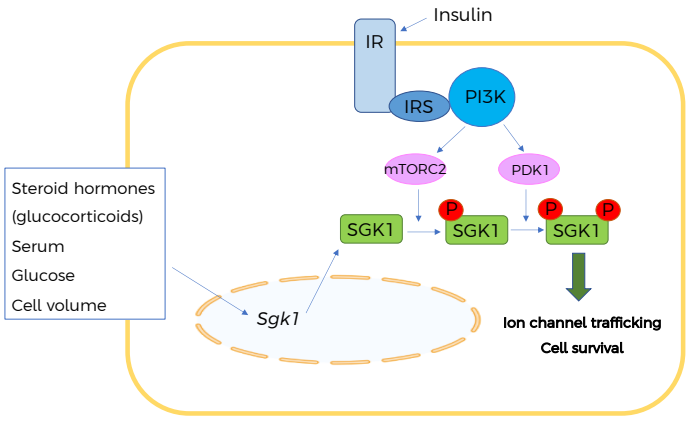

Figure 8. SGK1 regulation at transcriptional and post-transcriptional levels. Glucocorticoids, serum, glucose and cell volume are factors that stimulate *Sgk1* transcription. At post-transcriptional level, SGK1 might be double phosphorylated in residues S422 by mTORC2 and T253 by PDK1 in the IRS/IP3 pathway. IR: insulin receptor, IRS: insulin receptor substrate, PI3K: phosphatidylinositol 3-kinase, PDK1: phosphoinositide-dependent protein kinase 1, and mTORC2: mammalian target of rapamycin complex 2.

Isoform SGK1.2 expression is very low in all tissues and its function has not been further evaluated. SGK1.1 mRNA expression is restricted to brain tissue, where it is present in pyramidal neurons of hippocampus and cortex, although its specific subcellular localization has not been investigated in detail due to the lack of specific antibodies (Arteaga et al. 2008; Wesch et al. 2010). On the other hand, even though its distribution overlaps with SGK1 in the brain and its mRNA levels have been shown to be lower, SGK1.1 is the most abundant protein isoform in brain. This is explained by its greater stability due to the absence of the proteasomal degradation signal in the NH_2-terminus present in SGK1, which leads to rapid degradation by the ubiquitin/proteasomal system (Arteaga et al. 2006). Neuronal and ubiquitous isoforms share high structural similarity with similar activation and catalytic domains, which makes it possible that functional roles proposed for SGK1 in the brain are actually mediated by SGK1.1. However, it is important to notice that, unlike SGK1, SGK1.1 is not regulated by glucocorticoids as it does not present a GRE on its promoter region, which might imply that roles related to chronic stress in the nervous system are mediated by the ubiquitous isoform (SGK1) whereas other functions may be associated to SGK1.1 activity. Stimuli inducing SGK1.1 expression should be further investigated, although it

has been already demonstrated that its transcription is up-regulated upon cell depolarization (Arteaga et al. 2008). This mechanism is known to induce the expression of genes that are important for neuronal plasticity (West et al. 2001).

Another crucial aspect about SGK1.1 is the presence of a positively charged cluster of residues intercalated with bulky hydrophobic residues on its N terminus. These residues form a motif that binds PtdIns(4,5)P_2, tethering the kinase to the plasma membrane (Arteaga et al. 2008; Wesch et al. 2010). PtdIns(4,5)P_2 is one of the phospholipidic components of plasma membranes and it has been characterized as a crucial modulator of different ion channels and transport proteins (Hilgemann et al. 2001; Delmas et al. 2005; Suh and Hille 2005; Pérez-Burgos and Alamilla 2010), including the M-channel (Delmas and Brown 2005). With this, it is reasonable to expect important roles of SGK1.1 on neuronal channels function and expression. In fact, it has been already described how SGK1.1 is able to reduce the activity of neuronal-specific channel ASIC1 by reducing the channel membrane expression (Arteaga et al. 2008). Further, SGK1.1 is able to up-regulate the neuronal-enriched delta subunit of the epithelial Na^+ channel (ENaC) membrane expression and activity (Wesch et al. 2010). Both mechanisms are independent of PY motifs and may not involve Nedd4-2 phosphorylation.

1.5 SGK1.1 is a new modulator of M-channels

Our group has previously demonstrated that SGK1.1 up-regulates Kv7.2/3 function in heterologous expression systems including *Xenopus laevis* oocytes and HEK293 cells (**Figure 9**). Co-expression of Kv7.2/3 and SGK1.1 led to a significant increased Kv7.2/3 current in both systems without altering the kinetic properties of the channel (Miranda et al. 2013). Rather, the observed effect on channel activity was explained by increased channel membrane abundance, demonstrated by flow cytometry. Co-injection of Kv7.2/3 with an inactive mutant of SGK1.1, SGK1.1(K220A), or a mutant that neutralizes polybasic motifs at the N terminus, SGK1.1(K21N/K22N/R23G), did not produce significant changes in current levels, suggesting that the effect of SGK1.1 depends on its kinase activity and membrane localization (**Figure 9**). Therefore, it would be expected that the effect of SGK1.1 is

abolished by activation of phospholipase C (PLC) or inositol phosphatases, which transiently reduce PIP_2 levels at the plasma membrane. This effect, along with M-current modulation by muscarinic pathway, constitutes a convergent route that relies on PIP_2 levels for the regulation of neuronal excitability (Miranda et al. 2013).

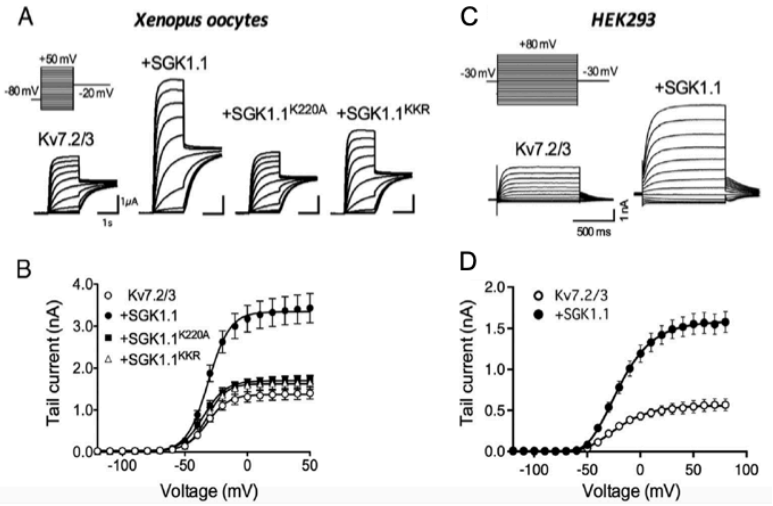

Figure 9. SGK1.1 increases Kv7.2/3 current in heterologous expression systems. (A) Currents elicited in Xenopus oocytes after co-injection of mRNAs from Kv7.2 and Kv7.3 alone (first panel) or in combination with wild type SGK1.1 (second panel), mutant SGK1.1(KKR) (third panel) or inactive mutant SGK1.1(K220A) (fourth panel). (B) Average activation curves and corresponding fits to Boltzmann equations (solid lines) for the indicated combinations. (C) Representative current families elicited in HEK293 cells transfected with Kv7.2 and Kv7.3 coding DNA with or without SGK1.1. (D) Average activation curves and corresponding fits to Boltzmann equations for the indicated construct combinations. From Miranda et al. 2013.

To evaluate the effect of SGK1.1 under physiological conditions, our laboratory developed a transgenic mouse model using a bacterial artificial chromosome (BAC) containing the whole *Sgk1* gene modified by homologous recombination in *E. coli* to introduce a mutation that renders the kinase constitutively active (S422D in SGK1 and S515D in SGK1.1). Transgenesis using this BAC induces gene expression controlled by endogenous promoters, generating the corresponding splice isoforms with their normal tissue-distribution pattern. Superior cervical ganglion (SCG) neurons isolated from transgenic mice (Tg.sgk1) showed enhanced M-currents compared to those in

control animals. Furthermore, decreased excitability and more negative resting potential were found in these neurons (Figure 10) (Miranda et al. 2013).

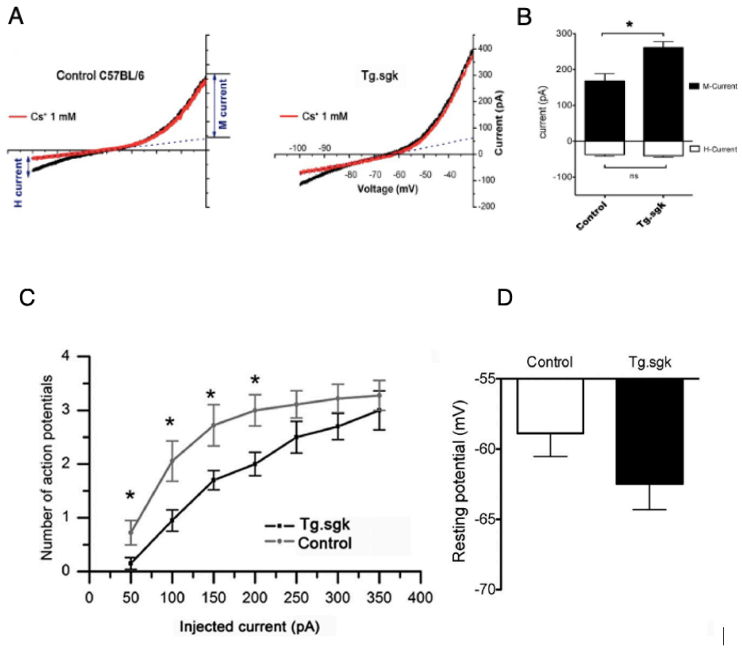

Figure 10. SCG neurons isolated from B6.Tg.sgk1 mice show a significant increase in M-current. (A) Representative voltage-ramp current responses elicited from SCG neurons isolated from control mice C57BL6/J (left panel) and B6.Tg.sgk1 (right panel) before (black line) and after (red line) adding 1 mM Cs^+. M-current amplitude at -30 mV was measured by subtracting the leak from the total current. The amplitude of the leak current (dotted line) was determined from extrapolated current-voltage (I/V) curves. (B) Average M-current (positive, black bars) and H-current (negative, white bars) in SCG neurons isolated from control mice (n=17) and from transgenic mice (n=21). (C) Representation of the average number of action potentials generated in response to stimulus of different amplitude (pA) for control (gray line) or Tg.sgk1 (black line) mice. Average resting membrane potential measured in SCG neurons from control (white bar, n=20) and transgenic (black bar, n=18). Error bars represent the SEM, *p<0.05. Modified from Miranda et at. 2013.

Lately, our group has published new results (Armas-Capote et al. 2020) revealing the potent anticonvulsant effect of SGK1.1 in our transgenic mouse model using the KA epileptic paradigm. We have demonstrated that the Tg.sgk1 mice are resistant to KA-induced seizures and show no lethality after acute SE (Figure 11).

Progression to more severe and convulsive stages (stage 4), was significantly reduced in B6.Tg.sgk1 mice compared to B6.WT. Also, a significant higher percentage

of B6.WT mice showed tonic-clonic seizures (stage 6) and around 30% of them reached stage 7 (SE-induced death), according to previous reports regarding kainic acid model (McLin and Steward 2006) and in contrast to the zero mortality rate found in transgenic mice (Figure 11).

Experiments with middle age and female mice were performed and proved that age and gender have minor influence on this phenotype with the more notable difference being mortality rates, that became similar between genotypes in middle age and female mice.

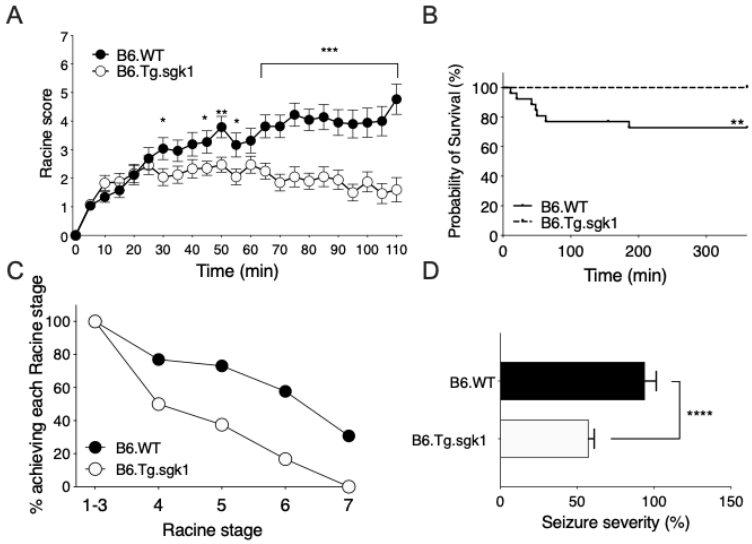

Figure 11. B6.Tg.sgk1 mice show reduced seizure severity and lower lethality after systemic administration of kainic acid. Seizure behaviour of B6.Tg.sgk1 (n=24) vs B6.WT (n=26) adult mice was evaluated after intraperitoneal injection of 20 mg/kg of kainic acid. Seizure activity was scored during monitored time (2 h) using a modified Racine scale (Racine 1972). A) Raw Racine scores represented as mean ± SEM each 5 min over the monitored time for both genotypes (Multiple t-test, *p<0.05, **p<0.01). B) Kaplan-Meier analysis in monitored mice. Survival of adult B6.Tg.sgk1 mice is significantly higher compared to rates observed in wild type animals (p=0.004, Log-rank (Mantel-Cox) test). C) Cumulative plot representing the percentage of mice reaching the indicated Racine stages. Stage 7 corresponds to death associated to SE. D) Average seizure severity score for WT and Tg.sgk1 mice. Values were calculated as the sum of all raw scores divided by the monitored time and represented as mean ± SEM (Unpaired t-test, ****p<0.0001). Modified from Armas-Capote 2017.

In addition, EEG recordings allowed our group to assess the impact of SGK1.1 on generalized seizures number (GS) and find that increased SGK1.1 activity reduces

the number and duration of GS without affecting its onset activity in hippocampus and cortex (Armas-Capote et al. 2020). Electrophysiological analysis of action potential characteristics and intrinsic membrane properties including resting membrane potential and membrane resistance was performed on CA1 pyramidal neurons from B6.Tg.sgk1 and B6.WT showing no significant alterations on these features, hence indicating that neuron response capacity is not changed in transgenic mice (Armas-Capote 2017).

The relevance of SGK1.1 activity on M-current up-regulation was evaluated in CA1 pyramidal neurons from hippocampal slices obtained from B6.WT and B6.Tg.sgk1 mice. This system has been widely used as a neuronal model to study the M current since its first use in 1982 (Halliwell and Adams 1982). In concordance with previous results in SCG neurons (Miranda et al. 2013), M-current amplitude was increased in CA1 pyramidal neurons from transgenic mice (Armas-Capote et al. 2020), an effect that was reversible when an SGK1-inhibitor was added to the medium. Consistently with the increase in the M-current, CA1 neurons showed significantly lower firing frequency upon depolarizing pulses (Figure 12).

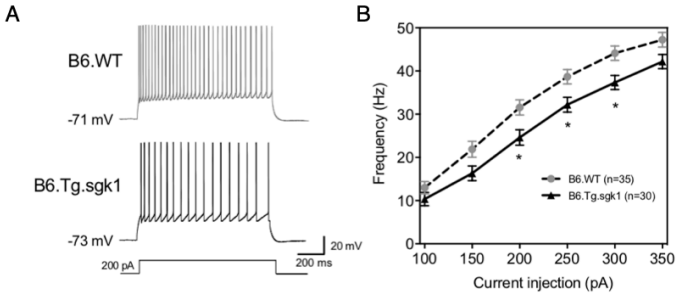

Figure 12. Reduced excitability in CA1 pyramidal neurons with increased SGK1.1 activity. (A) Representative traces recorded in CA1-PN after a 200 pA current injection in B6.WT (gray) and B6.Tg.sgk1 (black) mice. (B) Frequency-current relationships for CA1-PN from B6.WT (gray) and B6.Tg.sgk1 (black) mice. Multiple t-test *p<0.05.

Overall, these results suggest that the anticonvulsant role of SGK1.1 can be explained, at least in part, by up-regulation of M-current function and reduced neuronal excitability. Also, they have encouraged us to continue uncovering the potential role of SGK1.1 as a new therapeutic target for epilepsy. We now propose to further elucidate

the M-current up-regulation as the key mechanism underlying the observed protection against seizures.

1.6 SGK1.1 as a neuroprotective factor

On the basis of SGK1 and SGK1.1 isoforms sharing their catalytic domain, it is tempting to hypothesize that they might also be sharing some downstream substrates as the very well-known antiapoptotic factor AKT and SGK1 do. As previously mentioned, the ability of SGK1 to phosphorylate FoxO family members has already been described and related to the pro-survival and anti-apoptotic roles of SGK1. Some of these studies suggest that SGK1 could be modulating the cellular response to growth factors along with AKT (Brunet et al. 2001) and reducing levels of hyperglycemia-induced apoptosis (Ferrelli et al. 2015) by regulating the apoptotic activity of FKHRL1 (or FoxO3A). Herein, we propose an evaluation of SGK1.1 downstream targets that might shed some light not only on its effect as an anticonvulsant but also on its potential as a neuroprotective factor upon SE-induced cellular damage in the brain. Different approaches have been used to evaluate neuroprotective roles in a seizure-induce damage condition. For example, the use of histochemistry to detect neuronal death along with evaluation of pro- and anti-apoptotic factors in the brain has allowed the description of Bim and Bcl-x_L as downstream targets of FoxO-3A and apoptotic modulators involved in damage caused by epilepsy (Kim et al. 2014). Altogether, this work has focused on uncovering a potential dual role of SGK1.1. First, its ability to up-regulate the M-current and second its potential as an anti-apoptotic factor.

HYPOTHESIS AND AIMS OF THE STUDY

2. HYPOTHESIS AND AIMS OF THE STUDY

We hypothesized that activation of SGK1.1 plays a regulatory role protecting against epileptic seizures, via two mechanisms. On one hand, it reduces excitability through up-regulation of Kv7 neuronal channels. Secondly, it acts as a neuroprotector in the context of epilepsy-induced neuronal damage. Therefore, activation of SGK1.1 may constitute a potent therapeutic target for epilepsy through its dual mode of action.

The main goal of this project was to identify the molecular mechanisms underlying the protective role of SGK1.1 as anti-convulsant and neuroprotector.

Specific aims are detailed next:

Aim 1. To uncover the mechanisms underlying SGK1.1-mediated protection against seizures

1.1 Further unveil the role of the M-current up-regulation by SGK1.1 on its anticonvulsant effect.
1.2 Characterize SGK1.1 antiepileptic effect using the pilocarpine model as a new seizure paradigm in the Tg.sgk1 animal model.

Aim 2. To assess the potential of SGK1.1 as a neuroprotective factor in the context of epilepsy-induced brain damage

2.1 Study the mechanisms of SGK1.1-dependent protection against seizure-induced neuronal death.
2.2 Elucidate the effect of epileptic seizures on glial cell activation processes in both wild type and transgenic mice.
2.3 Determine the impact of SGK1.1 activation on ectopic neurogenesis.

Aim 3. To characterize the ability of SGK1.1 to modulate different Kv7 channel combinations and epileptogenic mutations:

3.1 Study the ability of SGK1.1 to up-regulate channels formed by different Kv7 subunits
3.2 Evaluate the effect of SGK1.1 in presence of epilepsy mutants Kv7.2(R207W) and Kv7.2(A306T)

MATERIAL AND METHODS

3. MATERIAL AND METHODS

3.1 Statistical analysis

Statistical analysis was conducted using Graph Pad Prism Version 8. Prior to perform any statistical analysis, we assessed normality distribution of our data using D'Agostino-Pearson test or Shapiro-Wilk normality test. Once determined, we compare means of data using Student t-test, One-Way ANOVA or Two-Way ANOVA test for parametric distributions. For non-parametric distributions, we performed tests as Mann-Whitney or Kruskal-Wallis.

3.2 Animals

All the experimental procedures and animal handling have been approved by Universidad de La Laguna Ethics Committee and conform to Spanish and European guidelines for protection of experimental animals (RD53/2013; 2010/63/EU).

Transgenic mouse model (B6/FVB.Tg.sgk1)

This work is based on the use of a transgenic mouse model generated in our laboratory, B6.Tg.sgk1 (Miranda et al. 2013). Briefly, the transgenic line was created by pronuclear injection of C57BL/6J x SJL/J F2 embryos with a BAC containing the whole *Sgk1* gene carrying a point mutation (S422D in SGK1; S515D in SGK1.1) that renders the kinase constitutively active (**Figure 13**). Founder animals were crossed with wild type C57BL/6J for at least nine generations. All experiments described here were performed in homozygosis for the transgene obtained by crossing heterozygous animals. Wild type mice (B6.WT) were used as controls.

Figure 13. Schematic representation of the 3' end of Tg.sgk1 mRNA isoforms. It includes a triple HA tag (dark grey box) and a point mutation S422D/S515D that renders the kinase constitutively active (asterisk). Arrows indicate oligonucleotides used to detect the expression of endogenous and transgenic kinase (sequence indicated in table 5). Cross hatched box indicates the 3' untranslated region of the transcripts.

In order to obtain the transgenic genotype in a different genetic background, we backcross bred our B6.Tg.sgk1 mice into a FVB/NJ background for nine generations. We then crossed the heterozygous mice to obtain a homozygous FVB.Tg.sgk1 colony. FVB/NJ is a strain defined as more susceptible to seizure disorders, so a more severe convulsive phenotype would be expected.

Table 5. Oligonucleotides used throughout this work and their sequences. Sequences in blue and red correspond to restriction enzymes sites and bold corresponds to a stop codon.

OLIGO	SEQUENCE	PURPOSE
GST-Seq	5'-GGGCTGGCAAGCCACGTTTGGTG-3'	ANTIBODY SGK1.1
SGK1.1_F2 Nterm Cloning-F	5'-GCCGGATCCCCCAACTTGAAGTACACTGGCCC-3	
SGK1.1_ F2 Nterm Cloning-R	5'-CATGCGAATTC**TCA**TGGAGGGAGCATCCCCCTTGG-3'	
SCREEN-F SGK1	5'-GGA AGC AGC AGA AGC CTT CCT CGG-3'	GENOTIPING
SCREEN-R SGK1	5'-GAC TGC CAA GCT TCC AGG TGT GC-3'	
F-Sgk1 gRNA ex6	caccgCTTCTTGAAAGTGATCGGAA	CRISPR II
R-Sgk1 gRNA ex6	aaacTTCCGATCACTTTCAAGAAGc	
F-Sgk1 gRNA ex8	caccgGTCCTGGACTACATTAATGG	
R-Sgk1 gRNA ex8	aaacCCATTAATGTAGTCCAGGACc	
F-Check Sgk1 mouse	GTAAGGCTGTGTGCAGCGTA	
R-Check Sgk1 mouse	TCAAACCCAAACCAAGCAAT	
F-Sgk1 Check_human	AGCCAAGTCCTTCTCAGCAA	
R-Sgk1 Check_human	GGTAACATTCTCCCCACCAA	
KCNQ2 _R207W_F	GCAGATTCTGTGGATGATCCGCATG	*KCNQ2* MUTAGENESIS
KCNQ2 _R207W_R	CATGCGGATCAACCACAGAATCTGC	
KCNQ2 _Seq	AGTTTGCCCGGAAACCGTTCTGTGT	
KCNQ2 _A306T_F	TCTCCTTCTTCACGCTGCCTGCAG	
KCNQ2 _A306T_R	CTGCAGGCAGCGTGAAGAAGGAGA	

Genotyping

Genotyping was performed for experimental groups by PCR analysis of genomic DNA using primers (Table 5) flanking *Sgk1* stop codon and producing a 186 bp product with wild type *Sgk1* and a 267 bp product with transgenic *Sgk1*, attributable to the insertion of three consecutive copies of HA epitope. Figure 14 shows PCR products obtained from genomic DNA extracted by alkaline hydrolysis of mice tails from wild type or transgenic mice.

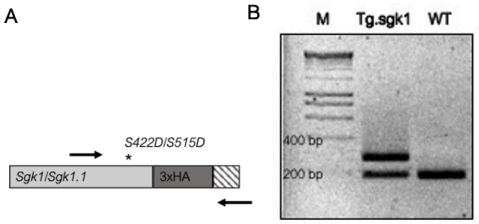

Figure 14. Genotyping. (A) Schematic representation of Sgk1 gene and location of the primers used for genotyping. (B) Agarose gel (2%) showing an example of PCR products for wild type Sgk1 (186 bp) and transgenic Sgk1 (267 bp). DNA from transgenic mouse contains both forms of the gene.

3.3 Epileptic paradigm and behavioral evaluation

Kainic acid administration and seizure behaviour evaluation

KA (Sigma, K0250-10MG) was freshly dissolved in isotonic saline pH 7.4 to a final concentration of 5 mg/ml. Status epilepticus was induced by intraperitoneal injection of KA 20 mg/kg in adult (4-5 months old) male mice. Dose response studies have defined seizure threshold in previous work from our lab (Miranda et al. 2013). Right after injection, a subset of adult B6.Tg.sgk1 and B6.WT mice were placed in clear glass cages and seizure behaviour was evaluated for 2 hours using a modified Racine scale (Racine 1972; Giménez-Cassina et al. 2012) explained in **Figure 15**. In addition to stages shown, we have included an extra stage (stage 7) corresponding to SE-induced death. Appropriate stages were assigned to every mouse each 5 min during the time of the experiment. Recorded parameters were: seizure progression during monitored time; survival rates and seizure severity scores. Differences in mortality rates between genotypes were evaluated using Kaplan-Meier estimator. Seizure severity scores were calculated as previously explained (Giménez-Cassina et al. 2012):

$$Seizure\ Severity = \Sigma\ (all\ scores\ of\ a\ given\ mouse)\ /\ time\ of\ experiment$$

The severity of all genotypes or conditions was normalized to WT mice (Giménez-Cassina et al. 2012).

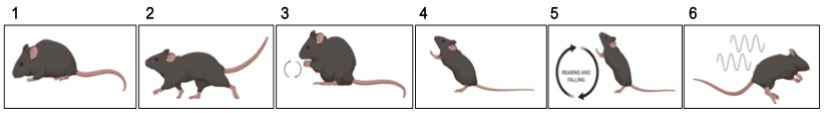

Figure 15. Seizure stages according to a modified Racine scale (Racine 1972). Stages of increasing severity used to characterize seizure behaviour. Illustrations of these stages are shown above: Stage 1: Immobility; Stage 2: Forelimb and/or tail extension, rigid posture; Stage 3: Repetitive movements, head bobbing; Stage 4: Rearing and falling; Stage 5: Continuous rearing and falling; Stage 6: Severe tonic-clonic seizures.

Kainic acid and XE991 double treatment

Previous work from our group demonstrated enhanced M-current activity in isolated SCG sympathetic neurons from B6.Tg.sgk1 leading us to hypothesize that up-regulation of the M-current is the mechanism underlying resistance to KA-induced seizures after SGK1 activation (Miranda et al. 2013). To confirm this hypothesis, we studied the seizure response in animals pre-treated with XE991 (Sigma Aldrich X2254), a specific M-current inhibitor. To that end, animals were ip injected with 10 mg/kg XE991 (Song et al. 2009) one hour prior to KA acid treatment. Seizure behaviour was valuated as described above.

Kainic acid and EMD638683 double treatment

As a new approach to further evaluate the role of SGK1.1 as an anticonvulsant in our transgenic mouse model B6.Tg.sgk1, we performed a behavioral test using the specific SGK1 inhibitor EMD638683 (MedChem Express HY-15193A) (Ackermann et al. 2011). Animals were ip injected with 1.6 mg/kg EMD638683 one day before KA injection. As described before, seizure behaviour was evaluated using Racine scale.

Pilocarpine administration and seizure behaviour evaluation

As part of our interest in studying the ability of SGK1.1 to protect mice against seizures, we used the PI model as a new epileptic paradigm. As shown in **figure 16**, 15 minutes prior to the experiment, a subset of adult B6.Tg.sgk1 and WT mice were ip injected with 1 mg/kg N-Methyl-scopolamine bromide (Sigma, S2250-1G) to block peripheral muscarinic receptors (Mazzuferi et al. 2012). Pilocarpine (Sigma, P6628-10G) was freshly dissolved in a dimethyl sulfoxide (DMSO): distilled water mix (1:9) to reach a final concentration of 40 mg/ml. Dose-response tests were performed (**Figure 23**) and a dose of 400 mg/kg was selected for the behavioral experiments. Right after ip injection, seizure progression was evaluated for 1 hour using the Racine scale. SE was terminated with 4mg/kg diazepam (Roche, 844241.6)

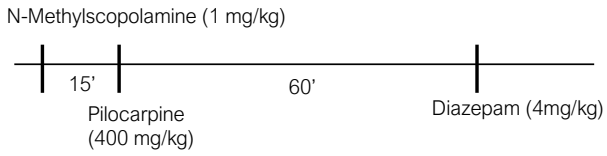

Figure 16. Schematic representation of pilocarpine model procedure. Before PI injection, animals are treated with N-Methylscopolamine to avoid peripheral effects. One hour later, seizure activity is terminated with diazepam.

3.4 Electrophysiology in brain slices

Intact hippocampal preparations of acute brain slices maintain much of the needed circuitry to generate electrographic seizures (Schwartzkroin 1986) and are thus very useful for studying the network activity under basal conditions, as well as after provoked seizures. In this study, we performed electrophysiological recordings in brain slices obtained from the animal model available in our laboratory and described previously. Brains from 4-6 weeks old male B6.WT and B6.Tg.sgk1 were dissected and perfused with ice-cold solution containing (in mM) 189 sucrose, 10 glucose, 26 $NaHCO_3$, 3 KCl, 5 $MgSO_4$, 0,1 $CaCl_2$, 1.25 NaH_2PO_4.. Coronal slices (350 μM) were obtained using a VT1000 vibratome (Leica). Before recording, slices were incubated for 1h at room temperature (22ºC) in artificial cerebrospinal fluid (ACSF) containing (in mM) 124 NaCl, 1.25 KH_2PO_4, 1,25 $MgSO_4$, 26 $NaHCO_3$, 10 glucose, 2 $CaCl_2$ and 0,4 ascorbic acid. ACSF was constantly bubbled with carbogen (95% O_2 - 5% CO_2). Whole-cell recordings were performed in CA1 pyramidal neurons (PN) with MultiClamp 700A (Molecular Devices).

Miniature inhibitory post-synaptic currents (mIPSC) were recorded at -70 mV in presence of tetrodotoxin (TTX, 1 μM), 7-nitro-2,3-dioxo-1,4-dihydroquinoxaline-6-carbonitrile (CNQX, 20 μM) and D-2-amino-5-phosphonovaleric acid (D-AP-5, 50 μM). TTX was added to block sodium channels, CNQX to block AMPA receptors and D-AP-5 to block NMDA receptors. The recording pipette was filled with an internal solution containing (in mM) 113 K-gluconate, 25 KCl, 10 HEPES, 0.2 EGTA, 4-Na-ATP and 0.3 Na_2GTP, pH 7.3 (320-340 mOsm; E_{Cl^-}: -42 mV). Miniature excitatory post-synaptic currents (mEPSCs) were recorded at -70 mV in presence of TTX (1 μM), picrotoxin (PiTX,

20 μM) and CGP-55845 (5 μM) in ACSF, and the recording pipette was filled with an internal solution containing (in mM) 130 K^+-gluconate, 8 KCl, 10 HEPES, 0.2 EGTA, 4 Na-ATP and 0.3 Na_2GTP, pH 7.3 (310-330 mOsm). In this case, PiTX was used to block GABA-activated chloride channels ($GABA_A$) and CGP-55845 to block $GABA_B$. Pipette resistance was in the range of 5-7 MΩ. Synaptic currents were filtered at 1 kHz (low pass), digitized (Digidata 1550B, Molecular Devices) and acquired by the pClamp software (Molecular Devices) with a computer. Cells were recorded for 10 minutes at room temperature (21-23 ºC). MiniAnalysis software was used for the analysis of the frequency and amplitude of mIPSCs and mEPSCs.

3.5 Western blot

Protein extracts were obtained by processing samples with lysis buffer TENT 1% (Tris-Base 0.5 M, pH 7.4, SDS 10%) containing phosphatase and proteinase inhibitors (Roche). Protein concentration was estimated using the bicinchoninic acid assay (BCA). Proteins were mixed with loading buffer and heated up to 95ºC for 5 minutes. After, they were separated by SDS denaturing gel electrophoresis (SDS-PAGE), transferred to a polyvinylidene fluoride membrane (PVDF) and analyzed by western blot (WB) using the specified antibodies. Chemiluminescence signals were analyzed using Image Lab® software 6.0 (Bio-Rad).

3.6 Antibodies

Primary antibodies: Antibodies against Bim (sc-374358) and Bcl-x_L (sc-8392) were obtained from Santa Cruz Biotechnology (Santa Cruz, CA); Parvalbumin (P3088) and GFAP (G3893) were obtained from Sigma-Aldrich; Bromodeoxyuridine (NBP2-14890) was obtained from Novus; Doublecortin (ab153668), Green Fluorescent Protein (GFP) (ab290), IBA-1 (ab5076), Kv7.2 (ab22897) and SGK1 (ab43606) were obtained from Abcam; NEDD4L (4013S), p-NEDD4L-S448 (8063S), p-NEDD4L-S342 (12146S), GSK3-β (9315) and p-GSK3αβ-Ser21/9 (9331) from Cell Signaling; HA (3F10) was obtained from Roche. Anti-SGK1.1 is a rabbit polyclonal antibody produced in our laboratory as described in the next subsection.

Secondary antibodies: Conjugated to Alexa Fluor®-488 (ab150141) was obtained from Abcam; Alexa Fluor®-594 (A-11005; A-11042) and Alexa Fluor®-488 (A-11008) were obtained from Thermo Fisher Scientific.

Generation of a specific SGK1.1 antibody

We designed and produced a specific antibody against a fusion protein between glutathione S-transferase (GST) and amino acids 41-80 from the SGK1.1-specific exon 2 (**Figure 17A**). The fragment of interest was amplified by PCR from mouse brain, analyzed by agarose gel electrophoresis and ligated to pGEX2T plasmid using BamHI and EcoRI (**Figure 17B**). Ligation reaction products were transformed into X-gold® (Agilent) bacteria following the manufacturer directions. DNA was extracted from transformed colonies with MACHEREY-Nagel NucleoSpin Plasmid Kit to analyse the presence of insert by PCR using F-GST-seq and R-Fr2 SGK1.1 as primers (**Table 5**). One of the positive colonies was used to inoculate 500 ml of LB medium. GST fusion protein expression was induced with isopropyl ß-D-1-thiogalactopyranoside (IPTG) 0.1 mM and protein was purified by affinity chromatography using glutathione-agarose beads in a column elution system, as previously described (Frangioni and Neel 1993). Eluates were analysed by SDS-PAGE electrophoresis to detect the fraction rich in proteins. This eluate was quantified using an albumin standard and diluted in phosphate-buffered saline (PBS) at 0.375 μg/μL. For rabbits' immunization, aliquots of 0.5 mL were mixed with 0.5 mL of complete or incomplete Freud adjuvant (Sigma) for the first and subsequent injections, respectively. A total of 6 immunizations were performed using New Zealand Rabbits acquired from the animal facility (SEGAI, ULL). Pre-immune serum was collected before the first immunization as control. Immune sera were collected after each immunization, beginning after the third immunization. The workflow to produce the antibody is summarized in **Figure 17D**.

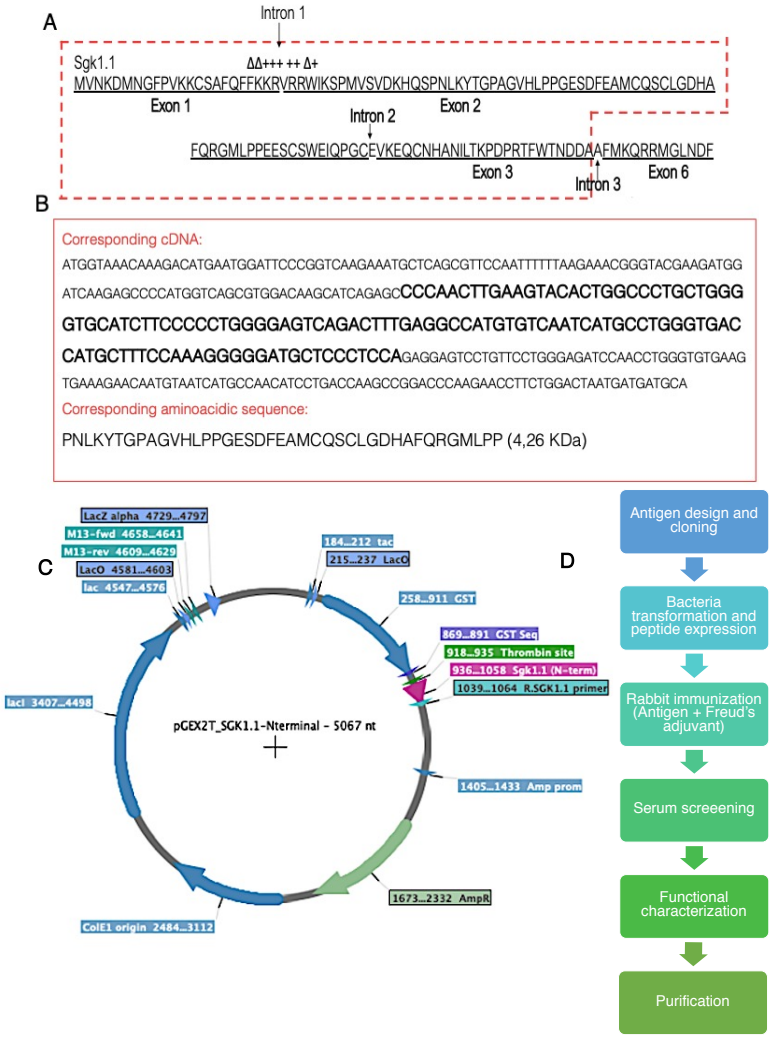

Figure 17. Design and production of anti-SGK1.1 antibody (A) Selected region corresponding to N-terminal domain of *Sgk1.1* gene is indicated by dotted line selection. (B) We selected the sequence in bold after performing antigenicity and solubility predictions in online platforms (PROSO, PROSO II, Spread and Predicted Antigenic Peptides Tool from the Universidad Complutense de Madrid) showing that this fragment of the codifying regions had the best properties to become an antigen. (C) pGEX2T includes an ampicillin resistance factor (light green) used to select and grow transformed bacteria and a lactose operon to control the expression of the GST fusion protein with IPTG. (D) First step includes epitope design and cloning in the appropriate vector. Bacteria transformation is required for expression and production of the protein of interest before purification of the GST-fused protein with glutathione. Rabbit immunization takes place each 3-4 weeks up to six injections. Finally, serum screening can be addressed by western blot or immunoprecipitation and purification of the final serum can be performed if necessary.

Denaturing immunoprecipitation

Protein extracts in 1% TENT from mouse brains were mixed with SDS 20% up to a final concentration of SDS 2% and heated up to 95 ºC for 4 min before overnight incubation with 1-2 µg of immunoprecipitation antibody (anti-SGK1.1) at 4 ºC. Then, protein-antibody complexes were bound to Protein G Magnetic Beads (EMD Millipore LSKMAGG02) for 1-2 h at room temperature. Beads were collected by centrifugation and washed twice with TENT 1%. Loading buffer was added to the pellets and magnetic beads were removed with a magnet before loading the proteins onto 10% acrylamide gels. Proteins were then transferred to PVDF membranes and probed with a monoclonal anti-HA antibody by western blot.

3.7 Brain damage analysis by histological procedures

Epileptogenesis leads to various biological changes including gliosis (Sofroniew 2014), uncontrolled inflammation (Vezzani et al. 2011), neurodegeneration (Dingledine et al. 2014) and aberrant neurogenesis (Jessberger and Parent 2015) among others. We were interested on evaluating the impact of these processes on mice surviving KA treatment and its different variants. Only mice reaching Racine stage 6 (generalized tonic-clonic seizures) were selected for the analysis, as it has been reported that the neuronal damage requires a threshold level of seizure intensity (Ben-Ari et al. 1980; Sperk et al. 1983; Ben-Ari 1985b). Most importantly, this design allowed us to directly assess SGK1.1 neuroprotective effect. Saline injected animals were used as controls. Three days after KA treatment, mice were deeply anesthetized (sodium pentobarbital, 40 mg/kg, ip) and perfused transcardially with saline (NaCl 0.9%) and paraformaldehyde (PFA 4%) in 0.1 M pH 7.4 PBS. Brains were carefully dissected and post-fixed in PFA for 24 hours at 4ºC before being transferred to sucrose 30% for cryoprotection overnight. Brains were kept at -80ºC until 30 µm thick coronal sections were obtained using a freezing microtome.

Neurodegeneration analysis by Fluoro-Jade C

Coronal slices were stained with Fluoro-Jade C (FJC), an anionic fluorochrome capable of selectively staining degenerating neurons in brain slices (Schmued et al. 1997). Neuronal degeneration was evaluated 72h after KA injection in WT and Tg.sgk1

mice following a previously described protocol (Afonso-Oramas et al. 2010). Briefly, selected slices were mounted onto 3-aminopropyltriethoxysilane (APS) coated slides and air-dried at RT for at least 12 hours. Slides were then immersed in 100% ethanol for 3 min, 70% ethanol for 1 min and distilled water for 1 min. They were then transferred to a 0.06% potassium permanganate solution for 15 min, rinsed with distilled water for 1 min and incubated in 0.001% FJC (HistoChem, Jefferson, AR) in 0,09% acetic acid for 30 min in dark conditions. Section were then were rinsed several times in distilled water, dehydrated, immersed in xylene and mounted with dibutylphthalate polystyrene xylene (DPX, Sigma M1289). Neurodegeneration was quantified in hippocampus, amygdalar complex, motor/visual cortex, somatosensorial/auditive cortex and piriform/entorhinal cortex using a confocal Leica TCS SP8 microscope. Nomenclature used for the different regions of the cortex varies depending on the bregma coordinates as shown in Figure 18. Five different sections were selected for each animal (from -1.355 to -3.08 in reference to Bregma, according to Allen Institute for Brain Science, 2014) providing a total of 5 individual values per region in each animal. Slices were mounted with DPX mounting solution. Images were taken with a confocal microscope (Leica TCS SP8) using 40X magnification and argon laser intensity of 15%. Image analysis was performed using ImageJ software. Measurements for all five sections were averaged to obtain one final measurement per region. Sections were also assessed qualitatively in other regions including thalamus, striatum and hypothalamus.

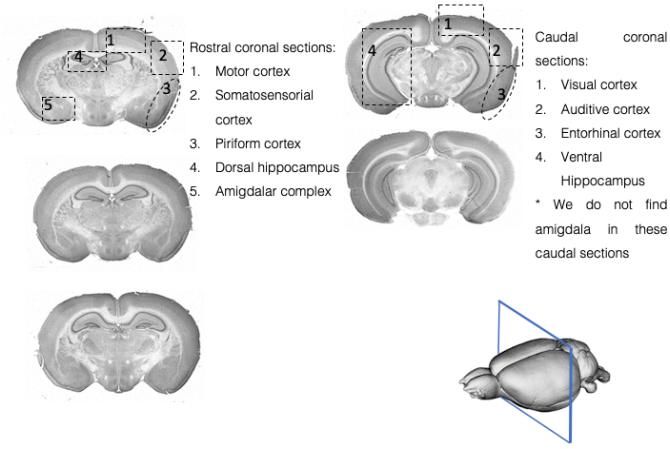

Figure 18. Coronal sections used for FJC analysis. 30 μm sections were obtained from rostral to caudal regions to scan the entire brain.

Gliosis evaluation by GFAP and IBA-1 immunohistochemistry

To assess the presence of reactive gliosis after KA injection, we measured expression of GFAP in astrocytes and IBA-1 in microglia on brain slices 72h post KA injection. One set of coronal sections (between -1.755 and – 2.155 mm from bregma) from the same mice previously analyzed for FJC was selected for evaluation of potential GFAP and IBA-1 changes after KA. Briefly, after three 5 min washes with PBS, sections were blocked with 4% goat serum for 1h before overnight incubation with 1:400 mouse anti-GFAP antibody or goat anti-IBA-1 antibody diluted in 2% goat serum. Sections were then washed 3-4 times in PBS before incubation with secondary goat anti-mouse Alexa Fluor® 594 antibody at 1:200 / rabbit anti-goat Alexa Fluor® 488 at 1:1000 for 2 hours. Finally, sections were washed and mounted with mowiol and DAPI for examination under confocal microscopy at 40x magnification. DPSS and Argon lasers were used to detect DAPI, green and red fluorescence.

3.8 Cell lines and transfection

HEK-293T (human embryonic kidney cells), HeLa (cervical cancer cells derived from Henrietta Lacks) and N2a (Neuro2A cells from mouse neuroblastoma) were obtained from American Type Culture Collection (Manassas, VA) and maintained in DMEM High Glucose (Biowest) supplemented with 10% fetal bovine serum (FBS), mycoplasm prevention reagent mycozap (Lonza) and antibiotics. Cells were transfected 24-48 hours before the experiment using Jetprime® (Polyplus Transfection, Illkirch) following the manufacturer's instructions.

3.9 Terminal deoxynucleotidyl transferase dUTP nick end labeling (TUNEL) Assay

To evaluate the potential anti-apoptotic role of SGK1.1, we performed the TUNEL assay (**Figure 19**) to quantify apoptosis after treatment with hydrogen peroxide (H_2O_2) using HEK293T cells. An empty vector (pECFP-N1) obtained from Clontech (#6900-1) was used as control. Fluorescently labeled SGK1.1 cDNA was generated by PCR and cloned into pECFP-N1 as described previously (Wesch et al. 2010). Cells were transiently transfected with constitutively active, nuclear and dominant negative mutants

of SGK1.1 (S515D, FF19,20AA, K220A respectively) obtained by Quick-change site-directed mutagenesis kit as described elsewhere (Arteaga et al. 2008; Wesch et al. 2010). SGK1.1 effects were compared to the well-known anti-apoptotic kinase AKT, which we used as positive control. Construct AKT-myr expressing a constitutively active form of AKT fused to a myristylation signal sequence was a gift from William Sellers (obtained from Addgene #9009 (Ramaswamy et al. 1999)). Cells were exposed to 1 mM H_2O_2 for 4h to induce apoptosis. TUNEL assays were performed according to the manufacturer's protocol (ApopTag® Fluorescein *In Situ* Apoptosis Detection Kit, Millipore, S7110). Apoptotic cells were detected as localized bright green nuclei in a blue background (DAPI) by confocal microscopy (Leica TCS SP8) at 63x magnification. Argon laser intensity was 15% for detection of blue and green fluorescence.

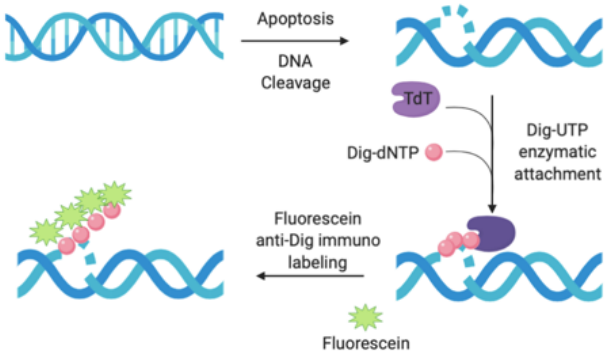

Figure 19. Schematic representation of the mechanism underlying TUNEL Assay. Briefly, this technique relies on the ability of the terminal deoxynucleotidyl transferase enzyme (TdT) to catalyze the addition of dUTP nucleotides to the free 3' ends of fragmented DNA in apoptotic cells. Commercial kits conjugate dUTPs to different tags such as digoxigenin (Dig) that can be easily recognized by secondary antibodies conjugated to fluorescent probes.

3.10 Neurogenesis quantification by bromodeoxyuridine immunohistochemistry

We tested the effect of SGK1.1 activation on ectopic neurogenesis using bromodeoxyuridine (BrdU) and doublecortin (DCX) markers on brain slices by immunohistochemistry. Mice injected with BrdU 150 mg/kg (Abcam, ab142567) were perfused with PFA 4% 24 hours after injection and 50 µm brain slices were obtained with a freezing microtome. After blocking with 1% bovine serum albumin (BSA), 1%

Triton X-100 in PBS and denaturalizing DNA with hydrochloric and boric acid (0.2N and 0.1M respectively), proliferating cells were detected with a rabbit anti-BrdU antibody at 1:500 and secondary anti-rabbit Alexa Fluor® 488 antibody at 1:1000 using confocal microscopy and 40x magnification. Number of proliferating cells in hilus (ectopic) and subgranullar layer (basal) of DG were quantified in transgenic and WT mice. Additionally, the amount of adult neuronal proliferation was evaluated by the presence of DCX+ neuroblasts in DG using a specific chicken anti-DCX antibody at 1:500 and a secondary anti-chicken Alexa Fluor® 594 antibody at 1:1000 (Chugh et al. 2015).

3.11 CRISPR/Cas9

We designed a model to knockout the expression of *Sgk1* gene in the mouse N2a cell line, using CRISPR-Cas9. CRISPR-Cas is a form of acquired immune response against viruses and their genetic material described in bacteria and archaea. E. Charpentier and J. Doudna proposed its application for editing the genome in 2013 (Charpentier and Dounda 2013). Since then, types and applications of CRISPR-Cas have expanded exponentially.

Breaking cas system (Oliveros et al. 2016) was used to design the guide RNAs (gRNAs) directed to exon 6 and exon 8 containing protospacer adjacent motif (PAM) ending regions (Figure 20A). Both exons are common to the coding regions of the ubiquitous *Sgk1* and the neuronal isoform *Sgk1.1*. Designed gRNAs (Table 6) were cloned separately in the BbsI site of pX459 vector (Addgene #62988), which also encodes Cas9 protein, ampicillin resistance for positive selection in bacteria and puromycin resistance for positive selection of transfected N2a cells.

N2a were transfected with both constructs (pX459-gRNA exon 6 and pX459-gRNA exon 8) using JetPrime®. After 36 hours, 3 µg/ml of puromycin were added. Surviving cells were split sufficiently diluted so individual colonies could be collected and expanded as clones. Genomic DNA from individual colonies was analyzed by PCR with oligos to detect gene rearrangements (Figure 20B). Protein extracts were analyzed by western blot to detect expression of SGK1 (Figure 20C).

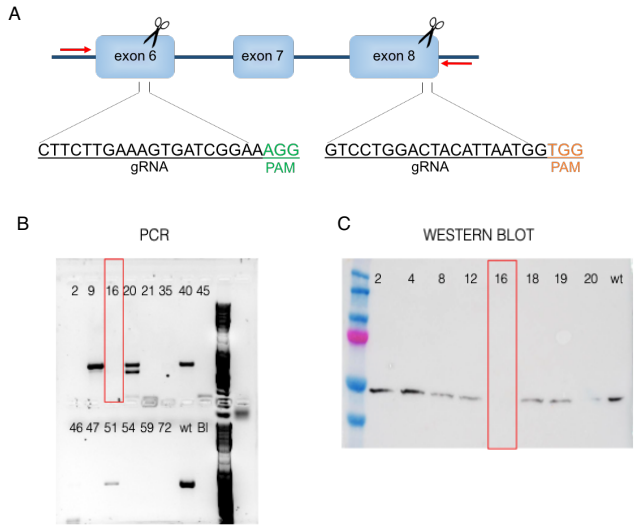

Figure 20. *Sgk1*-KO N2a cells generation by CRISPR/Cas9. (A) Sgk1 gene scheme. Arrows indicate place of hybridization of the guides and PAM sequences (NGG) required for Cas to cut the DNA are indicated in green and orange at the end of each targeted exon. (B) Screening PCR and (C) western blot to detect presence of *Sgk1* gene and SGK1 protein expression respectively. Clone 16 was designated as *Sgk1*-Knock out.

3.12 Immunocytochemistry

24 h after transfection, cells were washed with PBS^{++} ($MgCl_2$ 1 mM, $CaCl_2$ 0.1 mM) and fixed with formaldehyde (FA) 4% for 30 min. Then cells were incubated with permeabilization buffer containing 0.3% Triton and 0.1% BSA in PBS for 15 min before blocking with 10% normal goat serum in PBS. After blocking, cells were incubated with primary antibodies in blocking solution at 4ºC overnight. On the second day, cells were washed with PBS^{++} before incubation with secondary antibodies for 1h at RT and mounting with mowiol and DAPI.

3.13 Proximity Ligation Assay (PLA)

PLA technique allows detection of molecular associations between endogenous or heterologously-expressed proteins. This technique is based on the recognition of protein proximity by using one pair of primary antibodies tagged with DNA probes that only hybridize if the two proteins of interest are within a 40 nm radius. Interactions between different combinations of Kv7.2/3 channel subunits, SGK1.1 and Nedd4-2

were detected following the manufacturer protocol (Duolink, Olink Biosciences) using our newly developed rabbit anti-SGK1.1 antibody, mouse anti-GFP antibody for XFP-tagged Kv7.2 and Kv7.3 subunits and XFP-tagged SGK1.1, and rabbit anti-Nedd4-2 antibody. Experiments were performed on *Sgk1*-knockout N2a cells. Cells were transiently transfected with variants of SGK1.1, Nedd4-2, Kv7.2 and Kv7.3 on different combinations 24 hours prior to PLA assay using JetPrime®. Cells expressing SGK1.1(S515D) and NR1-GFP and cells expressing the channel subunits only, Kv7.2/3, were used as negative controls. The first condition was used to normalize and the latter was used for statistical comparisons.

Plasmids: pcDNA3.1 containing NMDAR1 (NR1) fused to YFP was obtained from Addgene (#17928). pSRC5 plasmids carrying human Kv7.2 and Kv7.3 tagged with CFP and YFP were kindly provided by Dr. Alvaro Villarroel (CSIC Institute of Biofisika, Vizcaya, Spain). Mutations in Kv7.2 were generated by site-directed mutagenesis using the oligos indicated in Table 6 and QuikChange kit according to manufacturer's protocol (Stratagene, San Diego, CA). Mouse SGK1.1 (wild type and constitutively active mutant S515D) cloned into pcDNA3.1/V5-His-TOPO (Invitrogen) were kind gifts from Dr. Cecilia Canessa (Yale University, New Haven, CT). Kinase-dead mutant K220A was obtained as described elsewhere (Wesch et al. 2010). All SGK1.1 constructs were also cloned into pECFP-N1 and pEYFP-N1 (Clontech) plasmids for their use in some conditions of the experiment.

Results were analyzed as average number of puncta/cell area using the software provided by the manufacturer (Duolink Image Tool).

3.14 Two Electrode Voltage Clamp (TEVC)

Channel subunit cRNA preparation and *Xenopus laevis* oocyte injection

TEVC is a very useful electrophysiological technique to test the functional effect of introduced mutations as well as the role of specific signaling components on ion channels function. We used this tool to evaluate the ability of SGK1.1 to modulate different Kv7 channel combinations. pSRC5 plasmids carrying human Kv7.2 and Kv7.3 were kindly provided by Dr. Alvaro Villarroel (CSIC Institute of Biofisika, Vizcaya, Spain) and pTLN plasmids carrying human Kv7.1, Kv7.3(A315T) and Kv7.4-5 as well as

KCNE1 cloned into pRAT were given by Dr. Geoffrey Abbott (University of California, Irvine, CA). pTLN plasmids incorporate Xenopus laevis β-globin 5' and 3' UTRs flanking the coding region to enhance translation and cRNA stability. SGK1.1 constructs were obtained as explained in the previous section. cRNA transcripts encoding human Kv7.1-5 were generated by *in vitro* transcription using the T7 or SP6 polymerase mMessage mMachine kits (Thermo Fisher Scientific). Transcription was performed after vector linearization, from cDNA. cRNA was quantified by spectrophotometry.

Xenopus laevis frogs were anesthetized with tricaine 1.7% (w/v) and ovaries were dissected and maintained in ND96 solution containing (mM): 96 NaCl, 2 KCl, 1 $MgCl_2$, 20 HEPES (pH 7.6) and antibiotic until oocytes were defolliculated with collagenase 1.63 mg/ml. After one-hour treatment with collagenase oocytes were placed in ND96 solution with 1.8 mM $CaCl_2$. Stage V and VI *Xenopus laevis* oocytes were injected with Kv7 channel α (and ß in the case of Kv7.1/KCNE1) subunit cRNAs (10 ng), alone or with SGK1.1 cRNA (10 ng). Oocytes were incubated at 16 ºC in ND96 solution with daily washing for 1-2 days prior to TEVC recording.

TEVC recordings were performed at room temperature with an OC-725C amplifier (Warner Instruments, Hamden, CT) and pClamp8 software (Molecular Devices, Sunnyvale, CA). Oocytes were placed in a small volume oocyte bath containing (mM): 96 NaCl, 4 KCl, 1 $MgCl_2$, 1 $CaCl_2$, 10 HEPES (pH 7.6) under a dissecting microscope. Chemicals were sourced from Sigma. Pipettes were of 1-5 MΩ resistance when filled with 3M KCl. Currents were recorded in response to pulses ranging between -80 mV and +40 mV at 20 mV intervals from a holding potential of -70 mV, followed by a -30 mV pulse (inset) to yield current-voltage relationships and current magnitude. TEVC data analysis was performed with Clampfit 10.6 (Molecular Devices).

RESULTS

4. RESULTS

SECTION 1: SEIZURE BEHAVIOUR

4.1 Tg.sgk1 mice show reduced seizure severity and lower lethality during acute KA-induced SE

As previously demonstrated, activation of SGK1.1 confers a significant protection against KA-induced seizures in B6.Tg.sgk1 mice (Miranda et al. 2013; Armas-Capote et al. 2020). Herein we show new sets of data that: a) demonstrate that pharmacological inhibition of SGK1 isoforms abrogates the protective effect of the kinase; b) clarify the key role of M-current up-regulation on this protective mechanism by SGK1.1; and c) show that the anticonvulsant effect of SGK1.1 is independent of genetic background. Seizure behaviour was evaluated using the Racine scale. For comparisons, some graphs show seizure behaviour of B6.Tg.sgk1 and B6.WT mice treated only with KA, data that have been already published and presented in a previous thesis from our laboratory (Armas-Capote 2017; Armas-Capote et al. 2020).

4.1.1 Inhibition of SGK1.1 by EMD638683 abolishes the protective effect of SGK1.1 after KA

EMD638683 is a highly selective inhibitor of SGK1 (Ackermann et al. 2011) that might counteract the protective effect of *Sgk1* activation in our transgenic mice when administrated prior to kainic acid treatment. As shown in **Figure 21**, inhibition of the kinase reverted the protective effect and abolished the differences in seizure behaviour between genotypes (Martin-Batista et al. 2021). The time course (**Figure 21A**), proportions reaching each Racine stage (**Figure 21C**) and seizure severity (**Figure 21D**) were similar between genotypes and mortality rates increased for both groups compared to animals treated only with KA (grey traces). However, survival rate of transgenic mice was significantly reduced (**Figure 21B**). About 60% of B6.Tg.sgk1 died after 120 min, whereas only 40% of B6.WT did. Although it is not clear why the two groups show these differences on lethality, it is important to point out the main finding

of this experiment: SGK1.1 enzymatic activity is the key mechanism underlying the protective effect observed in the KA model of epilepsy.

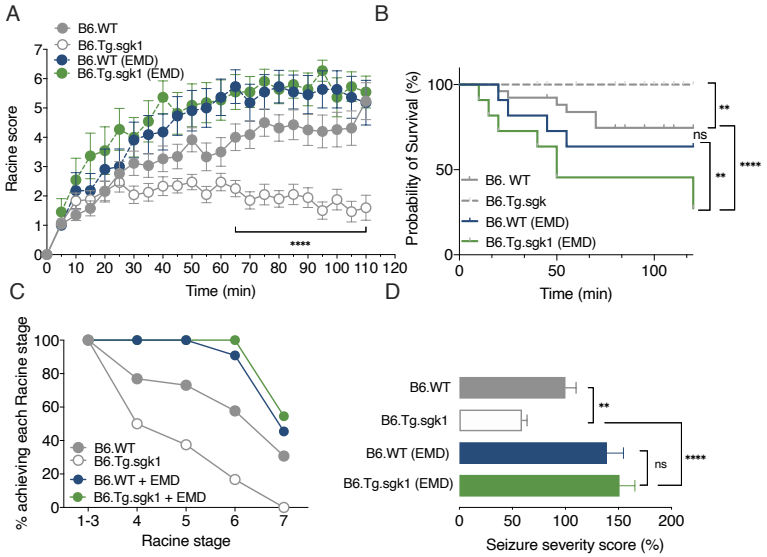

Figure 21. Inhibition of SGK1.1 with EMD638683 equalizes the seizure behaviour between genotypes. 4-5 months old B6 mice were ip injected with EMD638683 (1,6 mg/kg) and Kainic acid (20 mg/kg). Grey symbols represent the groups treated only with KA for comparisons. (A) Average of raw Racine stages was assigned to WT and Tg.sgk1 mice each five minutes during monitored time (Multiple t-test, B6.WT, B6.Tg.sgk1, n=26; B6.WT(EMD), B6.Tg.sgk1(EMD) n=21). (B) Kaplan-Meier survival analysis shows significant differences in mortality rates associated to KA seizure between genotypes (Log-rank Mantel-Cox test, **p<0.01, ****p<0.0001, ns not significant). (C) Cumulative plot representing percentage of mice reaching indicated Racine stages. For clarity, stages 1,2 and 3 (no generalized seizures) are grouped as '1-3' in the graph. (D) Mean seizure severity scores were assigned to B6.WT and B6.Tg.sgk1 mice. Values are mean ± SEM normalized to B6.WT. One-Way ANOVA with Sidak's correction, **p<0.01, ****p<0.0001, ns not significant.

4.1.2 Reduced seizure severity in B6.Tg.sgk1 mice depends on M-current activation

We evaluated the role of M-current up-regulation in the epileptic phenotype of transgenic mice by treating the animals with a specific M-current inhibitor, XE991. As shown in Figure 22, the protective effect of SGK1 activation was abolished in transgenic mice pre-treated with XE991. First, a higher percentage (80%) of B6.Tg.sgk1 mice reached Racine stage 6 (Figure 22C) compared to levels found with exclusive KA

treatment (16%). Also, lethality rates rose to around 50% in both genotypes, with no significant differences between them (Figure 22B). Seizure progression was also worse, with both groups following a tendency to more severe stages throughout the whole experiment, similarly to progression observed for B6.WT treated with KA only (Figure 22A). Accordingly, no differences in seizure severity were observed in WT *vs* transgenic mice after treatment with the inhibitor (Figure 22D). This result strongly suggests that up-regulation of M-current constitutes the mechanism underlying protection against SE driven by SGK1 activation (Martin-Batista et al. 2021).

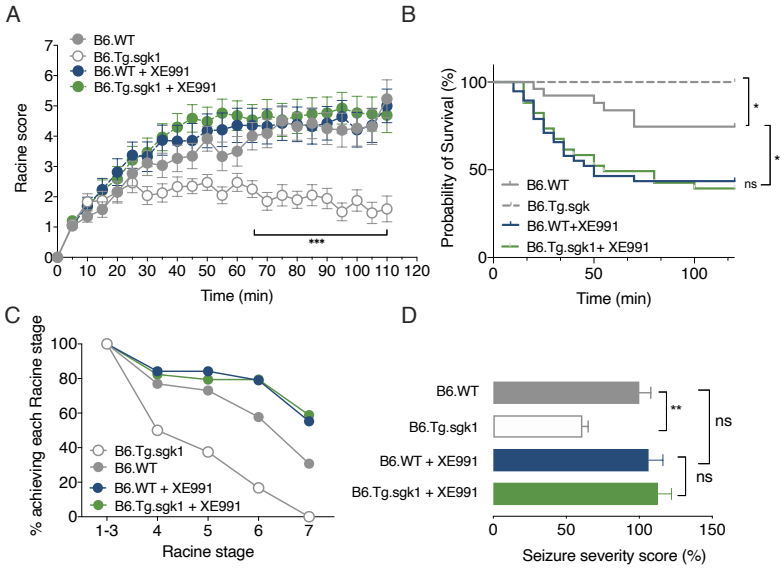

Figure 22. Tg.sgk1 mice show reduced seizure severity and mortality after systemic KA administration via M-current activation. Analysis of seizure behaviour after intraperitoneal KA injection in B6.WT (n=26), B6.Tg.sgk1 (n=26),B6.WT + XE991 (n=26) and B6.Tg.sgk1 + XE991 (n=24) male mice. (A) Raw Racine stage score (mean ± SEM) in 5 min intervals over the monitored period. Multiple t-test; ***p<0.0005. (B) Kaplan-Meier survival analysis of mice monitored for seizure activity. Differences in lethality are abolished after inhibition of the M-current with XE991. Log-rank (Mantel-Cox) test; *p<0.05; ns, not significant. (C) Cumulative plot representing the percentage of mice reaching the indicated Racine stages for B6.WT and B6.Tg.sgk1 before and after treatment with XE991. For clarity, stages 1,2 and 3 (no generalized seizures) are grouped as '1-3' in the graph. (D) Integrated seizure severity for both genotypes, with and without previous treatment with XE991. Values are mean ± SEM normalized to B6.WT. One-Way ANOVA with Tukey's correction; **p<0.01; ns, not significant.

To further examine the role of the M-current in SGK1.1-mediated protection against seizures, we used a different epileptic paradigm. PI is a muscarinic agonist whose mechanism of action involves activation of PLC and PtdIns(4,5)P_2 disruption from the plasma membrane, thus down-regulating the M-current. Therefore, we expected similar levels of seizure severity and lethality in both WT and Tg.sgk1 mice. After deciding which was the most appropriate dose of PI based on the reached seizure severity score (Figure 23), we performed the PI-based epileptic paradigm. As shown in Figure 24, progression in time did not yield average scores above 4. For wild type mice, SE-associated lethality was 13% (Figure 24B) and only 40% of them reached Racine stage 6 (Figure 24C). As expected, transgenic mice were not protected against PI-induced seizures. Time-course evolution was similar to wild type mice; animals were motionless for the first minutes after injection and subsequently progressed to more severe stages, in agreement with previous reports (Turski et al. 1983). Lethality rate scaled up to 15% and almost 50% of B6.Tg.sgk1 mice reached stage 6 (Figure 24B-C). In agreement with these observations, no differences in seizure severity scores were observed in WT *vs*. transgenic mice (Figure 24D). These observations further support our hypothesis that anticonvulsant role of SGK1.1 relies on M-current upregulation, which is inhibited upon activation of muscarinic receptors M_1 by PI.

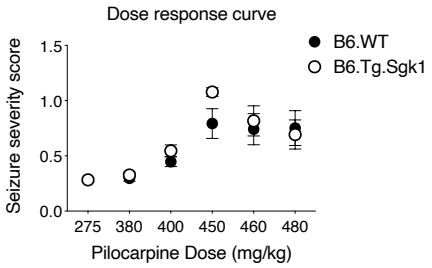

Figure 23. Different doses of pilocarpine (275-480 mg/kg) were evaluated according to the seizure severity score. Integrated seizure severity score was calculated for B6.WT and B6.Tg.sgk1 after treatment with PI at different doses in order to select the best dose regarding lethality rate and seizure severity. A final dose of 400 mg/kg was chosen for behavioral experiments.

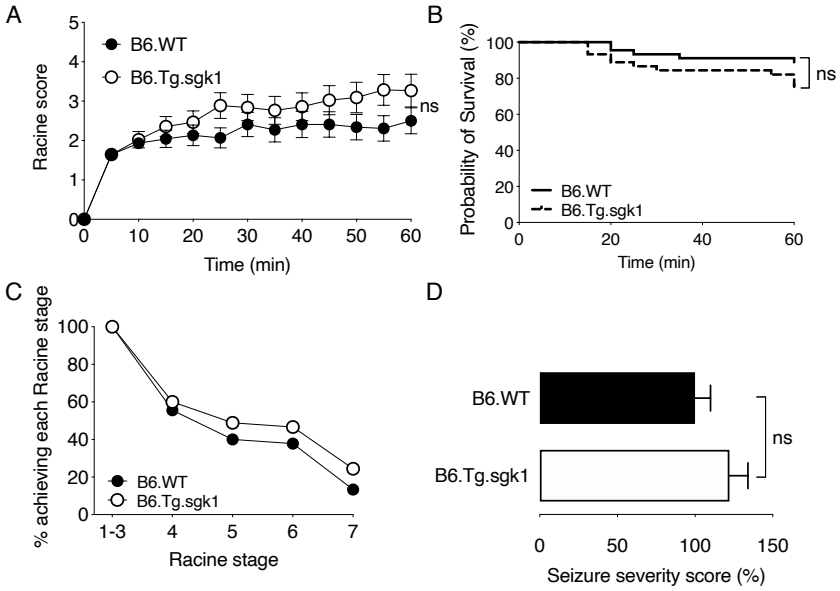

Figure 24. Activation of muscarinic pathway by pilocarpine abolishes the SGK1.1-mediated resistance to KA-induced seizures. A subset of B6.WT (n=45) and B6.Tg.sgk1 (n=45) mice were ip injected with N-methylscopolamine (1 mg/kg) 1 h prior to PI injection (400 mg/kg) for seizure behaviour evaluation using the Racine scale. (A) Raw Racine stages score (mean ± SEM) in 5 min intervals during the monitored period (Multiple t-test; ns, not significant). (B) Kaplan-Meier survival analysis showing the mortality rates associated to PI-induced seizures in both genotypes (Log-rank (Mantel-Cox) test; ns, not significant). (C) Cumulative plot showing the percentages of mice reaching indicated Racine stages for both genotypes. For clarity, stages 1,2 and 3 (no generalized seizures) are grouped as '1-3' in the graph. (D) Integrated seizure severity for both mice genotypes represented mean ± SEM normalized to B6.WT. (Unpaired t-test with Welsch's correction; ns, not significant).

4.1.3 SGK1.1-dependent protection against seizures is retained in FVB/NJ genetic background

It has been reported that the phenotype of genetically modified mice can be notably influenced by the genetic background in which the mutation is maintained. This effect can lead to alterations in, for instance, the susceptibility to seizure disorders (Schauwecker 2002). C57BL/6 strain has been extensively used as animal model, however its use in epilepsy research has been controversial due to its low sensitivity to various convulsant agents and the reported resistance to neuronal death processes

(Schauwecker 2000; McCord et al. 2008) although this seems to depend on experimental conditions (Zhang et al. 2012).

Previously, our laboratory has shown that the anticonvulsant effect of SGK1.1 is maintained in FVB mice (Armas-Capote 2017). However, the results referred to a reduced sample of animals that we have expanded in this work. Herein we show updated results supporting the previous finding that FVB.Tg.sgk1 mice are resistant to seizure activity progression. After injection, all mice reached Racine stage 1 during the first 5 minutes, similarly to C57BL6/J mice (data from Armas-Capote et al 2019). Progression to more severe stages was also fast, with an average Racine score above 3 at 30 minutes time point. However, FVB.Tg.sgk1 mice progressed to less severe seizure stages after 30 minutes in contrast to their WT counterpart, who suffered sustained tonic-clonic seizures until the end of the experiment (Figure 25A). SE lethality rate for transgenic mice kept unchanged (0%) while it slightly decreased for FVB.WT (20%) (Figure 25B) compared to 30% of B6.WT. Although this difference between genotypes is not significant (p=0.07), results suggest that activation of SGK1.1 also protects against death associated to SE in this genetic background. As shown in Figure 25C, a higher percentage of FVB.Tg.sgk1 mice (60%) reached stage 6, compared to B6.Tg.sgk1 (16%). This increase was also found in WT counterparts; 80 % of FVB.WT reached tonic clonic seizures compared to 60% of B6.WT. Nevertheless, transgenic mice remained protected against seizures, with less animals reaching stages 4-7. In agreement with this observation, quantification of the average seizure severity score showed significantly reduced severity in FVB.Tg.sgk1 mice (Figure 25D).

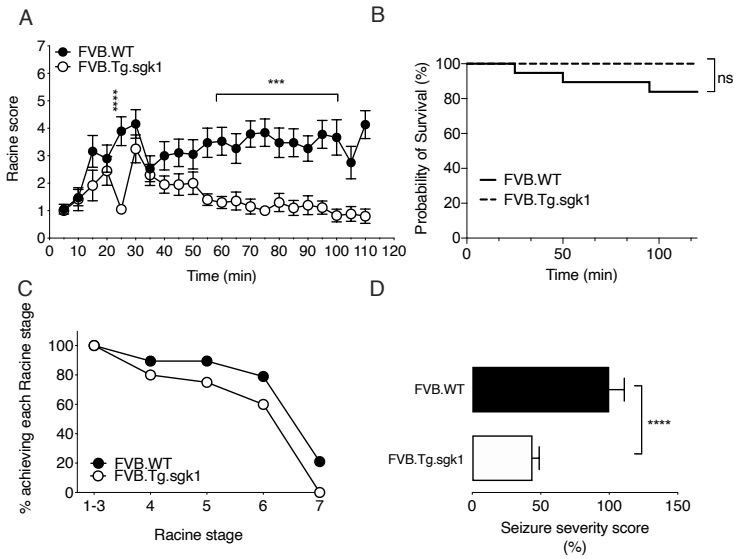

Figure 25. SGK1.1 protective role against KA-induced seizures is independent of genetic background. Analysis of seizure behaviour after intraperitoneal KA injection in FVB.WT (n=19) and FVB.Tg.sgk1 (n=20) male mice. A) Raw Racine stage score (mean ± SEM) in 5 min intervals for FVB mice of both genotypes. Multiple t-test; ***p<0.0005; ****p<0.0001. B) Kaplan-Meier survival analysis in monitored mice. Although lethality is higher for FVB.WT mice, difference with FVB.Tg.sgk1 is not statistically significant (p=0.07, Log-rank (Mantel-Cox) test). C) Cumulative plot representing the percentage of mice reaching the indicated Racine stages. For clarity, stages 1,2 and 3 (no generalized seizures) are grouped as '1-3' in the graph. D) Integrated seizure severity score for FVB.WT and FVB.Tg.sgk1. Seizure severity was significantly reduced in FVB.Tg.sgk1 compared to WT. Data are mean ± SEM. Unpaired t-test with Welch's correction; ****p<0.0001.

4.2 B6.Tg.sgk1 CA1 pyramidal neurons show unaltered basal synaptic transmission

As part of our interest in understanding the anticonvulsant effect of SGK1.1, we wondered if the basal transmission of our transgenic mice could be modulated by the transgene. Thus, we evaluated basal inhibitory and excitatory synaptic transmission in CA1-Pyramidal neurons (PN) from B6.WT and B6.Tg.sgk1 in basal conditions. As observed in Figure 26, we analyzed basal synaptic transmission by recording mEPSC (Figure 26A-D) and mIPSC (Figure 26E-H) in hippocampal CA1-PN. Our results demonstrate that activation of SGK1.1 in B6.Tg.sgk1 mice does not affect the frequency of mEPSC (Figure 26B) and mIPSC (Figure 26F). Moreover, we did not observe any

difference between genotypes on the amplitude of mEPSC (Figure 26C) nor mIPSC (Figure 26G) which suggests that SGK1.1 activation does not modulate levels of AMPA/NMDA (mEPSC) nor $GABA_A$ (mIPSC) postsynaptic receptors. Therefore, our data proves that both inhibitory and excitatory transmission is unaltered in transgenic mice (Armas-Capote et al. 2020).

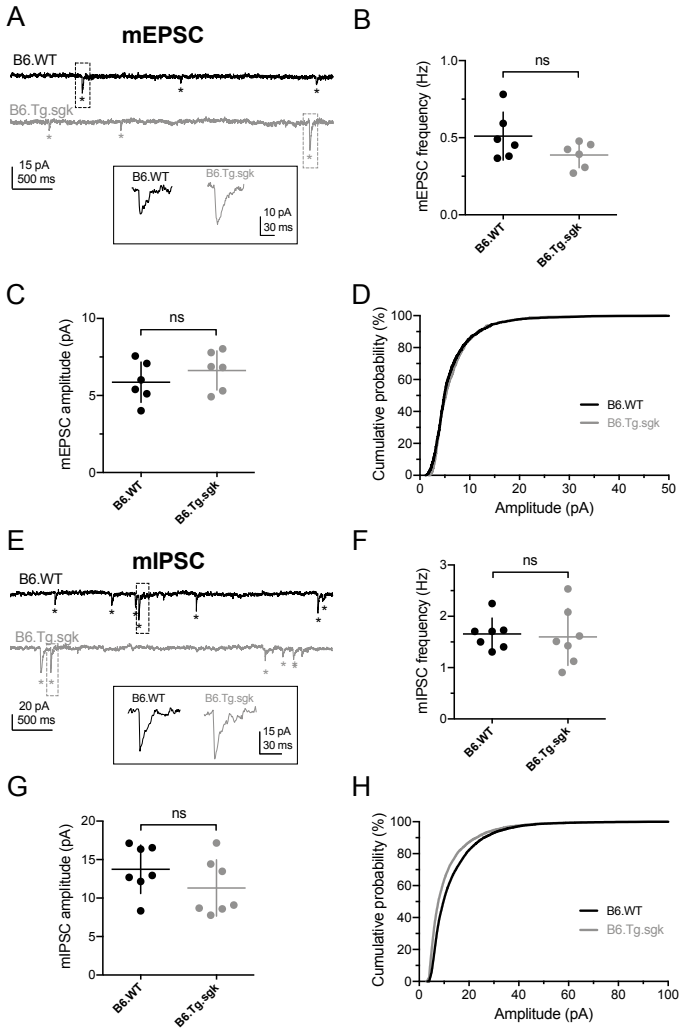

Figure 26. Basal synaptic transmission is not altered in B6.Tg.sgk1 mice. (A) Representative current traces recorded at–70mV in CA1-PN from B6.WT (gray) and B6.Tg.sgk1

(black) mice in the presence of 1 µM TTX, 50 µM PiTX, and 5 µM CPG-55845 to isolate mEPSCs. Asterisks denote mEPSC events. Insert shows representative mEPSCs in an expanded scale. (B) Frequency, (C) amplitude, and (D) cumulative probability distribution of amplitudes of mEPSC in B6.WT (gray) and B6.Tg.sgk1 mice (black). (E) Representative current traces recorded at −70 mV in CA1-PN from B6.WT (gray) and B6.Tg.sgk1 (black) mice in the presence of 1 µM TTX, 50 µM AP5, and 20 µM CNQX to isolate mIPSCs. Asterisks denote mIPSC events. Insert shows representative mIPSCs in an expanded scale. (F) Frequency, (G) amplitude, and (H) cumulative probability distribution of amplitudes of mIPSC in B6.WT (gray) and B6.Tg.sgk1 mice (black). Unpaired two-tailed t-test; ns, not significant.

4.3 Phosphorylation of Nedd4-2 by SGK1.1: a proposed mechanism for M-current up-regulation

Previous experiments performed in *Xenopus laevis* oocytes indicate that SGK1.1 counteracts the inhibitory effect of Nedd4-2 on the M-current (Miranda et al. 2013). Considering these findings, and as part of our interest in elucidating the molecular pathway underlying the M-current up-regulation by SGK1.1, we hypothesized that SGK1.1, like its ubiquitous counterpart SGK1, might be able to phosphorylate and inhibit the ubiquitin-ligase, preventing the degradation of the channel. So far, no direct evidence supporting this model is available. To directly test whether SGK1.1 and SGK1 share common phosphorylation targets, we analyzed the levels of phosphorylation in two sites of Nedd4-2; serine (S) 448 (equivalent to S328 in murine Nedd4-2) and S342 (equivalent to S222 in murine Nedd4-2). These two sites are known to be phosphorylated by ubiquitous SGK1 (Debonneville et al. 2001). We observed a significant increase in phosphorylation levels of Nedd4-2 in HEK293 cells transiently co-transfected with constitutively active SGK1.1(S515D) mutant and Nedd4-2, but not in cells expressing an inactive mutant of the kinase, SGK1.1(K220A) (Figure 27A).

Additionally, phosphorylation of endogenously-expressed GSK3-β, another known target of SGK1 (Kobayashi et al. 1999), was increased when SGK1.1(S515D) was transiently transfected in HeLa cells (Figure 27B). In this case, the reason to choose the HeLa cell line was that these cells endogenously express GSK3-β.

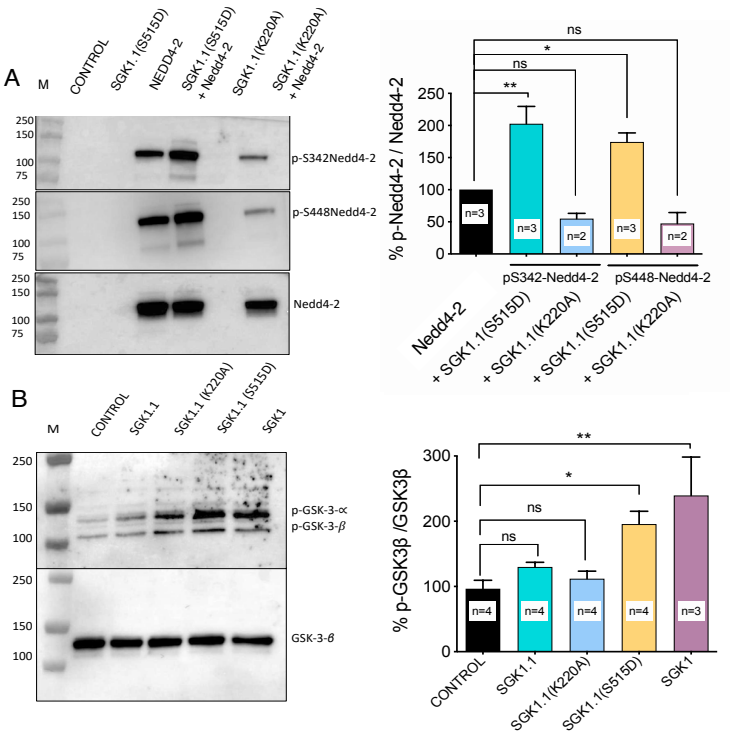

Figure 27. SGK1.1 enhances phosphorylation levels of Nedd4-2 and GSK-3-β in heterologous expression systems. (A) Left: Representative immunoblot of p-S342Nedd4-2 (above) and p-S448-Nedd4-2 (middle) (110/135 KDa). Total Nedd4-2 (115 KDa) was used as internal standard (below). Right: Quantification of p-S342Nedd4-2 and P-S448-Nedd4-2 levels relative to total Nedd4-2 in untransfected cells, SGK1.1(S515D) (constitutively active mutant) + Nedd4-2 and SGK1.1(K220A) (kinase inactive mutant) + Nedd4-2. The results are the mean ± SEM from at least two independent experiments. Significant differences are indicated by *p<0,05, **p<0.01, ns no significant (One-Way ANOVA, Sidak's correction for Multiple comparisons). (B) Left: Representative immunoblot of p-S21-GSK-3-α (51 KDa) and p-S9-GSK-3-β (46 KDa). Total GSK-3β (46 KDa) was used as internal standard. HeLa cells were transfected with wild type SGK1.1, SGK1.1(K220A), SGK1.1(S515D), and SGK1. Untransfected cells were used as control. Right: Quantification of p-S9-GSK-3-β levels relative to total GSK-3-β in untransfected cells, cells transfected with SGK1.1, SGK1.1(K220A), SGK1.1(S515D) and SGK1. The results are the mean ± SEM from at least three independent experiments. One-way ANOVA, Dunnett's correction for Multiple comparisons, significant differences are indicated by *p<0.05; **p<0.01, ns no significant.

Altogether, our data suggest that SGK1 and SGK1.1 share phosphorylation targets, at least in heterologous expression systems. Whether Nedd4-2 is also downstream of the SGK1.1 signaling pathway in neurons remained unexplored. To address this question, we quantified Nedd4-2 phosphorylation levels in hippocampal

tissue from B6.WT and B6.Tg.sgk1 mice. Our results showed significantly higher phosphorylation levels at S448 in B6.Tg.sgk1 mice compared with B6.WT (Figure 28A). Importantly, this difference was not observed when the tissue was incubated with the SGK1 inhibitor EMD638683 (Figure 28B). Thus, our data demonstrate that Nedd4-2 is a substrate of SGK1.1 in hippocampal neurons, constituting a regulatory pathway underlying M-current modulation by this kinase in hippocampus (Armas-Capote et al. 2020). Levels of phosphorylation at site S342 were unchanged in B6.Tg.sgk1 (Figure 28D-E).

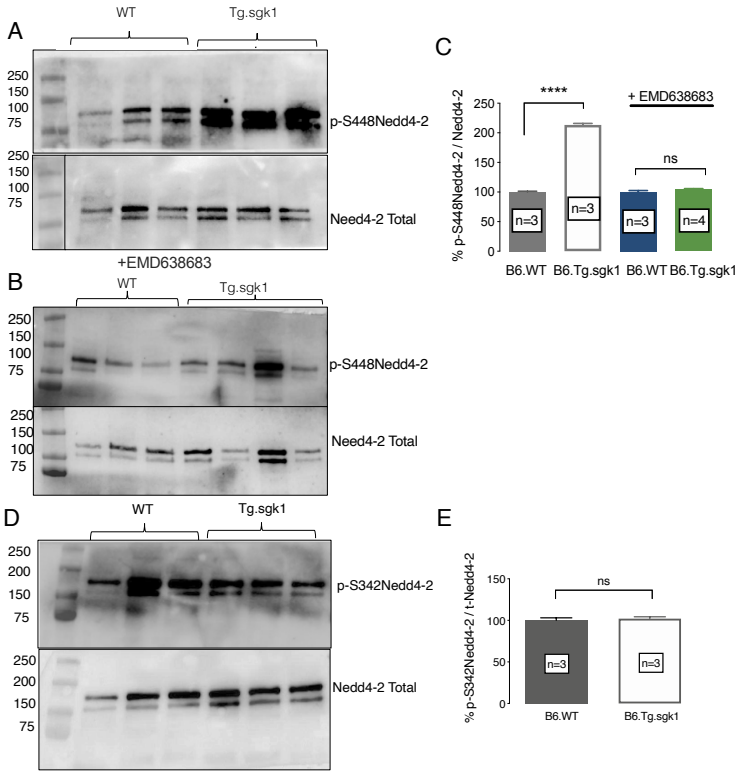

Figure 28. SGK1.1 phosphorylates Nedd4-2 in mouse hippocampus. (A) Representative immunoblots detecting p-S448 and total Nedd4-2 in hippocampus lysates from B6.WT (n=3) and B6.Tg.sgk1 (n=3-4) mice, without (A) and with (B) pre-treatment with EMD638683. (C) Quantification of p-S448Nedd4-2 (relative to total Nedd4-2). The results are the mean ± SEM from at least three independent experiments. One-Way ANOVA with Sidak's correction for Multiple comparisons; ****p<0.0001; ns, not significant. (D) Representative immunoblot showing p-S342 and total Nedd4-2 in hippocampus lysates from B6.WT (n=3) and B6.Tg.sgk1 (n=3) mice. (E) Quantification of p-S342Nedd4-2 relative to total Nedd4-2. The results are the mean ± SEM from at least three independent experiments. Unpaired t-test; ns, not significant.

SECTION 2: NEUROPROTECTION

4.4 SGK1.1 protects mice from KA-induced neuronal cell death

SE triggers a series of negative outcomes in the brain that include neuronal death, which might contribute to the occurrence of new spontaneous and recurrent seizures. To evaluate the role of SGK1.1 on neurodegeneration, we quantified neuronal death on brain slices from B6.WT and B6.Tg.sgk1 mice 72 h after KA injection. For this purpose, we only used mice that reached Racine stage 6 and therefore had comparable levels of seizure activity (Figure 29A). Activation of SGK1.1 confers significant protection against neuronal death in different brain areas including hippocampus, somatosensorial-auditive and piriform-entorhinal cortex (Figure 29B). Transgenic mice showed significantly reduced levels of FJC positive cells per area when compared to wild type animals (Figure 29C) (Martin-Batista et al. 2021).

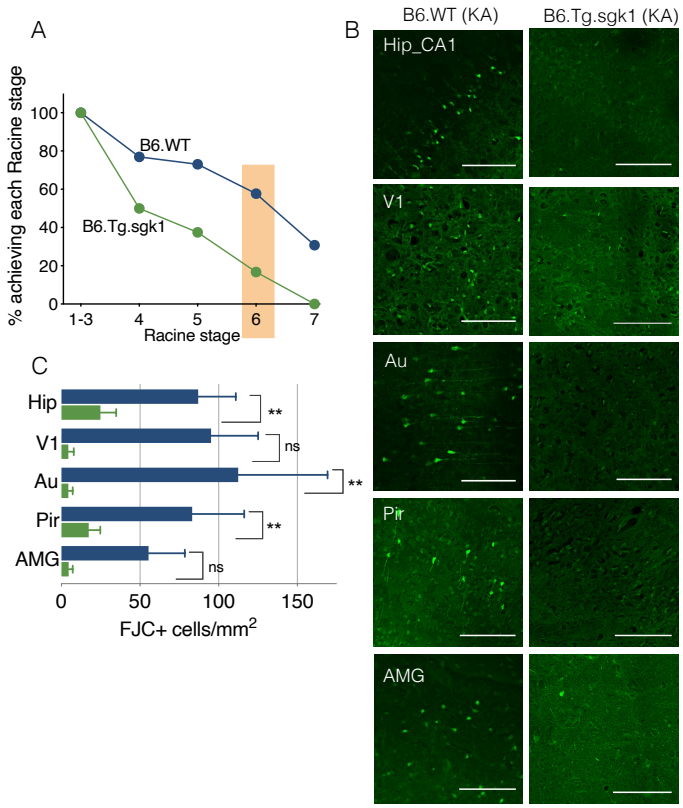

Figure 29. FJC staining reveals significant differences in neuronal death between B6.WT and B6.Tg.sgk1. FJC staining was performed on 30 µm brain slices from B6.WT and B6.Tg.sgk1 n=5 (5 slices per mouse), 72 h after KA treatment. (A) Panels show representative images of FJC-stained sections from CA1 of hippocampus (Hip_CA1), motor/visual cortex (V1), auditive/somatosensorial cortex (Au), piriform/entorhinal cortex (Pir) and amygdalar complex (AMG) at 40x magnification. Scale bar = 100 µm. (B) Quantitative analysis of neurodegeneration events normalized to area (mm^2) in denoted regions for both genotypes. Transgenic mice show significantly reduced levels of neuronal death after KA treatment. Mann-Whitney test, **p<0.01, ns no significant.

The next approach that we used was evaluating neuronal injury on mice treated with EMD638683 in combination with KA to elucidate the effect of SGK1.1 inhibition on neuronal death. As observed in Figure 30, levels of neurodegeneration were similar between wild type and transgenic mice reaching the same Racine state when we inhibited SGK1.1 with EMD638683. Thus, the neuroprotective effect is lost when we inhibit the kinase activity (Martin-Batista et al. 2021).

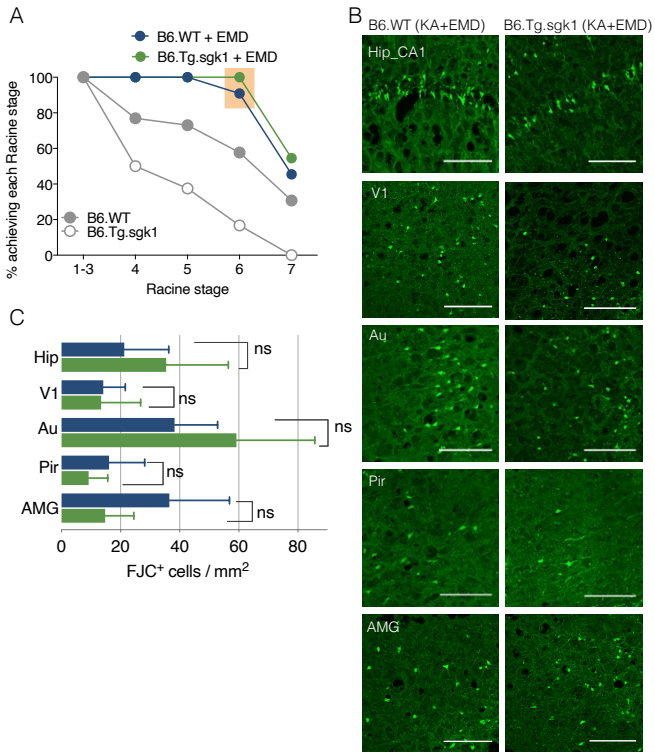

Figure 30. SGK1.1-induced neuroprotection depends on kinase activity. FJC staining was performed on 30 μm slices from B6.WT (n=8) and B6.Tg.sgk1 (n=5) (5 slices per mouse) 72 h after KA treatment + EMD638683. (A) Representative confocal images corresponding to FJC staining of brain sections from B6.WT (left column) and B6.Tg.sgk1 mice (right column) pretreated with EMD638683. Brain regions shown are CA1 of hippocampus (Hip_CA1), motor/visual cortex (V1), auditive/somatosensorial cortex (Au), piriform/entorhinal cortex (Pir) and amygdalar complex (AMG). Scale bar = 100 μm. (B) Quantitative analysis of FJC+ cells in EMD638683-pretreated mice in the areas shown in B. Data are mean ± SEM (Mann-Whitney test; ns, not significant).

We then tested whether M-current up-regulation is also needed for neuroprotection. To address this question, we evaluated the incidence of neurodegeneration on brain slices from mice treated with XE991 and KA after reaching Racine stage 6 (Figure 31A). Differences between genotypes became less noteworthy when XE991 was administrated along with KA (Figure 31B and 31C). However, we still observed a clear tendency to lower levels of neuronal death in the transgenic mice, where the piriform/entorhinal cortex is the most protected area with significant differences compared to WT. This result not only supports our hypothesis that SGK1.1

exerts a dual role as an anticonvulsant and as a neuroprotective factor but suggests that there must be alternative mechanisms in addition to M-current regulation playing a role in the neuroprotective effect (Martin-Batista et al. 2021).

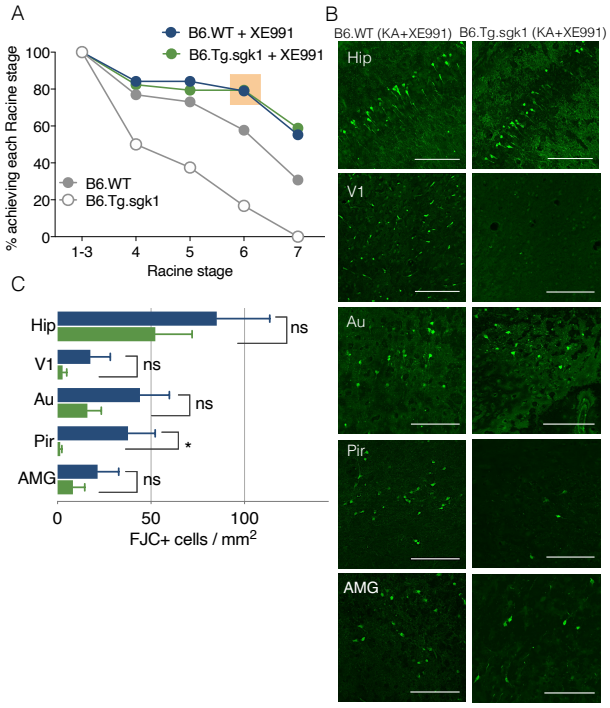

Figure 31. FJC staining on KA + XE991-treated B6 mice demonstrates SGK1.1 activity-dependent neuroprotection includes M-current dependent and independent mechanisms. FJC staining was performed on 30 μm slices from B6.WT and B6.Tg.sgk1 n=7 (5 slices per mouse) 72 h after XE991 + KA treatment. (A) Panels show representative images of FJC stained sections from CA1 in hippocampus (Hip_CA1), Motor/visual cortex (V1), Auditive/somatosensorial cortex (Au), Piriform/entorhinal cortex (Pir) and Amigdalar complex (AMG) at 40x magnification. Scale bar = 100 μm. (B) Quantitative analysis of FJC positive cells normalized to area (mm^2) on slices from WT and transgenic in the selected areas. Data are mean ± SEM (Mann-Whitney test, *p>0.05, ns not significant).

4.5 Activation of SGK1.1 reduces levels of reactive gliosis after status epilepticus

We were interested on quantifying the manifestation of gliosis, a very well-described feature of epileptic brains, on brain slices from WT and Tg.sgk1 after SE. To evaluate astrogliosis, we have used GFAP marker and quantified its expression. GFAP is the main intermediate filament in astrocytes and is responsible for the cytoarchitecture and functions of these cells. Upregulation of GFAP is an indicator of reactive astrogliosis in pathologic conditions (McKeon and Benarroch 2018).

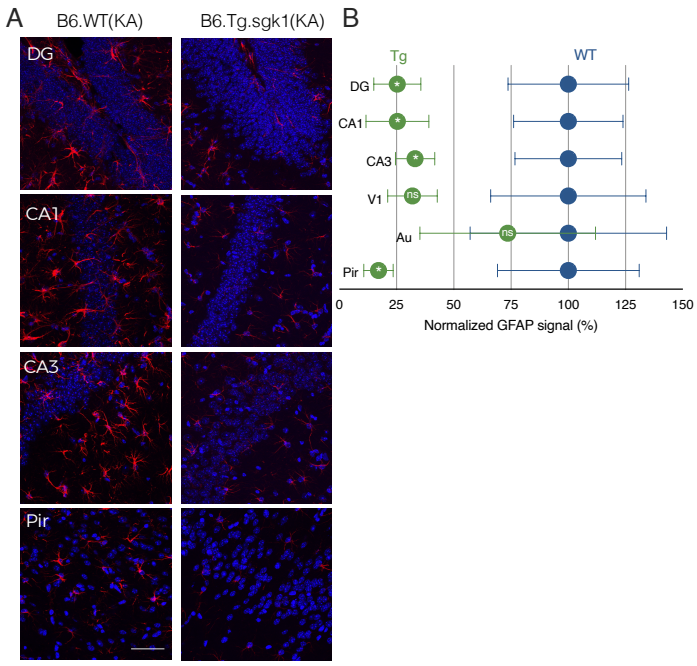

Figure 32. Astrogliosis in hippocampi and cortex from KA-injected B6.WT and B6.Tg.sgk1 mice. (A) Representative images showing GFAP signal (red, Alexa Fluor® 594) and DAPI (blue) for B6.WT and B6.Tg.sgk1 72h after kainic acid injection at 40x magnification in hippocampus regions (CA1, CA3 and dentate gyrus -DG-) and cortex (piriform cortex -Pir-). Scale bar= 50 μm. B) Average quantification of GFAP levels in transgenic mice compared to normalized levels in WT on indicated brain areas (DG, CA1, CA3, Visual cortex (V1), Auditive cortex (Au) and Pir). Values are represented as mean ± SEM. Multiple t-test, significant differences are indicated by *p<0,05; ns, not significant. (B6.WT, n=5. B6.Tg.sgk1, n=5).

Similarly to previous studies (Chen et al. 2005), we found increased GFAP expression in the hippocampus and cortex on day 3 post KA injection (Figure 32). Most importantly, activation of SGK1.1 in transgenic mice was accompanied by significantly reduced levels of astrogliosis after seizures in different brain areas including hippocampus and cortex (Figure 32) (Martin-Batista et al. 2021).

Furthermore, we quantified the expression of IBA-1 marker to evaluate microgliosis on brain slices from the same mice. IBA-1 is an actin-binding protein that is constitutively expressed in microglia and is involved in membrane ruffling during ramification and activation of these cells (Ahmed et al. 2007).

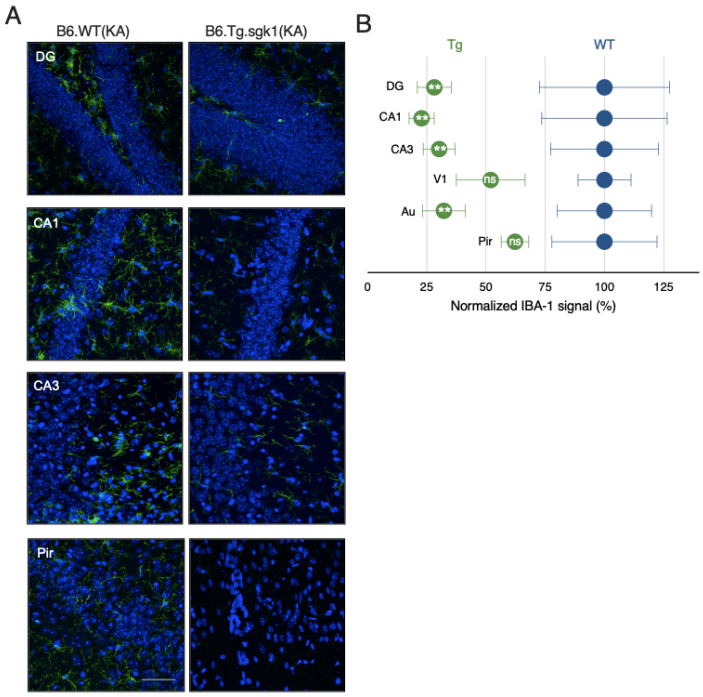

Figure 33. Microgliosis analysis in B6.WT and B6.Tg.sgk1 demonstrates increased IBA-1 levels in wild type mice after KA treatment. (A) Representative images showing IBA-1 reactivity (green, Alexa 488) and cell nuclei in blue (DAPI) for B6.WT and B6.Tg.sgk1 after kainic acid (right) injection at 40x magnification in hippocampus regions (CA1, CA3 and dentate gyrus -DG-) and Pir. Scale bar= 50 μm. (B) Average quantification of IBA-1 levels in transgenic mice compared to normalized levels in WT on specified brain areas (DG, CA1, CA3, V1, Au and Pir). Values are represented as mean ± SEM. Multiple t-test. Significant differences are indicated by *p<0,05; **p<0,01; ns, not significant (B6.WT, n=5. B6.Tg.sgk1, n=5).

Quantitative analysis revealed that levels of reactive microglia were significantly lower in hippocampal and cortical areas of transgenic mice compared to wild type 72 hours after KA-induced status epilepticus (Figure 33) (Martin-Batista et al. 2021).

Taken together, our results demonstrate that activation of SGK1.1 significantly reduces astro- (Figure 32) and microgliosis (Figure 33) after SE. Given that all the mice used for this study underwent the most severe Racine stage (6), these results indicate that SGK1.1 contributes to a lesser reactivity of glial cells. This might involve a reduction in the levels of inflammation and structural changes in the injured brain of transgenic mice.

4.6 SGK1.1-mediated protection against neuronal death and gliosis is independent of mouse strain

As part of our interest on validating SGK1.1 as a target for epilepsy treatment in different genetic backgrounds, we also evaluated neurodegeneration and gliosis in the FVB strain. Importantly, our results demonstrate that the neuroprotective effect of the kinase is maintained independently of genetic background. FVB.Tg.sgk1 showed significantly reduced levels of neuronal death (Figure 34) and gliosis (Figures 35 and 36) after KA-induced SE compared to WT (Martin-Batista et al. 2021).

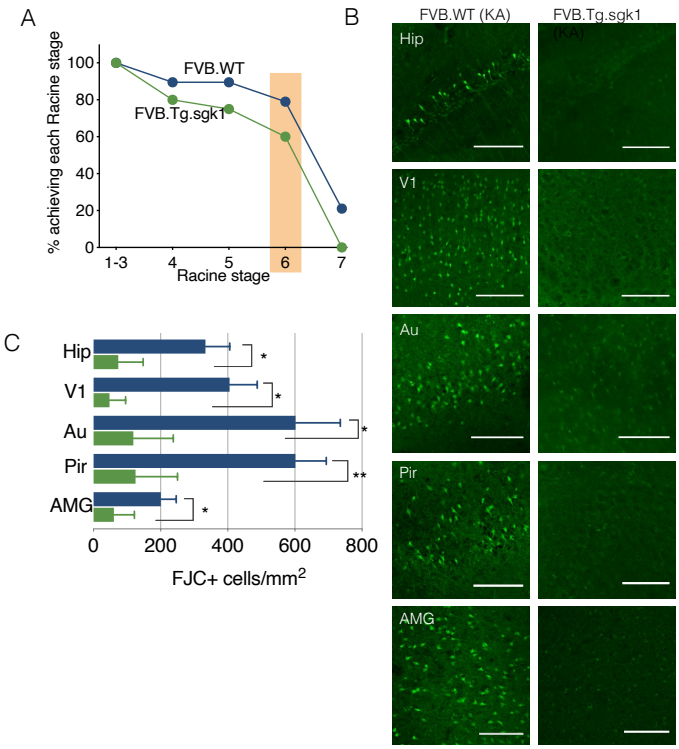

Figure 34. FJC staining demonstrates SGK1.1-mediated protection against neurodegeneration is independent of strain. FJC staining was performed on 30 μm brain slices from FVB.WT n=5 and FVB.Tg.sgk1 n=7 (5 slices per mice) 72h after KA treatment. (A) Panels show representative images of FJC positive neurons in CA1 of hippocampus (Hip_CA1), visual/motor cortex (V1), auditive/somatosensorial cortex (Au), piriform/entorhinal cortex (Pir) and amygdalar complex (AMG) from WT and Tg.sgk1 mice at 40x magnification. Scale bar =100 μm. (B) Quantification of FJC positive cells normalized to area (mm^2) in both genotypes. (Data shown as mean ± SEM. Mann-Whitney test, *p<0.05; **p<0.01).

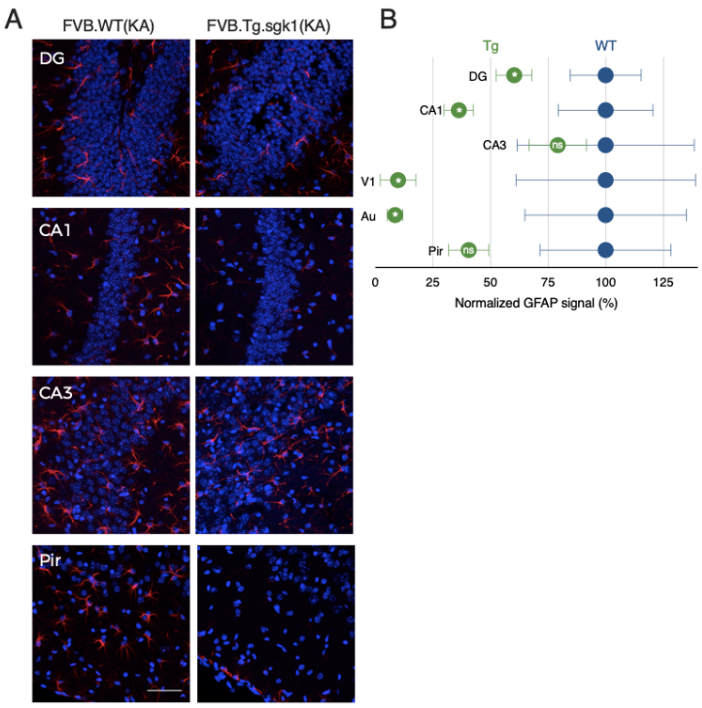

Figure 35. Astrogliosis in hippocampus and cortex of KA-injected FVB.WT and FVB.Tg.sgk1 mice. (A) Representative images showing GFAP signal (red, Alexa Fluor® 594) and DAPI (blue) for FVB.WT and FVB.Tg.sgk1 72 h after kainic acid injection at 40x magnification in hippocampal regions (CA1, CA3 and dentate gyrus -DG-) and Pir. Scale bar= 50 μm. B) Quantification of GFAP levels in transgenic mice compared to normalized levels in WT. Transgenic mice show significantly reduced levels of astrogliosis in CA1, visual (V1) and auditive cortex (Au). Values are represented as mean ± SEM, significant differences are indicated by *p<0,05; ns, not significant. Multiple t-test (FVB.WT, n=6. FVB.Tg.sgk1, n=6).

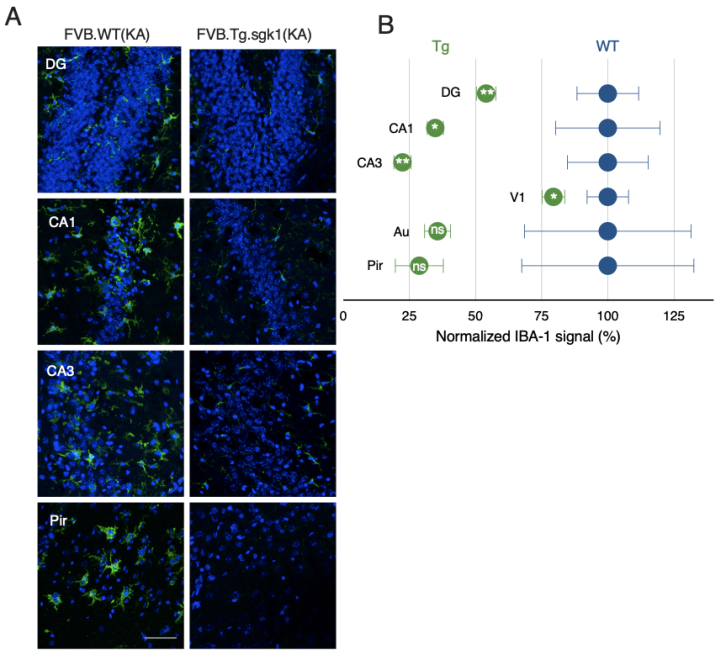

Figure 36. Reactive microglia in hippocampus and cortex of KA-injected FVB.WT and FVB.Tg.sgk1 mice. (A) Representative images showing IBA-1 signal (green, Alexa 488) and DAPI (blue) for FVB.WT and FVB.Tg.sgk1 72 h after kainic acid treatment at 40x magnification in hippocampal regions (CA1, CA3 and dentate gyrus -DG-) and Pir. Scale bar = 50 µm. (B) Average quantification of GFAP levels in transgenic mice compared to normalized levels in WT in the indicated brain areas (DG, CA1, CA3, V1, Au and Pir). Values are represented as mean ± SEM, significant differences are indicated by *p<0.05, **p<0.01 (Multiple t-test. FVB.WT and FVB.Tg.sgk1 n=5).

4.7 SGK1.1 is mainly expressed in pyramidal neurons

We next asked whether the effect of constitutively active SGK1.1 on reactive gliosis is directly due to expression of this kinase in glial cells or indirectly related to reduced neuronal death. We have previously reported that SGK1.1 mRNA is preferentially expressed in pyramidal neurons of the cortex and hippocampus (Wesch et al. 2010), but the protein distribution has never been described previously, due to the lack of isoform-specific antibodies. To overcome this limitation, we developed a new rabbit polyclonal antibody that recognizes SGK1.1 specifically. First, we used western blot and immunoprecipitation approaches to evaluate the functionality and specificity of our homemade antibody. Preimmunize serum did not give any signal whereas

blotting with post-immune serum revealed a band at the expected position (Figure 37A-B). The serum also worked for protein extracts obtained from WT and Tg hippocampal tissue (Figure 37C) and immunoprecipitation of these proteins with anti-SGK1.1 produced a specific band only present in samples from transgenic mice. The reason is that we used anti-HA for blotting and only the transgene is tagged with HA (Figure 37D). We then investigated the distribution of the kinase in transfected HEK293T cells where plasma membrane localization of SGK1.1 is clearly observed (Figure 38A) and in the mouse brain (Figure 38B-F).

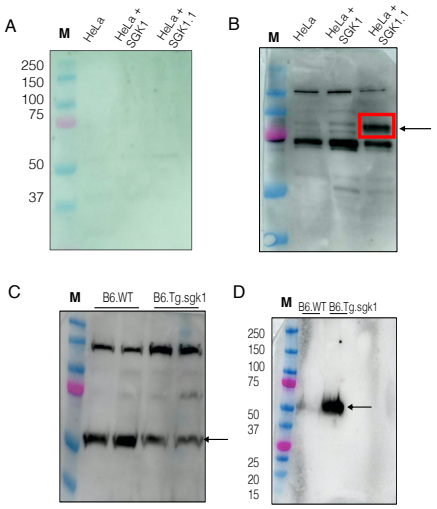

Figure 37. Characterization of a new rabbit polyclonal anti-SGK1.1 antibody. (A) Protein extracts from HeLa cells before and after transfection with SGK1.1 and SGK1 blotted with pre-immune serum. (B) Protein extracts from HeLa cells before and after transfection with SGK1.1 and SGK1 blotted with serum after sixth immunization. Selected band corresponds to SGK1.1 fused to CFP (87 KDa). (C) Brain extracts from B6.WT and B6.Tg.sgk1 mice were separated in a SDS-PAGE gel, transferred to a PVDF membrane and blotted with anti-SGK1.1. Both, wild type and transgenic express SGK1.1 and the corresponding band is detected with our antibody (60 KDa). (D) Denaturing immunoprecipitation shows the specificity of our anti-SGK1.1. Protein extracts from B6.WT and B6.Tg.sgk1 hippocampi were used for immunoprecipitation with anti-SGK1.1 and probed with anti-HA. Only SGK1.1-HA from transgenic mice was detected.

Immunohistochemical localization of SGK1.1 in mouse brain tissue revealed a very specific neuronal expression limited to the plasma membrane and absence of nuclei mark. In addition, double immunohistochemistry revealed that SGK1.1 is not

expressed in parvalbumin (PV)-positive interneurons. Within pyramidal neurons, expression is detectable in the soma and neuronal processes (Martin-Batista et al. 2021). Finally, we performed double inmuhistochemistry with SGK1.1 and GFAP and concluded no co-localization between SGK1.1 and GFAP. This result suggests that the kinase is not expressed in astroglia. Observed localization strongly suggests that the primary site of SGK1.1 action is neuronal and that the decrease in reactive gliosis is secondary to decreased neuronal death.

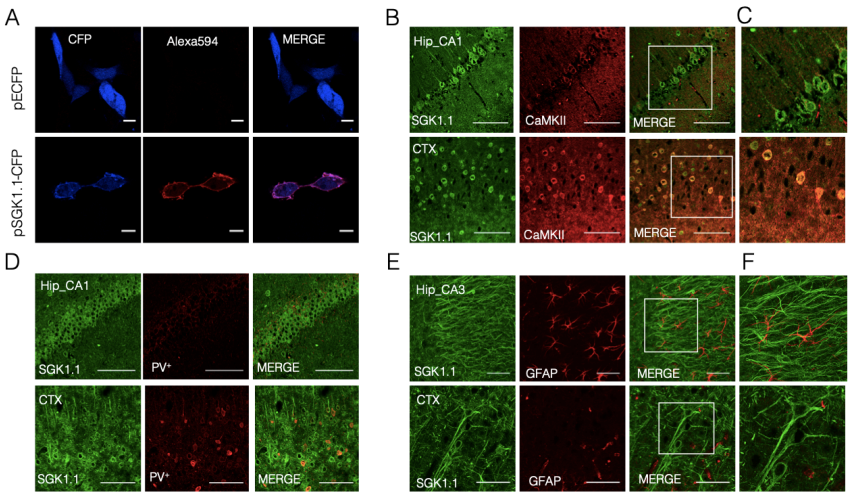

Figure 38. SGK1.1 is selectively expressed at the soma and processes of pyramidal neurons. (A) Representative confocal images of HEK293T cells transfected with an empty vector (pECFP-N1) or a vector expressing SGK1.1-CFP and stained with anti-SGK1.1 rabbit polyclonal antibody. Scale bar = 10 μm. (B) Representative confocal images of WT brain slices showing SGK1.1 (green, Alexa Fluor® 488) and CaMKII (red, Alexa Fluor® 594) immunostaining of hippocampus CA1 (Hip_CA1) and visual cortex (CTX) areas. Scale bar = 100 μm. (C) Magnification of white-framed regions in B. (D) Representative confocal images showing SGK1.1 (green) and PV (red) immunostaining of hippocampus CA1 (Hip_CA1) and visual cortex (CTX) from WT brain slices. (E) Representative confocal images showing SGK1.1 (green, Alexa Fluor® 488) and GFAP (red, Alexa Fluor® 594) expression of hippocampus CA3 (Hip_CA3) and visual cortex (CTX). (F) Magnification of white-framed areas in E.

4.8 SGK1.1 exerts an antiapoptotic role comparable to AKT

As mentioned before, SGK1 and AKT share a 54% identity in their catalytic domain. Furthermore, all SGK1 isoforms conserve the same catalytic domain and, therefore, it would be expected that they share very similar substrate specificity, as we have shown with Nedd4-2 and GSK-3ß. Downstream targets might include apoptosis-

related factors that contribute to neuroprotection in an epileptic-induced brain damage condition. Thus, we studied the possible role of SGK1.1 as an anti-apoptotic kinase. To do so, we performed TUNEL assay in HEK293T cells expressing different SGK1.1 variants to test the ability of the kinase to reduce apoptosis and compare it to the well-known antiapoptotic effect of AKT. As shown in **Figure 39**, apoptosis levels after treatment with H_2O_2 were significantly reduced in cells expressing AKT, as well as in those expressing activated SGK1.1(S515D) compared to control cells (pECFP-N1). In contrast, cells transfected with inactive SGK1.1(K220A) and SGK1.1(FF19,20AA) (mutant unable to interact with the plasma membrane and located in nuclei) were not protected against apoptosis and even showed significantly higher levels than control, suggesting a dominant negative effect over the endogenous kinase.

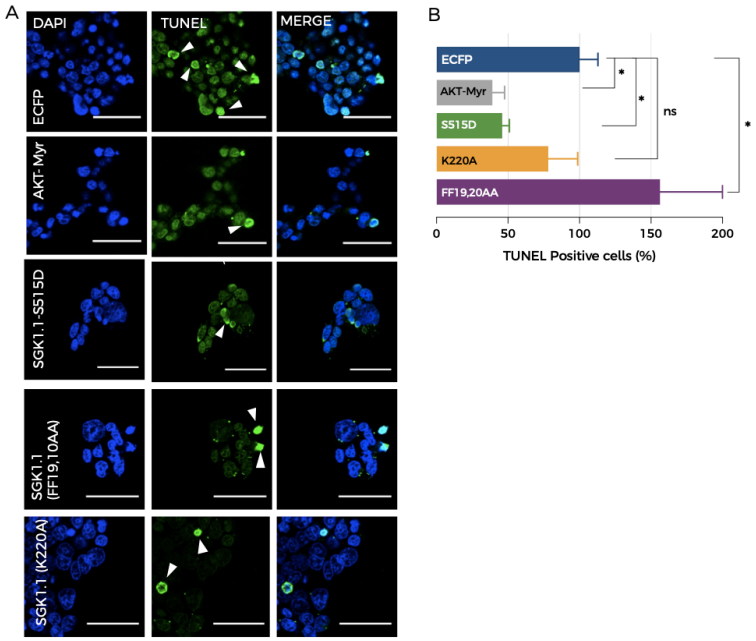

Figure 39. SGK1.1 activation leads to a significant anti-apoptotic effect similarly to AKT. Levels of apoptosis were detected as TUNEL-positive cells after a treatment with H_2O_2 1 mM for 4 h. (A) Panels show representative images of DAPI and Fluorescein (TUNEL) stained cells transfected with the indicated constructs. Arrows indicate TUNEL positive cells. Scale bar = 10 µm. (B) Quantitative analysis of TUNEL positive cells after treatment. Data shown as mean ± SEM from 5 independent experiments (One-Way ANOVA, Fisher's test for Multiple comparisons; ns, not significant; *p<0.05).

Our data support the hypothesis of SGK1.1 playing an anti-apoptotic role that prevents cells from H_2O_2-induced apoptosis (Martin-Batista et al. 2021) which constitutes a highly promising feature if we are to propose this kinase as a new therapeutic target for epilepsy.

4.9 Activation of SGK1.1 reduces levels of pro-apoptotic mediator Bim and up-regulates Bcl-X_L

Different apoptosis markers, including the Bcl-2 interacting mediator of cell death (Bim) and cleaved caspase-3, are overexpressed after seizures in hippocampus (Kim et al. 2014). Herein, we quantified the levels of Bim in hippocampus extracts from B6.WT and B6.Tg.sgk1 mice 24 h after KA-induced SE. There are three different splicing isoforms of Bim: Bim_s, Bim_L and Bim_{EL} (Putcha et al. 2001). Based on molecular mass, we have detected all three isoforms on our membranes. Western blot showed that total Bim abundance was significantly decreased in Tg.sgk1 mice compared to WT after treatment (Figure 40) (Martin-Batista et al. 2021). This result supports the hypothesis of SGK1.1 having an anti-apoptotic effect that may protect against neurodegeneration in our transgenic mice.

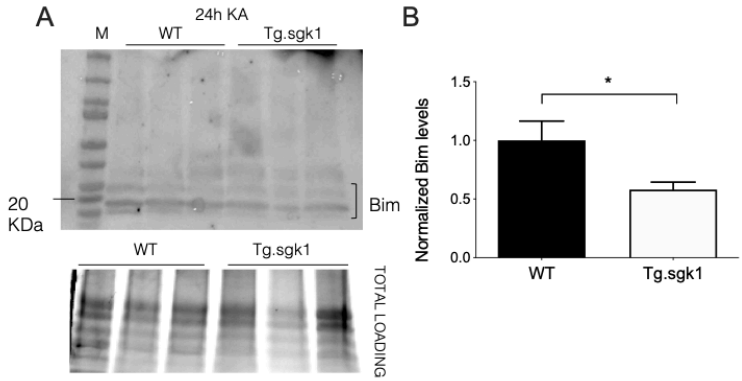

Figure 40. Bim levels are significantly reduced in Tg.sgk1 mice after status epilepticus. (A) Representative western blot and (B) quantification of Bim in the hippocampus of wild type and transgenic mice at 24 h after kainic acid (KA) administration. Total protein track was used as loading control. Data shown as mean ± SEM from WT n=4 and Tg.sgk1 n=6 from three independent replicates. Unpaired t-test, *p<0.05.

We then quantified the expression of one of the anti-apoptotic protein members of Bcl-2 family, Bcl-x_L. Bcl-x_L has been proposed to reduce apoptosis, maintain cell viability in CNS and prevent mitochondrial permeability transition in response to pro-apoptotic factors (Boise et al. 1993; Krajewska et al. 2002; Jonas et al. 2014). Our results show that activation of SGK1.1 increases the level of Bcl-x_L in transgenic mice after KA (**Figure 41**), which may underly the neuroprotective role of SGK1.1 (Martin-Batista et al. 2021).

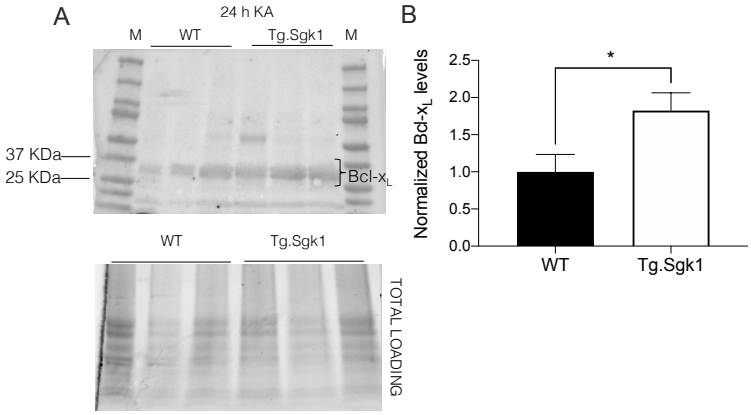

Figure 41. Bcl-x_L levels are significantly lower in B6.WT after status epilepticus. (A) Representative western blot and (B) quantification of Bcl-x_L in the hippocampus of wild type and transgenic mice at 24 h after kainic acid (KA) administration. Total protein track was used as loading control. Data shown as mean ± SEM from WT n=4 and Tg.sgk1 n=6 from three independent replicates. Unpaired t-test, *p<0.05.

4.10 Activation of SGK1.1 does not alter neurogenesis processes in hippocampus

It has been proposed that ectopic neurogenesis after seizure-induced damage could be producing neurons with different electrophysiological properties, related to hyperexcitable circuits and responsible for the maintenance of epileptic activity (Ribak et al. 2000). Also, previous studies suggested that SGK1 might be related to ectopic neurogenesis in hippocampus induced by glucocorticoids hormones (Anacker et al. 2013). If SGK1.1 is to be proposed as a valid pharmacological target in the treatment of epilepsy, it is important to determine whether constitutive activation of SGK1.1 has side effects on neurogenesis in our animal model. Therefore, we quantified ectopic neurogenesis in hippocampus from WT and Tg.sgk1 mice under basal conditions,

using *in vivo* incorporation of BrdU to proliferating neuronal precursors. Number of proliferating cells in hilus (ectopic) and subgranullar layer (basal) of DG were quantified in transgenic and WT mice. Our experiment demonstrated that Tg.sgk1 mice do not show altered neurogenesis in the hippocampus compared to WT because levels of ectopic neurogenesis (BrdU/DCX-positive cells in hilus) were similar between genotypes (Figure 42).

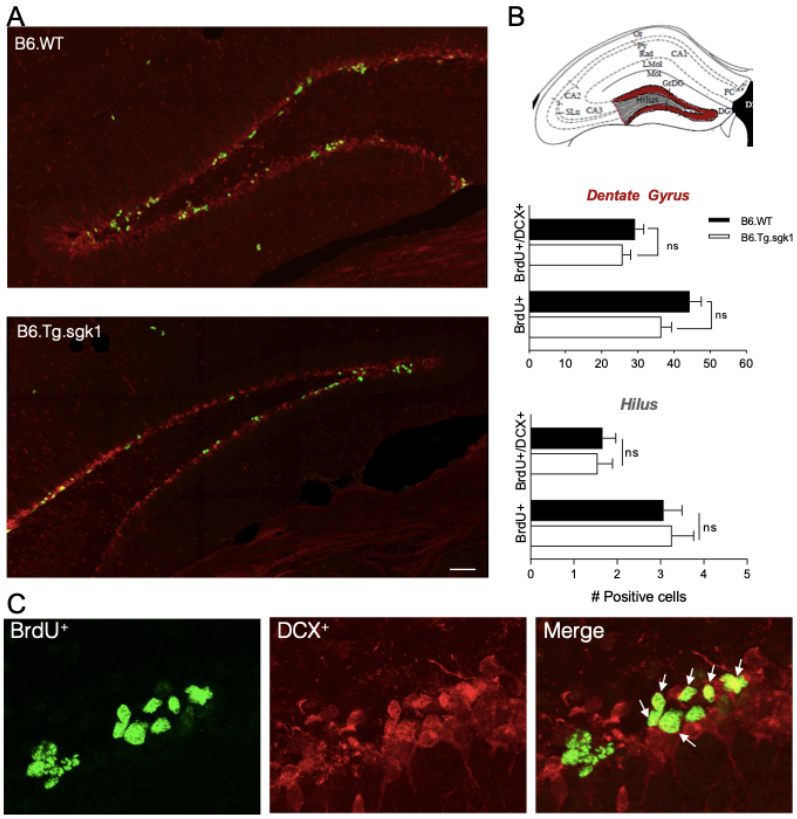

Figure 42. Activation of SGK1.1 does not alter neurogenesis processes in hippocampus. (A) Representative images showing neurogenesis phenomena in B6.WT (top) and B6.Tg.sgk1 (bottom) in dentate gyrus of hippocampus. (B) Schematic representation of hippocampus showing analyzed regions for quantification of neurogenesis in DG (red) and hilus (grey). Graphs show quantification of BrdU+ and DCX+ cells per brain section in granular cells of DG and hilus. BrdU and DCX+ cells localized in DG account for normal neurogenesis while BrdU and DCX+ cells localized in hilus constitute ectopic neurogenesis. Data shown as mean ± SEM (Unpaired t-test, ns no significant. B6.WT and B6.Tg.sgk1 n=4). (C) Representative images showing BrdU+ cells, DCX+ neurons and merge in DG.

Altogether, we have presented a series of results demonstrating not only that activation of SGK1.1 does not alter basal processes (Figure 42), but it leads to a very powerful protection against brain damage associated to seizures including neurodegeneration (Figures 29 and 34), astrogliosis (Figures 32 and 35) and reactive microglia (Figures 33 and 36). A proposed mechanism for neuroprotection might be a reduction of apoptosis (Figure 39) and regulators such as Bim (Figure 40) and Bcl-x_L (Figure 41), in addition to increased M-current.

SECTION 3: REGULATION OF Kv7 CHANNEL FAMILY AND Kv7.2 EPILEPSY-INDUCING MUTANTS BY SGK1.1

We examined the ability of SGK1.1 to modulate different Kv7 channel subunit combinations, with special attention to channels incorporating epilepsy mutations. This information is essential to predict possible side effects of SGK1.1 activation, as well as its potential to overcome at least some inherited forms of epilepsy.

Heterologous expression in *Xenopus laevis* oocytes of Kv7.2/3 resulted in slow activating, slow deactivating, non-inactivating and voltage-dependent K^+ currents measured by TEVC (Figure 43A), similarly to our previously published results (Miranda et al. 2013). Both wild type and constitutively active SGK1.1 led to a significant increase of the tail current measured at -30 mV (Figure 43C). WT SGK1.1 also produced a significant hyperpolarization of oocyte RMP (Figure 43E).

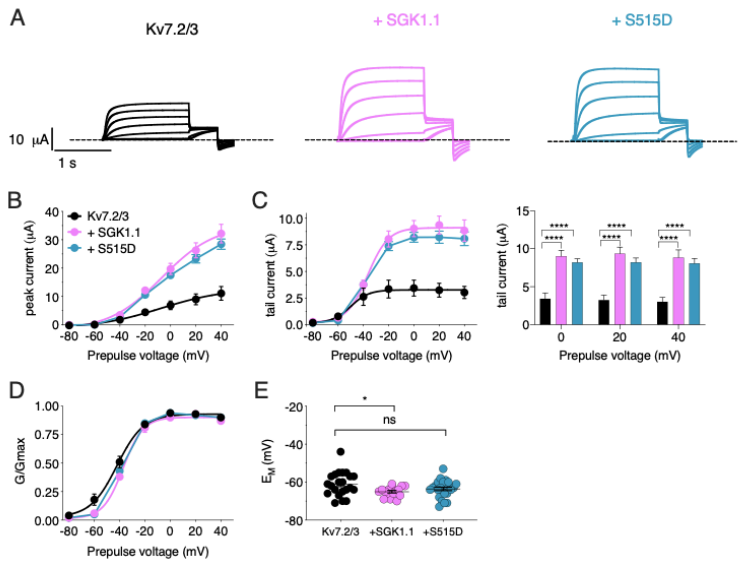

Figure 43. WT and constitutively active (S515D) SGK1.1 increases heteromeric Kv7.2/3 currents at similar levels, supporting previously obtained results. (A) Currents elicited in Xenopus oocytes after coinjection of cRNAs from Kv7.2/3 channel alone (first panel) or in combination with wild-type (second panel) or constitutively active (third panel) SGK1.1. (B) Peak current/voltage relationship. (C) Tail current (left) and tail currents measured at -30 mV after 0, +20 or +40 mV depolarizing pulses for the indicated construct combinations (right). Values represent mean ± SEM (Two-way ANOVA Tukey's Multiple comparisons test; ****p<0.0001). (D) Normalized conductance. (E) Resting membrane potentials (One-Way ANOVA Tukey's Multiple Comparisons test, *p<0.05; ns, not significant). Legends are indicated on graph B.

4.11 SGK1.1 does not affect homomeric Kv7.4 and Kv7.5 currents, but up-regulates heteromeric Kv7.3/5 channels

Oocytes microinjected with cDNAs coding for Kv7.4 or Kv7.5 led to smaller K^+ currents than those elicited by heteromeric Kv7.2/3 (**Figure 44A and 44F**). Co-expression of SGK1.1 did not up-regulate the homomeric channels. In fact, produced an inhibitory effect of the Kv7.4-mediated tail current (**Figure 44C**). RMP was not altered by the presence of SGK1.1 in any of the conditions (**Figure 44E and 44J**).

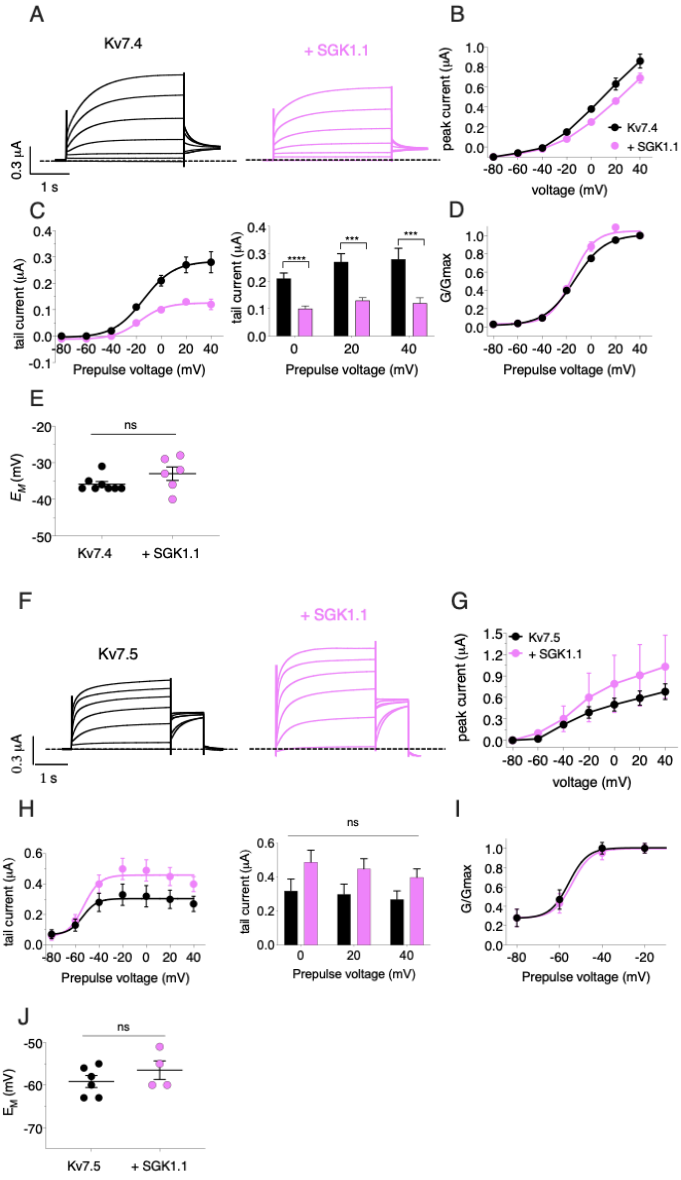

Figure 44. SGK1.1 fails to increase homomeric Kv7.4 and Kv7.5 currents, similarly to previously reported results for homomeric Kv7.2/3. (A) Currents elicited in Xenopus oocytes after microinjection of Kv7.4 channel alone (first panel) or in combination with wild-type SGK1.1 (second panel). (B) Peak current/voltage relationship. (C) Tail current (left) and tail currents measured at -30 mV after 0, +20 or +40 mV depolarizing pulses for the indicated construct combinations (right). Values represent mean ± SEM (Multiple t-test Holm-Sidak correction method;***p<0.0005, ****p<0.0001). (D) Normalized conductance. (E) Resting membrane potentials

(Unpaired t-test; ns, not significant). Legends are indicated on graph B. (F) Currents elicited after expression of Kv7.5 channel alone (first panel) or in combination with wild-type SGK1.1 (second panel). (G) Peak current/voltage relationship. (H) Tail current (left) and tail currents measured at -30 mV after 0, +20 or +40 mV depolarizing pulses for the indicated construct combinations (right). Values represent mean ± SEM (Multiple t-test Holm-Sidak correction method; ns, not significant) (right). (I) Normalized conductance. (J) Resting membrane potentials (Unpaired t-test; ns, not significant). Legends are indicated on graph G.

When we expressed heteromeric Kv7.3/5, a previously described combination associated to M-current (Schroeder et al. 2000), currents of bigger amplitude were measured compared to those elicited by Kv7.5 alone. These currents were also sensitive to SGK1.1, with significant increases in the tail currents at 0, +20 and +40 mV (Figure 45C). Also, RMP was significantly reduced by SGK1.1 (Figure 45E).

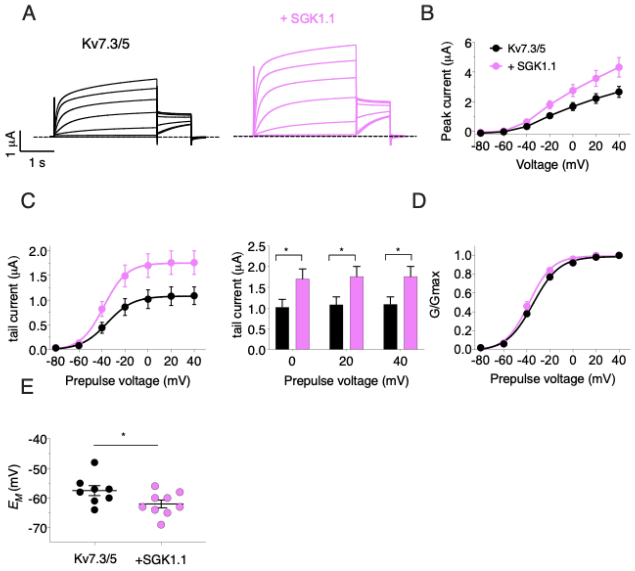

Figure 45. SGK1.1 increases heteromeric Kv7.3/5 currents like heteromeric Kv7.2/3, supporting the need for heteromeric channel assembly to observe SGK1.1 effects. (A) Currents elicited in Xenopus oocytes after coinjection of cDNAs from Kv7.3/5 channel alone (first panel) or in combination with wild-type SGK1.1 (second panel). (B) Peak current/voltage relationship. (C) Tail current (left) and tail currents measured at -30 mV after 0, +20 or +40 mV depolarizing pulses for the indicated construct combinations (right). Values represent mean ± SEM (Multiple t-test Holm-Sidak correction method; *p<0.05). (D) Normalized conducance. (E) Resting membrane potentials (Unpaired t-test, *p<0.05). Legends are indicated on graph B.

4.12 SGK1.1 does not affect the major repolarizing cardiac current Kv7.1/KCNE1 (I_{KS}).

Co-expression of Kv7.1 and accessory subunit KCNE1 resulted in characteristic cardiac K^+ currents, with a slower voltage-dependent activation compared to M-channel (Figure 46A). Co-expression of SGK1.1 did not have any effect neither on current amplitude, nor conductance. Accordingly, RMP was unaltered (Figure 46C-E).

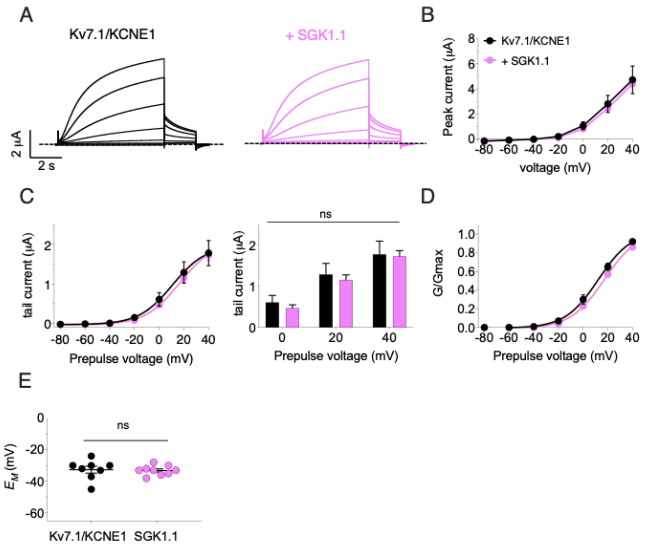

Figure 46. SGK1.1 does not affect the major repolarizing cardiac current Kv7.1/KCNE1 (I_{KS}). (A) Currents elicited in Xenopus oocytes after coinjection of cDNAs from Kv7.1/KCNE1 channel alone (first panel) or in combination with wild-type SGK1.1 (second panel). (B) Peak current/voltage relationship. (C) Tail current (left) and tail currents measured at -30 mV after 0, +20 or +40 mV depolarizing pulses for the indicated construct combinations (right). Values represent mean ± SEM (Multiple t-test Holm-Sidak correction method; ns, not significant). (D) Normalized conductance. (E) Resting membrane potentials (Unpaired t-test; ns, not significant). Legends are indicated on graph B.

4.13 Activated SGK1.1 up-regulates Kv7.2 epilepsy mutations R207W and A306T in heteromeric assembly with Kv7.3

Expression of epilepsy mutant Kv7.2(R207W) along with Kv7.3 led to smaller currents than wild type channel and with altered voltage-dependent activation kinetics,

as observed in Figure 47A and described elsewhere (Dedek et al. 2001). R207W is a *KCNQ2* mutant that neutralizes a charged amino-acid residue within the voltage sensor domain, slowing voltage-sensor dependent channel activation and resulting in BFNC (Dedek et al. 2001). Co-expression of wild type SGK1.1 did not produce any change in the amplitude of the currents. However, constitutively active SGK1.1(S515D) significantly up-regulated the tail current at different voltages (Figure 47D). RMP was not modified by any variant of the kinase (Figure 47).

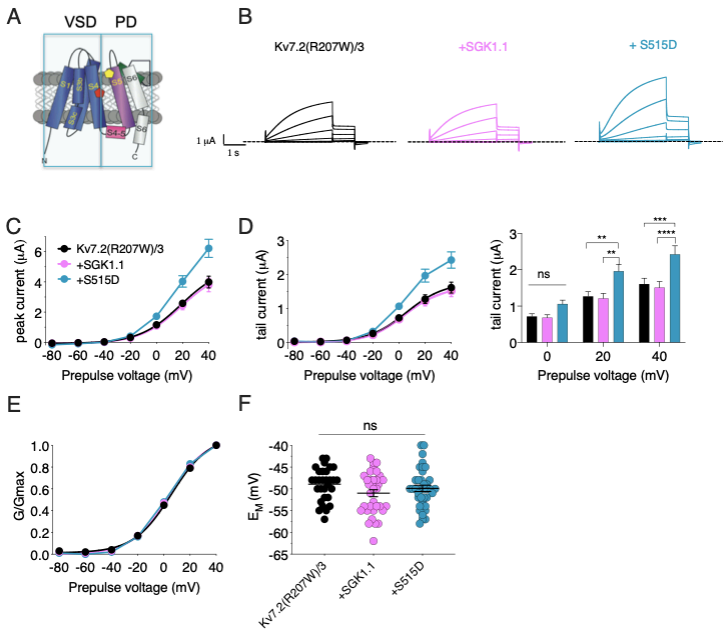

Figure 47. Constitutively active form SGK1.1(S515D) up-regulates heteromeric Kv7.2/3 channel in presence of Kv7.2 epilepsy mutation R207W while WT SGK1.1 fails to. (A) Schematic representation of Kv7 channel structure. The basic organization of potassium channels is a tetramer with each monomer containing one pore-forming domain (PD) (transmembrane segments S1-S4) and a voltage sensor domain (VSD) (transmembrane segments S5-S6). Epilepsy mutants are represented as colored pentagons (R207W in red and A306T in yellow). (B) Currents elicited in Xenopus oocytes after coinjection of cDNAs from Kv7.2(R207W)/3 channel alone (first panel) or in combination with wild-type (second panel) or constitutively active (third panel) SGK1.1. (C) Peak current/voltage relationship. (D) Tail current (left) and tail currents measured at -30 mV after 0, +20 or +40 mV depolarizing pulses for the indicated construct combinations (right). Values represent mean ± SEM (Two-way ANOVA, Tukey's correction for multiple comparisons; ns, not significant; **p<0.01; ***p>0.0005; ****p<0.0001). (D) Normalized conductance. (E) Resting membrane potentials (One-Way ANOVA, Tukey's correction for multiple comparisons; ns no significant). Legends are indicated on graph C.

Co-expression of Kv7.2(A306T) with Kv7.3 did not induce detectable currents (data not shown). Therefore, we used a previously described mutation (A315T) in the pore of Kv7.3 that greatly increases current amplitude (Gomez-Posada et al. 2011). Our lab has previously demonstrated that SGK1.1 does not affect currents elicited by Kv7.3-A315T but does increase them in the presence of the heteromeric Kv7.2/3(A315T) channel (Miranda et al. 2013). Mutation A306T is in S5 segment of Kv7.2 subunit, within the pore domain. This mutant provokes reduced currents but retains much of the biophysics characteristics of Kv7.2 (Xiong et al. 2008). When analysing the currents elicited by mutant Kv7.2(A306T) in heteromeric assembly with Kv7.3(A315T) we observed similar findings to those found with R207W. Only the expression of SGK1.1(S515D) resulted in substantial increase of the current (Figure 48C) and no changes in RMP were observed (Figure 48F).

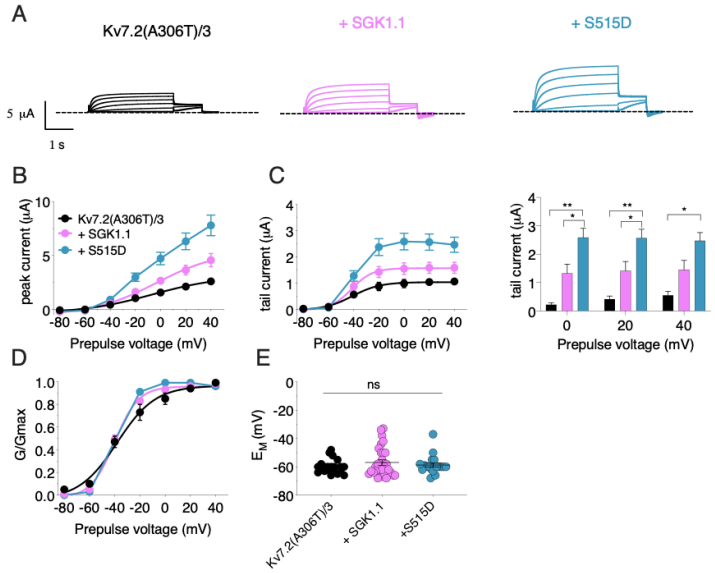

Figure 48. Constitutively active form of SGK1.1(S515D) up-regulates Kv7.2 epilepsy mutation A306T in heteromeric assembly with Kv7.3(A315T). (A) Currents elicited after coinjection of Kv7.2(A306T)/3 channel alone (first panel) or in combination with wild-type (second panel) or constitutively active (third panel) SGK1.1. (B) Peak current/voltage relationship. (C) Tail current (left) and tail currents measured at -30 mV after 0, +20 or +40 mV depolarizing pulses for the indicated construct combinations (right). Values represent mean ± SEM (Two-way ANOVA Tukey's correction for multiple comparisons; *p<0.05; **p<0.01). (D) Normalized conductance. (E) Resting membrane potentials (One-Way ANOVA, Tukey's correction for multiple comparisons; ns no significant). Legends are indicated on graph B.

In summary, our results support previously published data (Miranda et al. 2013) confirming the effect of SGK1.1 on M-current when both, Kv7.2 and Kv7.3 subunits, are expressed (Figure 43). Additionally, this time we have been able to show a similar result when expressing Kv7.3 and Kv7.5 subunits (Figure 45), which is a described combination associated to M-current (Schroeder et al. 2000; Shah et al. 2002). Expression of Kv7.4 and Kv7.5 alone did not lead to significant increases in current amplitudes (Figure 44). Similarly, SGK1.1 was not able to modulate cardiac I_{Ks} current (Figure 46). Most importantly, we wanted to evaluate the ability of SGK1.1 to regulate the M-current when it is affected by different epilepsy mutants, Kv7.2(R207W) and Kv7.2(A306T), (Singh et al. 1998; Dedek et al. 2001; Xiong et al. 2008) along with Kv7.3. Our data show that wild type SGK1.1 is unable to up-regulate the M-current when these mutants are expressed (Figures 47 and 48). Interestingly, when we co-expressed the constitutively active form of the kinase, SGK1.1(S515D), we did observe an up-regulation of the M-current.

4.14 SGK1.1 is in close proximity to Kv7.2/3 channels

On the basis of our electrophysiology results, we were interested on evaluating whether SGK1.1, Nedd4-2 and Kv7 channels are in close proximity in normal conditions and in the presence of epilepsy mutations. We used our newly developed rabbit anti-SGK1.1 to detect SGK1.1, a mouse anti-GFP to localize the tagged Kv7.2 and Kv7.3 subunits and an anti-Nedd4-2 to detect Nedd4-2. We performed the experiments on the N2a *Sgk1*-KO cells. As negative controls, we used cells transfected with NR1 and SGK1.1(S515D) and cells transfected only with the channel subunits Kv7.2 and Kv7.3.

As a control of expression of our constructs we have performed an immunocytochemistry assay on *Sgk1*-KO N2a cells to detect transfected SGK1.1, Kv7 and Nedd4-2. Our results show clear expression of SGK1.1 at the plasma membrane and expression of Kv7.2/3 and Nedd4-2 (Figure 49).

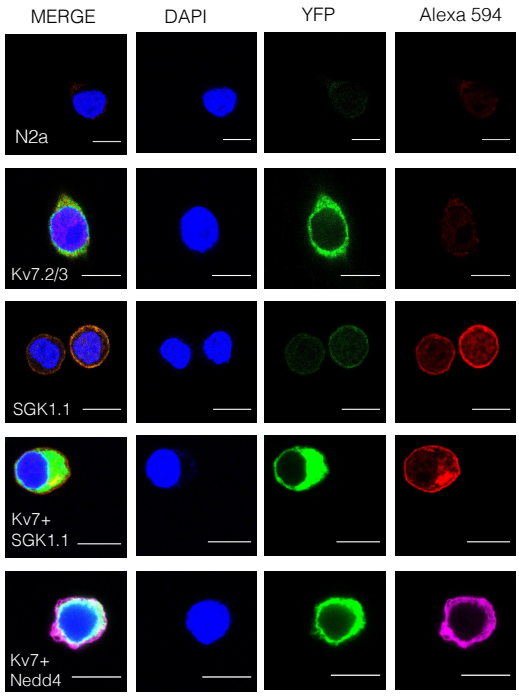

Figure 49. Representative confocal images showing expression of Kv7.2/3, SGK1.1 and Nedd4-2. 24h after transfection, *Sgk1*-KO N2a cells were permeabilized and incubated with adequate antibodies to detect each construct. Cells were stained with DAPI for nuclei detection. Transfection with Kv7 subunits was detected as green fluorescence as constructs were fused to YFP. To detect SGK1.1 we used our home-made anti-SGK1.1 and Alexa Fluor® 594 fused anti-rabbit. Nedd4-2 expression was detected with anti-Nedd4-2 and Alexa Fluor® 594 fused anti-rabbit (for a better identification Nedd4-2 signal was selected in magenta). As expected, untransfected N2a *Sgk1*-KO cells did not show signal from Kv7 nor SGK1.1 nor Nedd4-2.

As shown in Figure 50, PLA signals were significantly more numerous in cells co-expressing Kv7.2 or Kv7.3 together with activated SGK1.1(S515D) compared to the negative control cells expressing Kv7.2 and Kv7.3 alone. Our results indicate that SGK1.1(S515D) is localised in physical proximity with Kv7 channel. Co-expression of heteromeric Kv7.2/3 significantly increased the kinase association to the channel compared to homomeric Kv7.3. Differences in signal strength between homomeric and heteromeric structures suggest that association of SGK1.1(S515D) with the channel becomes facilitated in the heteromeric configuration, in agreement with previously published data showing that SGK1.1 effect requires the heteromeric assembly of

Kv7.2/3 channels (Miranda et al. 2013). Importantly, association between the kinase and the heteromeric channel was significantly impaired in the presence of K220A, a mutation in the ATP-binding cassette of the SGK1.1 that abolishes the kinase activity (Wesch et al. 2010). Also, molecular proximity between the kinase and the heteromeric channel was significantly reduced in the presence of one of the epilepsy mutations studied on this work, R207W, although PLA signals obtained from this condition were still significantly higher than those obtained from the negative control. In contrast, association levels did not change significantly in the presence of Kv7.2(A306T) (Figure 50B).

Phosphorylation at Ser448 by SGK1 has been described as a mechanism of inactivation of Nedd4-2 (Debonneville et al. 2001). As previously demonstrated, SGK1.1 also enhances levels of phosphorylation of Nedd4-2 leading to an up-regulation of Kv7.2/3 currents (Miranda et al. 2013; Armas-Capote et al. 2020). Therefore, we next wondered if we could detect the association between Nedd4-2 and SGK1.1(S515D). Our results proved that activated SGK1.1 associates with Nedd4-2, which is in agreement with previous reports suggesting a direct interaction between Kv7 and Nedd4-2 (Ekberg et al. 2007), and that this association significantly decreases in the presence of kinase dead mutant SGK1.1(K220A) (Figure 50D).

We then used PLA to evaluate the association of Nedd4-2 with the channel and the role of SGK1.1 in this complex. To do so, we transfected N2a *Sgk1*-KO cells with the indicated constructs (Figure 51A) and quantified the PLA signals given by co-expression of Kv7 and Nedd4-2 in presence or absence of SGK1.1 (Figure 51B). Our results demonstrate association between Kv7.2/3 and Nedd4-2 in basal conditions, as PLA signals were significantly augmented compared to those found in negative control cells. Importantly, the association between Kv7 and Nedd4-2 was significantly reduced when we co-expressed activated SGK1.1 but not in the presence of SGK1.1(K220A). Furthermore, association between the channel and the ubiquitin ligase was significantly diminished in presence of both epileptogenic mutations and co-expression of SGK1.1 intensified this effect in the case of Kv7.2(R207W) mutant. To gain further information about the effects of these mutations, we then tested the levels of protein expression of

Kv7.2 in both heterologous expression systems, injected oocytes and N2a cells. Both, R207W and A306T significantly decreased the abundance of the Kv7.2 in oocytes and neither WT SGK1.1 nor activated SGK1.1(S515D) increased its expression (Figure 51C-D, E-F).

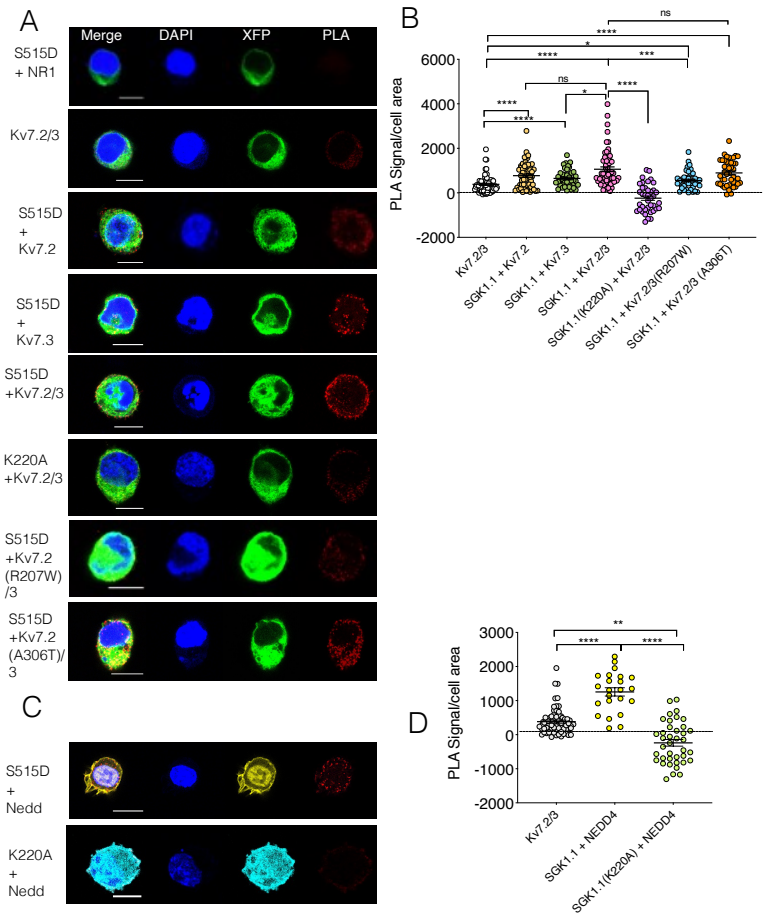

Figure 50. Association between activated SGK1.1 and heteromeric channel Kv7.2/3 is reduced in presence of epilepsy mutant Kv7.2(R207W) but not Kv7.2(A306T). (A) Proximity ligation assay (PLA) was performed on N2a *Sgk1*-KO cells transfected with the indicated constructs. Cells transfected with SGK1.1(S515D) and NR1 were used as negative control (see panel B and dotted line at 0 in panel B). (B) Quantification of PLA positive signals for each condition. (C) PLA showing signals from SGK1.1 and Nedd4-2 association. SGK1.1-transfected cells were detected as yellow/cyan bright cells depending on the plasmids used. (D) Quantification of PLA positive signals for conditions showed in C. (ANOVA Kruskal Wallis test, ns, not significant; *p<0.05; **p<0.01; ***p<0.0005 ****p<0.0001). Each dot represents an individual cell from at least three independent experiments.

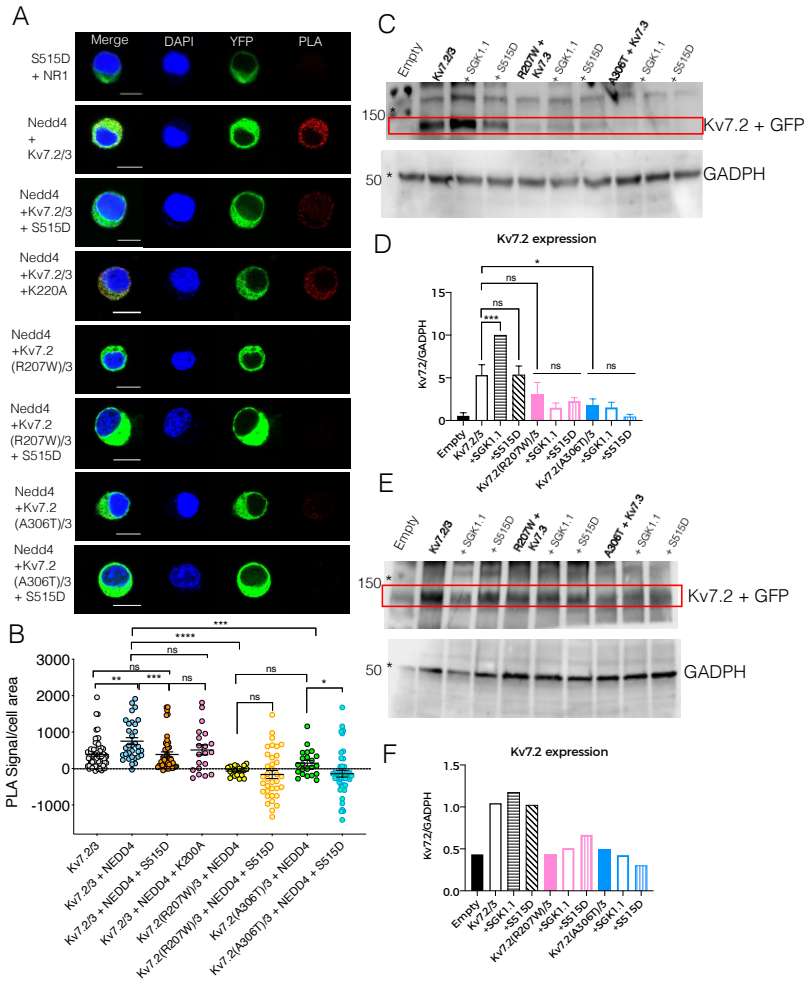

Figure 51. Kv7.2/3 heteromeric channel is located in close proximity to Nedd4-2 and this association weakens in presence of activated SGK1.1. (A) PLA was performed on N2a *Sgk1*-KO cells transfected with the indicated constructs. Dotted line at 0 represents the signal from cells transfected with SGK1.1(S515D) and NR1. (B) Quantification of PLA positive signals (ANOVA Kruskal Wallis test, ns, not significant; *p<0.05; **p<0.01; ***p<0.0005; ****p<0.0001). Each dot represents an individual cell from at least three independent experiments. (C) Representative western blot showing expression levels of Kv7.2 fused to YFP (top panel, 110 KDa) and GADPH (bottom panel, 50 KDa) from oocytes injected with the indicated constructs. (D) Quantitative analysis of Kv7.2 expression levels. Values are mean ± SEM from at least three independent experiments (ANOVA Sidak's test for multiple comparisons; ns, not significant; *p<0.05; ***p<0.0005). (E) Representative western blot showing expression levels of Kv7.2 fused to YFP (top panel, 110 KDa approximately) and GADPH (bottom panel, 50 KDa) from N2a Sgk1-KO cells transfected with the indicated constructs. Asterisks denote position of molecular weight marker. (F) Quantitative analysis of Kv7.2 expression levels.

DISCUSSION

5. DISCUSSION

In this study, we have evaluated the mechanisms of SGK1.1-mediated anticonvulsant effects, its contribution to neuroprotection after SE and the potential role of SGK1.1 activation as a therapeutic approach for hyperexcitability disorders. We have demonstrated that the ability of SGK1.1 to reduce KA-induced seizures essentially relies on M-current up-regulation. In contrast, epilepsy models that rely on muscarinic pathway activation totally counteract the effect of the kinase. Furthermore, we have proven the potent effect of SGK1.1 as a neuroprotective factor which is able to reduce levels of neuronal death and gliosis after SE in a way that is independent of the M-current modulation. Finally, we show that the activation of the kinase constitutes a strategy to up-regulate the M-current in presence of epilepsy mutations.

5.1 M-current up-regulation is the key mechanism underlying SGK1.1 mediated protection against seizures.

We have addressed the importance of the M-current on the observed anticonvulsant role of SGK1.1 using different approaches. Our data demonstrate that activation of SGK1.1 might constitute a key therapeutic approach to counteract hyperexcitability caused by excessive glutamatergic activity (Eid et al. 2004) and that it is effective only when M-channel is functional. First, we decided to evaluate the seizure behaviour in our mouse model using different epileptic paradigms. Both, XE991 + KA double treatment and PI treatment led to similar results; SGK1.1-mediated protection against seizures was abolished and both genotypes showed comparable seizure severity levels and mortality rates. As previously mentioned, PI is a M1 muscarinic agonist (Hamilton et al. 1997) leading to M-current blockade through activation of PLC and depletion of PIP_2. Similarly, XE991 directly binds to M-channel and inhibits the M-current (Zaczek et al. 1998). Therefore, these two approaches counteracted the protective effect of SGK1.1. In the case of PI it might be due to the fact that PIP_2 hydrolysis destabilizes SGK1.1 from the plasma membrane (Miranda et al. 2013) and also inhibits M-channels directly (Delmas and Brown 2005). In addition, we tested seizure behaviour in our transgenic mouse model after treatment with SGK1-specific

inhibitor EMD638683 and observed reversion of the protective effect. After treatment with EMD and KA both genotypes underwent similar levels of seizure severity and mortality rates getting close to seizure behaviour observed in WT mice treated only with KA. Given our findings, it seems that SGK1.1 protective effect relies on a functional M-channel. Although this can be taken as a limitation given the diverse epilepsy syndromes caused by Kv7.2 and Kv7.3 genetic mutations (Biervert et al. 1998; Singh et al. 1998; Dedek et al. 2001), many other forms of epilepsy can be alleviated with M-channel-mediated control of excitability. Moreover, personalized treatments directed to specific groups of patients are getting more attention from pharmacological perspectives and might constitute the future direction in clinical therapies (Abou-Khalil 2019). Further, given the news regarding retigabine and flupirtine withdrawal due to side effects, it would be useful to have new targets able to reproduce the effect on Kv7.2/3 channels without yielding the same deleterious effects, as they were not associated to the mechanism of action (Surur et al. 2019). Therefore, here we have a very promising target for the development of new treatments that has both the ability to up-regulate the M-current in the brain and the neuroprotective role that we have profusely described throughout this work.

Also important, and based on previous findings regarding the PTZ model of epilepsy (Armas-Capote 2017) and our results here, we can speculate about the absence of protective effect by SGK1.1 in the PTZ model of epilepsy. PTZ model relies on inhibitory transmission blockade to induce seizures and, because we have already demonstrated that activation of SGK1.1 is not leading to any change in basal excitatory nor inhibitory transmission, there must be another explanation underlying the differences observed between KA and PTZ models. Two different possibilities might be raised. On one hand it could be that PTZ model of epilepsy is actually also modulated by the muscarinic pathway (Gholami et al. 2012) which we have described already as a negative regulator of the M-current (Delmas and Brown 2005). In fact, other approaches directed to M-channel up-regulation resulted effective in reducing PTZ-induced seizures (Manville and Abbott 2019). Specific localization of SGK1.1 in pyramidal neurons might explain its null effect when GABAergic transmission, which is in majority occurring in interneurons, is blocked by PTZ.

Different mechanisms could explain our findings. First it could be that transgenic mice present reduced KA bioavailability. However, published results from our group (Armas-Capote et al. 2020) show comparable seizure latency values for Tg.sgk1 and WT mice, ruling out the possibility that KA reaches the brain at lower concentrations in transgenic mice. Second, it was demonstrated that expression levels of GluK receptors were unchanged in Tg.sgk1 (Armas-Capote 2017; Armas-Capote et al. 2020). Therefore, it excluded the option of a decreased response to KA in transgenic mice for this reason. Third, we have shown that both inhibitory and excitatory basal transmissions are not different between genotypes. Finally, previous results obtained in SCG cells (Miranda et al. 2013) and brain slices (Armas-Capote et al. 2020) support the hypothesis of lower neuronal excitability in relevant brain areas of transgenic mice. Also, we have demonstrated that the phosphorylation levels of Nedd4-2 are increased in hippocampus from transgenic mice, suggesting that Nedd4-2 is a phosphorylation substrate of SGK1.1. This finding supports previous results showing that in presence of SGK1.1, the ability of Nedd4-2 to target the channel for degradation is restrained (Miranda et al. 2013). Also, it has been proven that Kv7.2/3/5 respond to Nedd4-2 modulation although they lack the classical PY motif at the C-terminal region. Instead, they contain atypical PY motifs PPX-PPY and XPXPPY (Ekberg et al. 2007). Similarly, it has been demonstrated that SGK1.1 regulates ENaC and ASIC1 independently of PY motifs (Arteaga et al. 2008; Wesch et al. 2010). In agreement with this, our results here strongly support our hypothesis that SGK1.1 increases the M-channel membrane abundance through a mechanism at least partially dependent of Nedd4-2 activity.

We have also validated our findings in C57BL6/J in a different genetic background, FVB/NJ. Briefly, we demonstrated that the anticonvulsant effect of SGK1.1 is maintained in FVB mice and therefore its effect it is not restricted by genetic background. As previously reported (Royle et al. 1999; Frankel et al. 2001; Kasugai et al. 2007), we found some differences in seizure behaviour between C57 and FVB strains, with the latter presenting higher proportions of individuals reaching stages 4-6. However, we did not find higher levels of mortality compared to C57BL6/J and both, FVB.WT and FVB.Tg.sgk1, showed similar survival rates. This, along with previous

results (Armas-Capote 2017; Armas-Capote et al. 2020), demonstrates that the power of SGK1.1 as an anticonvulsant is independent of age, sex and genetic background, which commonly act as modifiers in the phenotypic effects of genetic manipulation.

5.2 SGK1.1 activation leads to a significant protection against SE-induced brain damage

One of the most frequent outcomes of status epilepticus in TLE, which is the most common form of epilepsy and the one we have modeled here, is hippocampal sclerosis. As previously mentioned, hippocampal sclerosis is characterized by pyramidal cell loss, granule cell dispersion, and axonal fiber sprouting (Blümcke et al. 2013; Thom 2014). Hippocampal sclerosis is the most common pathological finding in adults with drug-resistant TLE (Blümcke et al. 2013) and in large epilepsy surgical series it affects up to 66% of patients (Meencke et al. 1996; Novy et al. 2013). In animal models of TLE, including PI and KA, SE induces neuropathological changes such as neuronal loss in different brain regions and reorganization of mossy fibers. This abnormal reorganization has been proposed to serve as the anatomical basis for epileptogenesis (Cavalheiro et al. 1982; Ben-Ari 1985b; Tauck and Nadler 1985; Cavalheiro et al. 1991; Mathern et al. 1993; Mello et al. 1993). For instance, using EEG it has been demonstrated that KA-induced mossy fiber sprouting is strongly associated to epileptogenesis in hippocampus (Mathern et al. 1993) and in a PI model of epilepsy it was found that higher levels of cell loss correlate to longer latent periods (Mello et al. 1993). Although a growing bulk of evidence supports the viewpoint that neuroprotection does not prevent progression to acquired epilepsy (André et al. 2001; Löscher 2002; Pitkänen 2002; Brandt et al. 2003; Pitkänen 2004), some studies suggest that targeting neuronal death and inflammation pathways might be useful to alleviate the outcome of the disease. For instance, it has been shown that treatment with resveratrol after KA-induced SE restrains neurodegeneration, ectopic neurogenesis and inflammation (Mishra et al. 2015). Administration of valproate right after SE ameliorates the behavioral alterations associated to epileptogenesis including memory impairment, development delay and sensory-motor deficits (Brandt et al. 2006). Therefore, there is an increasing interest in the field of epilepsy research to develop new therapies directed to reduce the neuro- and glial pathology. Herein, we have experimentally demonstrated that

SGK1.1, which has been previously presented as a modulator of Kv7 channels (Miranda et al. 2013; Armas-Capote et al. 2020), exerts a dual role by additionally reducing seizure-induced cell damage in the brain. In contrast to other reports where it was shown that KA causes hippocampal restricted injuries (Raedt et al. 2009), we have identified neurodegenerative events in neocortical areas and amygdalar complex as well. Thus, we have shown that SGK1.1 significantly reduces the levels of neurodegeneration in hippocampus, cortex and amygdalar complex in B6 and FVB mice after KA treatment, showing a neuroprotective effect that is robust and independent of genetic background (Martin-Batista et al. 2021). This has an especial interest having into account previous reports showing strain-associated sensitivity to neuronal death. C57BL6 mice have been described as resistant to neurodegeneration and gliosis progression, whereas FVB strain is considered more vulnerable (Schauwecker and Steward 1997; McKhann et al. 2003; Kasugai et al. 2007). Although we have observed neuronal injury in both strains, FVB mice showed higher levels of neurodegeneration in all the analyzed brain areas compared to B6 counterparts.

Mechanisms involved in neuroprotection could coincide with those associated to a lesser seizure behaviour or imply additional ones. Different studies have shown that a reduced number of seizures leads to decreased brain damage (Henshall et al. 2013) and other M-current activators such as retigabine have been proven to exert a neuroprotective role only when seizures were significantly attenuated (Friedman et al. 2015). However, in our study we restricted our analysis to those mice reaching the most severe Racine stage (6) and observed that Tg.sgk1 brain injury was still reduced or absent in some regions. Therefore, we hypothesized that there must be an additional protection mechanism beyond decreased seizure severity. Acute kinase inhibition with the specific inhibitor EMD638683 led to equal levels of neuronal death in both genotypes but, to further evaluate the role of M-current up-regulation on neuroprotection, we used a different approach. Acute pre-treatment with the specific Kv7-blocker XE991 gave us an insight into a potential additional role of SGK1.1. Animals treated with XE991 and KA showed similar levels of neurodegeneration between genotypes. Strikingly, transgenic mice still showed significantly reduced neuronal death levels in piriform cortex (Martin-Batista et al. 2021). Importantly, evidence suggests that piriform cortex (PIRC) represents one of the earliest sites of neuronal loss after SE

(Scholl et al. 2013) and that due to excitability and connectivity properties of the area it is considered to be implicated in seizure generation and propagation (for a review, see Vismer et al. 2015). Our results suggest that activation of SGK1.1 modulates pathways preventing neuronal death independently of its role in membrane Kv7 modulation. Also, the fact that pharmacological inhibition of the kinase abolished the neuroprotective effect rules out the possibility of the observed effects being a consequence of long-term changes induced by the expression of the transgene. Different studies have demonstrated that seizure-induced neuronal loss can be diminished by molecular and pharmacological approaches limiting apoptotic cell death (Henshall et al. 2002; Roy et al. 2002). Interestingly, SGK1 isoforms share high homology to the catalytic domain of the well described anti-apoptotic kinase AKT (Kobayashi et al. 1999). Both AKT and its upstream activator PI3K have been demonstrated to reduce apoptosis and promote neuronal survival in the central nervous system (Datta et al. 1997; Crowder and Freeman 1998). The ubiquitous isoform SGK1 shows cell-survival and anti-apoptotic effects (Brunet et al. 2001; Ferrelli et al. 2015) and has been linked to neuroprotection in stroke (McCaig et al. 2019; Wang et al. 2019). Here, we have shown that the mechanism underlying this observed SGK1.1-mediated protection against neuronal death relies at least partially on the role of this kinase as an anti-apoptotic factor in the brain. First, our results show that SGK1.1 activation reduces H_2O_2-induced apoptosis similarly to AKT (Martin-Batista et al. 2021). Further, the existence of such homology makes it tempting to hypothesize that both kinases might share downstream substrates, including the anti-apoptotic transcriptional factor Bim, which has been related to SE-induced brain damage along with FoxO3a and caspase-3 (Kim et al. 2014). In line with this hypothesis, we have now showed that activation of SGK1.1 in Tg.sgk1 mice reduces Bim protein levels in hippocampus and up-regulates the expression of Bcl-x_L (Martin-Batista et al. 2021). Importantly, both members of the Bcl-2 family have been described as key regulators of the mitochondrial (intrinsic) apoptotic pathway (Youle and Strasser 2008) and related to seizure-induced brain damage (Murphy et al. 2010; Kim et al. 2014). Increased levels of Bim have been found in mice and rats after KA-induced SE and Bim-deficient mice show reduced levels of neurodegeneration (Putcha et al. 2001; Murphy et al. 2010). Bim localizes to intracellular membranes, where it has been proposed to induce apoptotic cell death via caspase activation (O'Connor et al. 1998).

This proapoptotic effect is blocked by interaction with Bcl-x_L, an anti-apoptotic factor found in mature neurons in the adult brain. Accordingly, Bcl-x_L-deficient mice show massive neuronal cell death (Motoyama et al. 1995). Our results showing modulation of both factors in transgenic mice are consistent with the observed reduced levels of neurodegeneration associated to activation of SGK1.1.

A potential implication of the anti-apoptotic role of SGK1.1 could be the existence of deleterious pro-proliferative effects (Brunet et al. 2001). In the framework of the observed neuroprotective effects of SGK1.1 activation, and taken into account previous reports of SGK1 effects (Anacker et al. 2013), we were especially concerned about the potential induction of aberrant hippocampal neurogenesis in the DG (Parent et al. 2006). It has been proposed that ectopic neurogenesis after seizure-induced damage could result in the alteration of neuronal electrophysiological properties, contributing to the generation of hyperexcitable circuits. This process has been involved in the maintenance of epileptic activity (Ribak et al. 2000; Parent et al. 2006). Conversely, some recent studies suggest that adult neurogenesis in the mouse DG might protect the hippocampus from neurodegeneration after PI-induced SE (Jain et al. 2019). Our data did not reveal significant differences in the levels of ectopic neurogenesis in the DG of Tg.sgk1 *vs.* WT mice, ruling out this possibility. It would be interesting to address whether there is any difference in ectopic neurogenesis between transgenic and wild type mice after KA treatment, both in acute conditions as well in animals undergoing recurrent spontaneous seizures.

Another common feature found in the resected hippocampi of TLE patients and animal models are proinflammatory mediators, reactive astrocytes and microgliosis, which might contribute to the disease development (Benkovic et al. 2004; Aronica et al. 2007; Van Gassen et al. 2008; Ravizza et al. 2008; Zanuzzi et al. 2019). However, how non-neuronal cells act on the progression of epilepsy is still debated. Thus, while it is well known that glial cells have important roles on the reparation of neuronal tissue post-injury, there are also some substances produced by astrocytes and microglia that can contribute to the neuropathological events in CNS diseases (for a clarifying review see Patel et al. 2019). For example, some studies have shown that levels of microgliosis and astrogliosis reach a peak at day 3 after KA-injection and then decrease at around day

7-9, consistent with the idea of inflammatory responses being necessary to repair the tissue (Zanuzzi et al. 2019). In contrast, animal models with genetically induced widespread gliosis and without other pathologies, developed spontaneous and recurrent seizures (Robel et al. 2015). In the present work, we have demonstrated that while SGK1.1 is not expressed in astrocytes, its neuronal activation prevents reactive gliosis in transgenic mice independently of genetic background, limiting the extent of overall brain damage (Martin-Batista et al. 2021). Thus, our results support the idea that, at least in the animal model we studied, gliosis occurs as a consequence of neuronal death. In order to ensure that the results were not due to the injection itself, we also performed the gliosis analysis on saline injected mice, where we observed basal lower levels of reactive astroglia and microglia and no differences between genotypes (data not shown).

Although epilepsy research has allowed to develop and improve different available treatments, there is still a great need for approaches able to control seizures in approximately 30% of the patients showing resistance to AEDs (Löscher and Schmidt 2011). New strategies suitable to diminish and reduce brain damage after SE might help to prevent the progression of the disease as well as the deterioration of neuronal tissue, which is usually accompanied by a long list of comorbidities and psychiatric dysfunctions (Tellez-Zenteno et al. 2007; Elliott et al. 2009; Kanner et al. 2010).

5.3 SGK1.1 activation up-regulates M-channel in presence of epilepsy mutations

On this work we have validated previous results showing the up-regulating effect of SGK1.1 on heteromeric channel Kv7.2/3 (Miranda et al. 2013), expanded them to other homo- and heteromeric combinations such as Kv7.3/5 and, for the first time, we have evaluated the effect of constitutively active SGK1.1 (mutant S515D, used in our transgenic mouse model). Our results suggest that activation of the kinase does not lead to an additional effect on M-current in oocytes, which might be explained by the already high levels of expression and/or activation state of wild type SGK1.1 once injected. Thus, we would be observing the maximum response already with wild type SGK1.1.

Regarding homomeric channels, we have shown that SGK1.1 fails to up-regulate Kv7.4 alone and, in fact, it produced an inhibitory effect at some prepulses of voltage. Importantly, Kv7.4 is a subunit mainly expressed in smooth muscle and ear, in contrast to the neuronal expression of SGK1.1 what makes it quite improbable to find a physiological situation where both proteins can be co-expressed and working together. However, some experiments have suggested low levels of expression in heart, brain and skeletal muscle and demonstrated that Kv7.4 assembles with Kv7.3 to produce a current comparable to M-current (Kubisch et al. 1999). Therefore, it would be interesting to address the effect of the kinase in presence of the heteromeric channel Kv7.3/4. SGK1.1 enhanced heteromeric Kv7.3/5 currents like heteromeric Kv7.2/3, supporting the need of heteromeric channel assembly to observe SGK1.1 effect as demonstrated before (Miranda et al. 2013). Given that SGK1-1 appears to up-regulate heteromers by stabilizing them in the membrane (Miranda et al. 2013), the lack of effect in homomeric channels suggests that their membrane stability may be regulated through a different pathway. It is important to note that Kv7.5 is expressed in brain, can form heteromeric channels with Kv7.3 and yields currents that can be inhibited by M1 muscarinic receptor activation (Schroeder et al. 2000). Therefore, the ability of SGK1.1 to up-regulate Kv7.3/5-elicited M-currents may be responsible for some of the anti-convulsant activity of the kinase. In fact, some studies demonstrating activation of Kv7.3/5 by retigabine suggested it could constitute a molecular target for this agent along with Kv7.2/3 (Wickenden et al. 2001).

Importantly, SGK1.1 was not able to modulate the major repolarizing cardiac current elicited by Kv7.1/KCNE1, ruling out the possibility of adverse side effects due to cardiac currents modulation. Although retigabine does not target cardiac potassium channels either (Gunthorpe et al. 2012), it targets Kv7 subtypes expressed in the periphery, such as the urothelium, provoking dysuria and other adverse effects (Clark et al. 2015). SGK1.1 is a very promising therapeutic target for epilepsy as it shares the mechanism of action of retigabine without the risk of activating potassium channels expressed in non-neuronal cell types. In any rate, this is a remote possibility since we have not detected SGK1.1 expression outside neurons.

As previously mentioned, among the different causes for epilepsy, genetic mutations affecting the functionality of Kv7.2-5 channels have been described in diverse forms of the disease. Herein, we have assessed the ability of SGK1.1 to up-regulate the M-current in the presence of two epilepsy mutations. Our results show that only when the kinase is constitutively active it can significantly up-regulate both, Kv7.2(R207W) and Kv7.2(A306T). Mutation R207W neutralizes a charged amino acid residue within the channel's voltage sensor domain and slows the voltage-sensor dependent activation, which can be easily perceived from the detected macroscopic currents. Moreover, and based on our results herein, it seems to yield to reduced protein expression at least in heterologous systems. This mutation results in BFNC and myokymia (Dedek et al. 2001). Myokymia results from hyperexcitability of the lower motor neurons where Kv7.2 seems to be expressed. Therefore, the effects of R207W are not limited to the brain. Further studies to examine the expression of SGK1.1 in the peripheral nervous system would be valuable. A306T is located in S6 segment and is associated to BFNC. As in the case of R207W, we have demonstrated herein that the presence of this modification in Kv7.2 provokes a reduction in the protein expression levels. Thus, our findings might contribute to the diagnosis of patients carrying these mutations because, other than being affected by the inner malfunction of the mutated channel, we can now suggest that the expression of the protein and the ability of wild type SGK1.1 to up-regulate it are disturbed. Therefore, activated SGK1.1 could constitute a strategy to increase the M-current in the presence of mutations that diminish this potassium current. Whether or not pharmacological activation of SGK1.1 might constitute a potential therapeutic approach should be further addressed.

As part of our interest in further understanding the effect of these mutants on SGK1.1 mechanism of action, we evaluated the physical proximity between the kinase and the channel by PLA. Our results demonstrated the molecular association of SGK1.1 with homo- and heteromeric Kv7.2/3, although PLA signals were significantly enhanced in heteromeric assembly conditions compared to homomeric Kv7.3. These findings support previous reports showing that SGK1.1 is only able to up-regulate the channel in heteromeric assembly (Miranda et al. 2013). The fact that SGK1.1 still associates to, but fails to regulate homomeric channels further supports our hypothesis that the mechanism controlling their plasma membrane levels is different from the one

regulating heteromeric combinations of Kv7 subunits. Association of SGK1.1 to the heteromeric channel was significantly impaired by the inactive mutant SGK1.1(K220A), suggesting that the catalytic activity of the kinase is crucial for its interaction with the channel and in agreement with previous results (Miranda et al. 2013). In addition, we were able to detect association of Nedd4-2 to SGK1.1 and, most importantly, to Kv7 channels in a SGK1.1-dependent manner. As observed in section 1, our results demonstrate the ability of SGK1.1 to increase phosphorylation of Nedd4-2 at residue Ser448 (Armas-Capote et al. 2020), similarly to SGK1. Ser448 phosphorylation is known to repress ubiquitination activity of Nedd4-2 (Debonneville et al. 2001), and might prevent M-channel degradation, stabilizing it in the membrane. Consistently, SGK1.1 is able to displace Nedd4-2 from its interaction with the M-channel.

Interestingly, co-expression of SGK1.1 with Kv7.2 epilepsy mutants produced divergent results. R207W mutant led to significant reduced levels of association to SGK1.1, which may be explained by the reduced channel subunit expression associated to the mutation. However, mutant A306T did not alter the association with the kinase, even in the presence of reduced protein abundance. Therefore, it appears that overall Kv7 subunit abundance is not a predictor of SGK1.1 association, which may be compartment-specific and depend on the relative abundance of the channel in the plasma membrane vs. intracellular compartments. In contrast, association between Nedd4-2 and Kv7 was significantly reduced in the presence of both epilepsy mutations. It may be that the presence of these mutations in the aminoacidic chain of the channel disturbs the ability of Nedd4-2 to interact with it. From this, it would be expected that the levels of expression at the membrane were higher and the currents were bigger. Nevertheless, currents elicited by these mutants are smaller than wild type which might be explained by the nature of the mutations and/or their lower expression levels. Regarding R207W, its interaction with SGK1.1 is significantly reduced compared to the WT channel although still significantly increased compared to the control. Therefore, given that interaction between Nedd4-2 and Kv7.2/3 diminishes in presence of this mutation, it could be that the complex composed by the three proteins breaks out and, although SGK1.1 interacts with Nedd4-2, the proximity with the channel is disturbed, explaining the lower levels of association observed between them.

In summary, it seems clear that SGK1.1 can still interact with the M-channel independently of the presence of Nedd4-2 in the complex. Because the protein expression levels of the channel in injected *Xenopus* oocytes were significantly reduced in presence of both mutations and because we did observe an up-regulating effect of the M-current by SGK1.1(S515D), we now wonder if there is any additional role of the kinase independent of Nedd4-2 pathway. For example, direct phosphorylation of the channel. Previous data from our lab have already elucidated that the inactive kinase K220A does not produce any effect on the M-channel (Miranda et al. 2013). Thus, altogether it seems that the kinase activity is needed for the up-regulation of the channel. Kv7 channel presents interaction sites for the phosphorylation reactions on serine, threonine and tyrosine residues (Ismailov and Benos 1995). For instance, the cytoplasmic N-terminal domain of Kv7.2 contains a consensus site for cAMP-dependent phosphorylation by PKA that is required for its stimulation by cAMP (Schroeder et al. 1998) and mass spectrometry studies have revealed different sites in S4-S5 loop of Kv7.2/3 within a sequence highly conserved among *KCNQ* family members (Surti et al. 2005). PKA phosphorylation consensus sequence overlaps with that of SGK1, and not only phosphorylates Kv7 but also Nedd4-2 at the same sites as SGK1. Hence it would be possible that SGK1.1 phosphorylates the channel likewise (Snyder et al. 2004). As it has been proposed for SGK1 (Bongiorno et al. 2011), it may be that SGK1.1 can interact directly with the RXRXXS/T consensus motif in the subunits of ion channels and/or via its PY motif indirectly with Nedd4-2. It would be convenient to test whether or not SGK1.1 is able to phosphorylate Kv7 channel subunits even though, so far, the consensus phosphorylation motif of SGK1 is not present neither in Kv7.3 nor in Kv7.2. This motif is identical to AKT's as expected from their similar catalytic domains. The use of specific antibodies targeting this motif has allowed the identification of AS160 as a substrate of AKT containing one Rab GAP (GTPase activating protein) domain (Kane et al. 2002). Rab proteins family are involved in membrane trafficking. Whether or not these proteins are also substrates of SGK1.1 should be addressed if we are to shed some light onto alternative mechanisms up-regulating the M-channel.

It is clear from our data that the interaction between SGK1.1/Nedd4-2/Kv7 is complex and may depend not only on total protein abundance, but also on enzymatic activity, subcellular localization and the presence or absence of certain epilepsy

mutations. Regardless of the mechanism, the fact that SGK1.1(S515D) significantly up-regulates the current might constitute a therapeutic target for patients carrying these mutations.

5.4 Summary, limitations, and future perspectives

The results presented on this thesis, together with other findings already published by our group, demonstrate that the expression of a constitutively active form of SGK1.1 constitutes a strategy to reduce seizures along with a wide spectrum of epilepsy-related alterations, including neuronal injury and gliosis. How well our results translate to human disease remains unexplored, but TLE models of epilepsy including the KA model, have been extensively used for the screening of AEDs that might be useful to treat drug resistant epilepsy (Löscher 2017). For example, carbamazepine and topiramate have been tested in systemic administered KA models of TLE (Grabenstatter et al. 2005; Grabenstatter et al. 2007; Ali et al. 2012; Grabenstatter and Dudek 2019). However, given the marked differences found between models, it is recommended to test on a series of models that contribute to the identification of specific limitations. In our case, the use of different models allowed us to gain further information regarding the mechanism of action of SGK1.1, although the protective effect of the transgene was only observable in the KA paradigm.

Also, it is important to consider that the transgenesis system that we have used maintains the endogenous promoter of the *Sgk1* gene and therefore the expression of the different isoforms follows their physiological patterns. Although it has been proven that SGK1.1 is the most abundant form in the brain (Arteaga et al. 2008), our model makes it difficult to attribute the observed anticonvulsant and neuroprotective effects exclusively to the presence of the neuronal isoform. Therefore, side effects due to SGK1 activity should also be considered. For instance, several reports mention the pro-proliferative effect of SGK1, which might lead to cancer, fibrosis and ectopic neurogenesis (Terada et al. 2008; Fagerli et al. 2011; Hall et al. 2012; Anacker et al. 2013). Nevertheless, no abnormal tumorigenesis has been observed in our mice (Sierra Ramos 2017) and we have not found increased ectopic neurogenesis compared to wild type mice. However, B6.Tg.sgk1 have shown levels of hypertension significantly higher

compared to B6.WT in a context of high-fat diet (Sierra Ramos 2017), indicating a potential complication of systemically increasing SGK1 activity. In addition, modulation of M-current has been related to some behavioral alterations (Fontán-Lozano et al. 2011; Hayashi et al. 2014) that should be considered when analyzing a new AED targeting the M channel. Our group performed a series of behaviour experiments showing no effect of the transgene in memory, anxiety-related conduct or locomotor and exploratory activity (Armas-Capote 2017). With all this, we propose to work on the design of specific SGK1.1 activators or agents able to reproduce its mechanism of action. M-current up-regulation remains as a very promising strategy that is being explored in order to develop more efficient AEDs after retigabine and flupirtine retrieval off the market (Surur et al. 2019). As mentioned before and based on our results, investigating the ability of SGK1.1 to phosphorylate Kv7 is likewise interesting and might open new therapeutic approaches. Different experimental approaches exist to evaluate the presence of particular phosphorylation modifications, including the design of specific antibodies, a technique already optimized in our group.

Regarding protection against brain damage, our results clearly support the hypothesis of SGK1.1 exerting an anti-apoptotic role that modulates different mediators of cell death associated to SE-induced brain injury. Kim et al., (2014) found that SE reduced the interaction between AKT and FoxO3a, leading to the consequent up-regulation of Bim. Similarly, it would be possible that the effect of SE in our TLE model has been restrained by SGK1.1, which might be targeting FoxO3a for phosphorylation and therefore yielding to the observed decreased levels of Bim in hippocampus from Tg.sgk1 mice. Modulation of apoptotic factors is supported by the observed reduction in neurodegeneration and gliosis, both measured 3 days after KA. In order to assess the effect of neuroprotection on epileptogenesis, it would have been interesting to evaluate behaviour and SRSs appearance in WT and Tg.sgk1 mice along time. Development of a chronic model of epilepsy to further evaluate these processes can be suggested from this work as a new line of study.

The electrophysiological study using *Xenopus* oocytes has allowed us to elucidate the potential ability of SGK1.1 to up-regulate the M-channel in presence of epileptogenic mutations. However, a step further would be to address this question in

animal models expressing these mutations. Treatment of these mice with an M-current activator such as retigabine could give us a first insight and the design of a SGK1.1 activator would be greatly valuable to advance on the study of its potential as therapeutic target in epileptic conditions related to these mutations. A novel project could in fact originate from this basis.

CONCLUSIONS

6. CONCLUSIONS

1. M-current up-regulation is the key mechanism for SGK1.1-mediated protection against KA-induced seizures, independently of genetic background
2. SGK1.1 limits brain damage after SE through M-current-dependent and independent mechanisms, being the latter due to its antiapoptotic activity.
3. Activated SGK1.1 rescues the activity of mutant Kv7.2/3 channels containing epileptogenic mutations.
4. We propose SGK1.1 as a potential therapeutic target to treat hyperexcitability related disorders like epilepsy.

REFERENCES

7.REFERENCES

Abou-Khalil BW. 2019. Update on Antiepileptic Drugs 2019. Contin. Lifelong Learn. Neurol. 25:508–536. doi:10.1212/CON.0000000000000715.

Ackermann TF, Boini KM, Beier N, Scholz W, Fuchß T, Lang F. 2011. EMD638683 , a Novel SGK Inhibitor with Antihyper- tensive Potency. Cell. Physiol. Biochem.:137–146.

Afonso-Oramas D, Cruz-Muros I, Barroso-Chinea P, Alvarez de la Rosa D, Castro-Hernandez J, Salas-Hernandez J, Giraldez T, Gonzalez-Hernandez T. 2010. The dopamine transporter is differentially regulated after dopaminergic lesion. Neurobiol. Dis. 40:518–530. doi:10.1016/j.nbd.2010.07.012.

Ahmed Z, Shaw G, Sharma VP, Yang C, McGowan E, Dickson DW. 2007. Actin-binding Proteins Coronin-1a and IBA-1 are Effective Microglial Markers for Immunohistochemistry. J. Histochem. Cytochem. 55:687–700. doi:10.1369/jhc.6A7156.2007.

Alexander S, Mathie A, Peters J. 2010. Ion Channels*. In: Comprehensive Toxicology. Vol. 164. Elsevier. p. 129–171.

Ali A, Dua Y, Constance JE, Franklin MR, Dudek FE. 2012. A once-per-day, drug-in-food protocol for prolonged administration of antiepileptic drugs in animal models. Epilepsia 53:199–206. doi:10.1111/j.1528-1167.2011.03314.x.

Allen Hauser W, Annegers JF. 1996. Descriptive epidemiology of epilepsy: Contributions of population-based studies from rochester, minnesota. Mayo Clin. Proc. 71:576–586. doi:10.4065/71.6.576.

Almeida A. 2013. Genetic determinants of neuronal vulnerability to apoptosis. Cell. Mol. Life Sci. 70:71–88. doi:10.1007/s00018-012-1029-y.

Alvarez de la Rosa D, Zhang P, Náray-Fejes-Tóth A, Fejes-Tóth G, Canessa CM. 1999. The serum and glucocorticoid kinase sgk increases the abundance of epithelial sodium channels in the plasma membrane of Xenopus oocytes. J. Biol. Chem. 274:37834–37839. doi:10.1074/jbc.274.53.37834.

Anacker C, Cattaneo A, Musaelyan K, Zunszain PA, Horowitz M, Molteni R, Luoni A, Calabrese F, Tansey K, Gennarelli M, et al. 2013. Role for the kinase SGK1 in stress, depression, and glucocorticoid effects on hippocampal neurogenesis. Proc. Natl. Acad. Sci. U. S. A. 110:8708–8713. doi:10.1073/pnas.1300886110.

Andersen MN, Krzystanek K, Petersen F, Bomholtz SH, Olesen SP, Abriel H, Jespersen T, Rasmussen HB. 2013. A phosphoinositide 3-Kinase (PI3K)-serum- and glucocorticoid-inducible

Kinase 1 (SGK1) pathway promotes Kv7.1 channel surface expression by inhibiting Nedd4-2 protein. J. Biol. Chem. 288:36841–36854. doi:10.1074/jbc.M113.525931.

André V, Ferrandon A, Marescaux C, Nehlig A. 2001. Vigabatrin protects against hippocampal damage but is not antiepileptogenic in the lithium-pilocarpine model of temporal lobe epilepsy. Epilepsy Res. 47:99–117. doi:10.1016/S0920-1211(01)00299-6.

Armas-Capote N. 2017. The serum and glucocorticoids regulated kianse 1.1 (SGK1.1) as an anticonvulsant factor. Universidad de La Laguna.

Armas-Capote N, Maglio LE, Pérez-Atencio L, Martin-Batista E, Reboreda A, Barios JA, Hernandez G, Alvarez de la Rosa D, Lamas JA, Barrio LC, et al. 2020. SGK1.1 Reduces Kainic Acid-Induced Seizure Severity and Leads to Rapid Termination of Seizures. Cereb. Cortex 30:3184–3197. doi:10.1093/cercor/bhz302.

Aronica E, Boer K, van Vliet EA, Redeker S, Baayen JC, Spliet WGM, van Rijen PC, Troost D, Lopes da Silva FH, Wadman WJ, et al. 2007. Complement activation in experimental and human temporal lobe epilepsy. Neurobiol. Dis. 26:497–511. doi:10.1016/j.nbd.2007.01.015.

Arteaga MF, Coric T, Straub C, Canessa CM. 2008. A brain-specific SGK1 splice isoform regulates expression of ASIC1 in neurons. Proc. Natl. Acad. Sci. U. S. A. 105:4459–4464. doi:10.1073/pnas.0800958105.

Arteaga MF, Wang L, Ravid T, Hochstrasser M, Canessa CM. 2006. An amphipathic helix targets serum and glucocorticoid-induced kinase 1 to the endoplasmic reticulum-associated ubiquitin-conjugation machinery. Proc. Natl. Acad. Sci. U. S. A. 103:11178–11183. doi:10.1073/pnas.0604816103.

Arundine M, Tymianski M. 2003. Molecular mechanisms of calcium-dependent neurodegeneration in excitotoxicity. Cell Calcium 34:325–337. doi:10.1016/S0143-4160(03)00141-6.

Auladell C, De Lemos L, Verdaguer E, Ettcheto M, Busquets O, Lazarowski A, Beas-Zarate C, Olloquequi J, Folch J, Camins A. 2017. Role of JNK isoforms in the kainic acid experimental model of epilepsy and neurodegeneration. Front. Biosci. - Landmark 22:795–814. doi:10.2741/4517.

Barhanin J, Lesage F, Guillemare E, Fink M, Lazdunski M, Romey G. 1996. KvLQT1 and IsK (minK) proteins associate to form the IKS cardiac potassium current. Nature 384:78–80. doi:10.1038/384078a0.

Bartolomei F, Khalil M, Wendling F, Sontheimer A, Régis J, Ranjeva JP, Guye M, Chauvel P. 2005. Entorhinal cortex involvement in human mesial temporal lobe epilepsy: An

electrophysiologic and volumetric study. Epilepsia 46:677–687. doi:10.1111/j.1528-1167.2005.43804.x.

Ben-Ari Y. 1985a. Limbic seizure and brain damage produced by kainic acid: Mechanisms and relevance to human temporal lobe epilepsy. Neuroscience 14:375–403. doi:10.1016/0306-4522(85)90299-4.

Ben-Ari Y. 1985b. Limbic seizure and brain damage produced by kainic acid: Mechanisms and relevance to human temporal lobe epilepsy. Neuroscience 14:375–403. doi:10.1016/0306-4522(85)90299-4.

Ben-Ari Y, Cossart R. 2000. Kainate, a double agent that generates seizures: Two decades of progress. Trends Neurosci. 23:580–587. doi:10.1016/S0166-2236(00)01659-3.

Ben-Ari Y, Lagowska J. 1978. [Epileptogenic action of intra-amygdaloid injection of kainic acid]. C. R. Acad. Sci. Hebd. Seances Acad. Sci. D. 287:813–6.

Ben-Ari Y, Lagowska J, Tremblay E, Le Gal La Salle G. 1979. A new model of focal status epilepticus: intra-amygdaloid application of kainic acid elicits repetitive secondarily generalized convulsive seizures. Brain Res. 163:176–179. doi:10.1016/0006-8993(79)90163-X.

Ben-Ari Y, Tremblay E, Ottersen OP, Meldrum BS. 1980. The role of epileptic activity in hippocampal and 'remote' cerebral lesions induced by kainic acid. Brain Res. 191:79–97. doi:10.1016/0006-8993(80)90316-9.

Ben-Ari Y, Tremblay E, Riche D, Ghilini G, Naquet R. 1981. Electrographic, clinical and pathological alterations following systemic administration of kainic acid, bicuculline or pentetrazole: Metabolic mapping using the deoxyglucose method with special reference to the pathology of epilepsy. Neuroscience 6:1361–1391. doi:10.1016/0306-4522(81)90193-7.

Benkovic SA, O'Callaghan JP, Miller DB. 2004. Sensitive indicators of injury reveal hippocampal damage in C57BL/6J mice treated with kainic acid in the absence of tonic-clonic seizures. Brain Res. 1024:59–76. doi:10.1016/j.brainres.2004.07.021.

Biervert C, Schroeder BC, Kubisch C, Berkovic SF, Propping P, Jentsch TJ, Steinlein OK. 1998. A potassium channel mutation in neonatal human epilepsy. Science (80-.). 279:403–406. doi:10.1126/science.279.5349.403.

Binder, Devin K.; Scharfman HE. 1997. Recent advances in epilepsy research.

Blümcke I, Thom M, Aronica E, Armstrong DD, Bartolomei F, Bernasconi A, Bernasconi N, Bien CG, Cendes F, Coras R, et al. 2013. International consensus classification of hippocampal sclerosis in temporal lobe epilepsy: A Task Force report from the ILAE Commission on Diagnostic Methods. Epilepsia 54:1315–1329. doi:10.1111/epi.12220.

Boise LH, González-García M, Postema CE, Ding L, Lindsten T, Turka LA, Mao X, Nuñez G, Thompson CB. 1993. Bcl-X, a Bcl-2-Related Gene That Functions As a Dominant Regulator of Apoptotic Cell Death. Cell 74:597–608. doi:10.1016/0092-8674(93)90508-N.

Bongiorno D, Schuetz F, Poronnik P, Adams DJ. 2011. Regulation of voltage-gated ion channels in excitable cells by the ubiquitin ligases Nedd4 and Nedd4-2. Channels 5:79–88. doi:10.4161/chan.5.1.13967.

Bonilha L, Elm JJ, Edwards JC, Morgan PS, Hicks C, Lozar C, Rumboldt Z, Roberts DR, Rorden C, Eckert MA. 2010. How common is brain atrophy in patients with medial temporal lobe epilepsy? Epilepsia 51:1774–1779. doi:10.1111/j.1528-1167.2010.02576.x.

Brandt C, Gastens AM, Sun M zhen, Hausknecht M, Löscher W. 2006. Treatment with valproate after status epilepticus: Effect on neuronal damage, epileptogenesis, and behavioral alterations in rats. Neuropharmacology 51:789–804. doi:10.1016/j.neuropharm.2006.05.021.

Brandt C, Potschka H, Löscher W, Ebert U. 2003. N-methyl-D-aspartate receptor blockade after status epilepticus protects against limbic brain damage but not against epilepsy in the kainate model of temporal lobe epilepsy. Neuroscience 118:727–740. doi:10.1016/S0306-4522(03)00027-7.

Brodie MJ, Barry SJE, Bamagous GA, Norrie JD, Kwan P. 2012. Patterns of treatment response in newly diagnosed epilepsy. Neurology 78:1548–1554. doi:10.1212/WNL.0b013e3182563b19.

Brown D. 1987. M-currents: an update.

Brown DA. 2008. Kv7 (KCNQ) potassium channels that are mutated in human diseases. J. Physiol. 586:1781–1783. doi:10.1113/jphysiol.2008.153007.

Brown DA, Adams PR. 1980. Muscarinic suppression of a novel voltage-sensitive K+ current in a vertebrate neurone. Nature 283:673–676.

Brown DA, Passmore GM. 2009. Neural KCNQ (Kv7) channels. Br. J. Pharmacol. 156:1185–1195. doi:10.1111/j.1476-5381.2009.00111.x.

Brunet A, Park J, Tran H, Hu LS, Hemmings BA, Greenberg ME. 2001. Protein Kinase SGK Mediates Survival Signals by Phosphorylating the Forkhead Transcription Factor FKHRL1 (FOXO3a). Mol. Cell. Biol. 21:952–965. doi:10.1128/MCB.21.3.952-965.2001.

Candelario-Jalil E, Al-Dalain SM, Castillo R, Martnez G, Fernndez OSL. 2001. Selective vulnerability to kainate-induced oxidative damage in different rat brain regions. J. Appl. Toxicol. 21:403–407. doi:10.1002/jat.768.

Carriero G, Arcieri S, Cattalini A, Corsi L, Gnatkovsky V, De Curtis M. 2012. A guinea pig model of mesial temporal lobe epilepsy following nonconvulsive status epilepticus induced by unilateral

intrahippocampal injection of kainic acid. Epilepsia 53:1917–1927. doi:10.1111/j.1528-1167.2012.03669.x.

Cavalheiro EA, Leite JP, Bortolotto ZA, Turski WA, Ikonomidou C, Turski L. 1991. Long-Term Effects of Pilocarpine in Rats: Structural Damage of the Brain Triggers Kindling and Spontaneous I Recurrent Seizures. Epilepsia 32:778–782. doi:10.1111/j.1528-1157.1991.tb05533.x.

Cavalheiro EA, Riche DA, Le Gal La Salle G. 1982. Long-term effects of intrahippocampal kainic acid injection in rats: A method for inducing spontaneous recurrent seizures. Electroencephalogr. Clin. Neurophysiol. 53:581–589. doi:10.1016/0013-4694(82)90134-1.

Chakir A, Fabene PF, Ouazzani R, Bentivoglio M. 2006. Drug resistance and hippocampal damage after delayed treatment of pilocarpine-induced epilepsy in the rat. Brain Res. Bull. 71:127–138. doi:10.1016/j.brainresbull.2006.08.009.

Chamorro-Muñoz MI, García-Martín G, Pérez-Errazquin F, Romero-Acebal M, García-Rodríguez A, Gutiérrez-Bedmar M. 2017. Epidemiological study of mortality in epilepsy in a Spanish population. Seizure 46:19–23. doi:10.1016/j.seizure.2017.02.004.

Charpentier E, Dounda JA. 2013. Rewriting a genome An accurate distance to the nearest galaxy. Nat. Biotechnol. 495:50–51.

Chen Z, Duan RS, Quezada HC, Mix E, Nennesmo I, Adem A, Winblad B, Zhu J. 2005. Increased microglial activation and astrogliosis after intranasal administration of kainic acid in C57BL/6 mice. J. Neurobiol. 62:207–218. doi:10.1002/neu.20099.

Cheng Y, Sun AY. 1994. Oxidative mechanisms involved in kainate-induced cytotoxicity in cortical neurons. Neurochem. Res. 19:1557–1564. doi:10.1007/BF00969006.

Chuang YC, Chen SD, Lin TK, Liou CW, Chang WN, Chan SHH, Chang AYW. 2007. Upregulation of nitric oxide synthase II contributes to apoptotic cell death in the hippocampal CA3 subfield via a cytochrome c/caspase-3 signaling cascade following induction of experimental temporal lobe status epilepticus in the rat. Neuropharmacology 52:1263–1273. doi:10.1016/j.neuropharm.2007.01.010.

Chugh D, Ali I, Bakochi A, Bahonjic E, Etholm L, Ekdahl CT. 2015. Alterations in Brain Inflammation, Synaptic Proteins, and Adult Hippocampal Neurogenesis during Epileptogenesis in Mice Lacking Synapsin2. PLoS One 10:e0132366. doi:10.1371/journal.pone.0132366.

Clark S, Antell A, Kaufman K. 2015. New antiepileptic medication linked to blue discoloration of the skin and eyes. Ther. Adv. Drug Saf. 6:15–19. doi:10.1177/2042098614560736.

Clifford DB, Olney JW, Maniotis A, Collins RC, Zorumski CF. 1987. The functional anatomy and pathology of lithium-pilocarpine and high-dose pilocarpine seizures. Neuroscience 23:953–968.

doi:10.1016/0306-4522(87)90171-0.

Cooper AD, Britton JW, Rabinstein AA. 2009. Functional and cognitive outcome in prolonged refractory status epilepticus. Arch. Neurol. 66:1505–1509. doi:10.1001/archneurol.2009.273.

Crespel A, Coubes P, Rousset MC, Brana C, Rougier A, Rondouin G, Bockaert J, Baldy-Moulinier M, Lerner-Natoli M. 2002. Inflammatory reactions in human medial temporal lobe epilepsy with hippocampal sclerosis. Brain Res. 952:159–169. doi:10.1016/S0006-8993(02)03050-0.

Crowder RJ, Freeman RS. 1998. Phosphatidylinositol 3-kinase and Akt protein kinase are necessary and sufficient for the survival of nerve growth factor-dependent sympathetic neurons. J. Neurosci. 18:2933–2943. doi:10.1523/jneurosci.18-08-02933.1998.

Curia G, Longo D, Biagini G, Jones RSG, Avoli M. 2008. The pilocarpine model of temporal lobe epilepsy. J. Neurosci. Methods 172:143–157. doi:10.1016/j.jneumeth.2008.04.019.

Datta SR, Dudek H, Xu T, Masters S, Haian F, Gotoh Y, Greenberg ME. 1997. Akt phosphorylation of BAD couples survival signals to the cell- intrinsic death machinery. Cell 91:231–241. doi:10.1016/S0092-8674(00)80405-5.

Debonneville C, Flores SY, Kamynina E, Plant PJ, Tauxe C, Thomas MA, Munster C, Chraibi A, Pratt JH, Horisberger JD, et al. 2001. Phosphorylation of Nedd4-2 by Sgk1 regulates epithelial Na(+) channel cell surface expression. EMBO J. 20:7052–7059. doi:10.1093/emboj/20.24.7052.

Dedek K, Kunath B, Kananura C, Reuner U, Jentsch TJ, Steinlein OK. 2001. Myokymia and neonatal epilepsy caused by a mutation in the voltage sensor of the KCNQ2 K+ channel. Proc. Natl. Acad. Sci. 98:12272–12277. doi:10.1073/pnas.211431298.

Delmas P, Brown DA. 2005. Pathways modulating neural KCNQ/M (Kv7) potassium channels. Nat. Rev. Neurosci. 6:850–862. doi:10.1038/nrn1785.

Delmas P, Coste B, Gamper N, Shapiro MS. 2005. Phosphoinositide lipid second messengers: New paradigms for calcium channel modulation. Neuron 47:179–182. doi:10.1016/j.neuron.2005.07.001.

DeLorenzo RJ, Garnett LK, Towne AR, Waterhouse EJ, Boggs JG, Morton L, Choudhry MA, Barnes T, Ko D. 1999. Comparison of status epilepticus with prolonged seizure episodes lasting from 10 to 29 minutes. Epilepsia 40:164–169. doi:10.1111/j.1528-1157.1999.tb02070.x.

Devinsky O, Spruill T, Thurman D, Friedman D. 2016. Recognizing and Preventing Epilepsy-Related Mortality: A Call for Action. Neurology 86:779–786.

Dingledine R, Varvel NH, Dudek FE. 2014. When and how do seizures kill neurons, and is cell death relevant to epileptogenesis? Adv. Exp. Med. Biol. 813. doi:10.1007/978-94-017-8914-1.

Drexel M, Preidt AP, Sperk G. 2012. Sequel of spontaneous seizures after kainic acid-induced status epilepticus and associated neuropathological changes in the subiculum and entorhinal cortex. Neuropharmacology 63:806–817. doi:10.1016/j.neuropharm.2012.06.009.

Eid T, Thomas MJ, Spencer DD, Rundén-Pran E, Lai JCK, Malthankar G V., Kim JH, Danbolt NC, Ottersen OP, De Lanerolle NC. 2004. Loss of glutamine synthetase in the human epileptogenic hippocampus: Possible mechanism for raised extracellular glutamate in mesial temporal lobe epilepsy. Lancet 363:28–37. doi:10.1016/S0140-6736(03)15166-5.

Ekberg J, Schuetz F, Boase NA, Conroy SJ, Manning J, Kumar S, Poronnik P, Adams DJ. 2007. Regulation of the voltage-gated K+ channels KCNQ2/3 and KCNQ3/5 by ubiquitination: Novel role for Nedd4-2. J. Biol. Chem. 282:12135–12142. doi:10.1074/jbc.M609385200.

Elliott JO, Lu B, Shneker B, Charyton C, Layne Moore J. 2009. Comorbidity, health screening, and quality of life among persons with a history of epilepsy. Epilepsy Behav. 14:125–129. doi:10.1016/j.yebeh.2008.10.013.

Engel T, Murphy BM, Hatazaki S, Jimenez-Mateos EM, Concannon CG, Woods I, Prehn JHM, Henshall DC. 2010. Reduced hippocampal damage and epileptic seizures after status epilepticus in mice lacking proapoptotic Puma . FASEB J. 24:853–861. doi:10.1096/fj.09-145870.

Fagerli U-M, Ullrich K, Stühmer T, Holien T, Köchert K, Holt RU, Bruland O, Chatterjee M, Nogai H, Lenz G, et al. 2011. Serum/glucocorticoid-regulated kinase 1 (SGK1) is a prominent target gene of the transcriptional response to cytokines in multiple myeloma and supports the growth of myeloma cells. Oncogene 30:3198–3206. doi:10.1038/onc.2011.79.

Ferrelli F, Pastore D, Capuani B, Lombardo MF, Blot-Chabaud M, Coppola A, Basello K, Galli A, Donadel G, Romano M, et al. 2015. Serum glucocorticoid inducible kinase (SGK)-1 protects endothelial cells against oxidative stress and apoptosis induced by hyperglycaemia. Acta Diabetol. 52:55–64. doi:10.1007/s00592-014-0600-4.

Firestone GL, Giampaolo JR, O'Keeffe BA. 2003. Stimulus-dependent regulation of serum and glucocorticoid inducible protein kinase (SGK) transcription, subcellular localization and enzymatic activity. Cell. Physiol. Biochem. 13:1–12. doi:70244.

Fisher R, Salanova V, Witt T, Worth R, Henry T, Gross R, Oommen K, Osorio I, Nazzaro J, Labar D, et al. 2010. Electrical stimulation of the anterior nucleus of thalamus for treatment of refractory epilepsy. Epilepsia 51:899–908. doi:10.1111/j.1528-1167.2010.02536.x.

Fisher RS, Acevedo C, Arzimanoglou A, Bogacz A, Cross JH, Elger CE, Engel J, Forsgren L, French JA, Glynn M, et al. 2014. ILAE Official Report: A practical clinical definition of epilepsy. Epilepsia 55:475–482. doi:10.1111/epi.12550.

Fisher RS, Cross JH, D'Souza C, French JA, Haut SR, Higurashi N, Hirsch E, Jansen FE, Lagae L, Mosh?? SL, et al. 2017. The ILAE classification of seizures. Stanford Epilepsy Cent. 58:531–542. doi:10.1111/epi.13671.

Fisher RS, Eggleston KS, Wright CW. 2015. Vagus nerve stimulation magnet activation for seizures: A critical review. Acta Neurol. Scand. 131:1–8. doi:10.1111/ane.12288.

Fisher RS, van Emde Boas W, Blume W, Elger C, Genton P, Lee P, Engel JJ. 2005. Epileptic seizures and epilepsy: definitions proposed by the International League Against Epilepsy (ILAE) and the International Bureau for Epilepsy (IBE). Epilepsia 46:470–472. doi:10.1111/j.0013-9580.2005.66104.x.

Fontán-Lozano Á, Suárez-Pereira I, Delgado-García JM, Carrión ÁM. 2011. The M-current inhibitor XE991 decreases the stimulation threshold for long-term synaptic plasticity in healthy mice and in models of cognitive disease. Hippocampus 21:22–32. doi:10.1002/hipo.20717.

Frangioni JV, Neel BG. 1993. Solubilization and Purification of Enzymatically Active Glutathione S-Transferase (pGEX) Fusion Proteins. Anal. Biochem. 210:179–187. doi:10.1006/abio.1993.1170.

Frankel WN, Taylor L, Beyer B, Tempel BL, White HS. 2001. Electroconvulsive thresholds of inbred mouse strains. Genomics 74:306–312. doi:10.1006/geno.2001.6564.

Franklin JL. 2011. Redox regulation of the intrinsic pathway in neuronal apoptosis. Antioxidants Redox Signal. 14:1437–1448. doi:10.1089/ars.2010.3596.

Friedman L, Slomko A, Wongvravit J, Naseer Z, Hu S, Wan W, Ali S. 2015. Efficacy of Retigabine on Acute Limbic Seizures in Adult Rats. J. Epilepsy Res. 5:46–59. doi:10.14581/jer.15010.

Fujikawa DG. 2005. Prolonged seizures and cellular injury: Understanding the connection. Epilepsy Behav. 7:3–11. doi:10.1016/j.yebeh.2005.08.003.

Galluzzi L, Blomgren K, Kroemer G. 2009. Mitochondrial membrane permeabilization in neuronal injury. Nat. Rev. Neurosci. 10:481–494. doi:10.1038/nrn2665.

Van Gassen KLI, De Wit M, Koerkamp MJAG, Rensen MGA, Van Rijen PC, Holstege FCP, Lindhout D, De Graan PNE. 2008. Possible role of the innate immunity in temporal lobe epilepsy. Epilepsia 49:1055–1065. doi:10.1111/j.1528-1167.2007.01470.x.

Gholami M, Saboory E, Zare S, Roshan-Milani S, Hajizadeh-Moghaddam A. 2012. The effect of dorsal hippocampal administration of nicotinic and muscarinic cholinergic ligands on pentylenetetrazol-induced generalized seizures in rats. Epilepsy Behav. 25:244–249. doi:10.1016/j.yebeh.2012.07.004.

Giménez-Cassina A, Martínez-François JR, Fisher JK, Szlyk B, Polak K, Wiwczar J, Tanner GR,

Lutas A, Yellen G, Danial NN. 2012. BAD-Dependent Regulation of Fuel Metabolism and KATP Channel Activity Confers Resistance to Epileptic Seizures. Neuron 74:719–730. doi:10.1016/j.neuron.2012.03.032.

Glien M, Brandt C, Potschka H, Löscher W. 2002. Effects of the novel antiepileptic drug levetiracetam on spontaneous recurrent seizures in the rat pilocarpine model of temporal lobe epilepsy. Epilepsia 43:350–357. doi:10.1046/j.1528-1157.2002.18101.x.

Gluck MR, Jayatilleke E, Shaw S, Rowan AJ, Haroutunian V. 2000. CNS oxidative stress associated with the kainic acid rodent model of experimental epilepsy. Epilepsy Res. 39:63–71. doi:10.1016/S0920-1211(99)00111-4.

Goldberg EM, Coulter DA. 2013. Mechanisms of epileptogenesis: A convergence on neural circuit dysfunction. Nat. Rev. Neurosci. 14:337–349. doi:10.1038/nrn3482.

Gomez-Posada JC, Aivar P, Alberdi A, Alaimo A, Etxeberria A, Fernandez-Orth J, Zamalloa T, Roura-Ferrer M, Villace P, Areso P, et al. 2011. Kv7 channels can function without constitutive calmodulin tethering. PLoS One 6:e25508. doi:10.1371/journal.pone.0025508.

Grabenstatter HL, Clark S, Dudek FE. 2007. Anticonvulsant effects of carbamazepine on spontaneous seizures in rats with kainate-induced epilepsy: Comparison of intraperitoneal injections with drug-in-food protocols. Epilepsia 48:2287–2295. doi:10.1111/j.1528-1167.2007.01263.x.

Grabenstatter HL, Dudek FE. 2019. Effect of carbamazepine on spontaneous recurrent seizures recorded from the dentate gyrus in rats with kainate-induced epilepsy. Epilepsia 60:636–647. doi:10.1111/epi.14680.

Grabenstatter HL, Ferraro DJ, Williams PA, Chapman PL, Dudek FE. 2005. Use of chronic epilepsy models in antiepileptic drug discovery: The effect of topiramate on spontaneous motor seizures in rats with kainate-induced epilepsy. Epilepsia 46:8–14. doi:10.1111/j.0013-9580.2005.13404.x.

Graham NSN, Crichton S, Koutroumanidis M, Wolfe CDA, Rudd AG. 2013. Incidence and associations of poststroke epilepsy the prospective South London stroke register. Stroke 44:605–611. doi:10.1161/STROKEAHA.111.000220.

Gunthorpe MJ, Large CH, Sankar R. 2012. The mechanism of action of retigabine (ezogabine), a first-in-class K + channel opener for the treatment of epilepsy. Epilepsia 53:412–424. doi:10.1111/j.1528-1167.2011.03365.x.

Hall BA, Kim TY, Skor MN, Conzen SD. 2012. Serum and glucocorticoid-regulated kinase 1 (SGK1) activation in breast cancer: requirement for mTORC1 activity associates with ER-alpha

expression. Breast Cancer Res. Treat. 135:469–479. doi:10.1007/s10549-012-2161-y.

Halliwell J V., Adams PR. 1982. Voltage-clamp analysis of muscarinic excitation in hippocampal neurons. Brain Res. 250:71–92. doi:10.1016/0006-8993(82)90954-4.

Hamilton SE, Loose MD, Qi M, Levey AI, Hille B, Mcknight GS, Idzerda RL, Nathanson NM. 1997. Disruption of the m1 receptor gene ablates muscarinic receptor-dependent M current regulation and seizure activity in mice. Proc. Natl. Acad. Sci. U. S. A. 94:13311–13316. doi:10.1073/pnas.94.24.13311.

Hayashi H, Iwata M, Tsuchimori N, Matsumoto T. 2014. Activation of Peripheral KCNQ Channels Attenuates Inflammatory Pain. Mol. Pain 10:1744-8069-10–15. doi:10.1186/1744-8069-10-15.

Henshall DC. 2007. Apoptosis signalling pathways in seizure-induced neuronal death and epilepsy. Biochem. Soc. Trans. 35:421–423. doi:10.1042/BST0350421.

Henshall DC, Araki T, Schindler CK, Lan JQ, Tiekoter KL, Taki W, Simon RP. 2002. Activation of Bcl-2-associated death protein and counterresponse of Akt within cell populations during seizure-induced neuronal death. J. Neurosci. 22:8458–8465.

Henshall DC, Diaz-Hernandez M, Miras-Portugal MT, Engel T. 2013. P2X receptors as targets for the treatment of status epilepticus. Front. Cell. Neurosci. 26:237. doi:10.3389/fncel.2013.00237.

Henshall JM, Dierens L, Sellars MJ. 2014. Quantitative analysis of low-density SNP data for parentage assignment and estimation of family contributions to pooled samples. Genet. Sel. Evol. 46:1–17. doi:10.1186/s12711-014-0051-y.

Hesdorffer DC, Logroscino G, Cascino G, Annegers JF, Hauser WA. 1998. Risk of unprovoked seizure after acute symptomatic seizure: Effect of status epilepticus. Ann. Neurol. 44:908–912. doi:10.1002/ana.410440609.

Hilgemann DW, Feng S, Nasuhoglu C. 2001. The complex and intriguing lives of PIP2 with ion channels and transporters. Sci. STKE 2001:1–9. doi:10.1126/stke.2001.111.re19.

Hille B. 2001. Ion channels of escitable membranes.

Honchar MP, Olney JW, Sherman WR. 1983. Systemic cholinergic agents induce seizures and brain damage in lithium-treated rats. Science (80-.). 220:323–325. doi:10.1126/science.6301005.

Ismailov II, Benos DJ. 1995. Effects of phosphorylation on ion channel function. Kidney Int. 48:1167–1179. doi:10.1038/ki.1995.400.

Itani OA, Liu KZ, Cornish KL, Campbell JR, Thomas CP. 2002. Glucocorticoids stimulate human

sgk1 gene expression by activation of a GRE in its 5′-flanking region. Am. J. Physiol. Metab. 283:E971–E979. doi:10.1152/ajpendo.00021.2002.

Jacobs MP, Leblanc GG, Brooks-Kayal A, Jensen FE, Lowenstein DH, Noebels JL, Spencer DD, Swann JW. 2009. Curing epilepsy: Progress and future directions. Epilepsy Behav. 14:438–445. doi:10.1016/j.yebeh.2009.02.036.

Jain S, LaFrancois JJ, Botterill JJ, Alcantara-Gonzalez D, Scharfman HE. 2019. Adult neurogenesis in the mouse dentate gyrus protects the hippocampus from neuronal injury following severe seizures. Hippocampus 29:683–709. doi:10.1002/hipo.23062.

Jessberger S, Parent JM. 2015. Epilepsy and adult neurogenesis. Cold Spring Harb. Perspect. Biol. 7. doi:10.1101/cshperspect.a020677.

Jonas EA, Porter GA, Alavian KN. 2014. Bcl-xL in neuroprotection and plasticity. Front. Physiol. 5:1–11. doi:10.3389/fphys.2014.00355.

Kamynina E, Staub O. 2002. Concerted action of ENaC, Nedd4-2, and Sgk1 in transepithelial Na(+) transport. Am. J. Physiol. Renal Physiol. 283:F377-87. doi:10.1152/ajprenal.00143.2002.

Kandratavicius L, Alves Balista P, Lopes-Aguiar C, Ruggiero RN, Umeoka EH, Garcia-Cairasco N, Bueno-Junior LS, Leite JP. 2014. Animal models of epilepsy: Use and limitations. Neuropsychiatr. Dis. Treat. 10:1693–1705. doi:10.2147/NDT.S50371.

Kane S, Sano H, Liu SCH, Asara JM, Lane WS, Garner CC, Lienhard GE. 2002. A Method to Identify Serine Kinase Substrates. J. Biol. Chem. 277:22115–22118. doi:10.1074/jbc.C200198200.

Kanner AM, Trimble M, Schmitz B. 2010. Postictal affective episodes. Epilepsy Behav. 19:156–158. doi:10.1016/j.yebeh.2010.06.024.

Kapur J, Lothman EW. 1989. Loss of inhibition precedes delayed spontaneous seizures in the hippocampus after tetanic electrical stimulation. J. Neurophysiol. 61:427–434. doi:10.1152/jn.1989.61.2.427.

Kapur J, Macdonald RL. 1997. Rapid seizure-induced reduction of benzodiazepine and Zn2+ sensitivity of hippocampal dentate granule cell GABA(A) receptors. J. Neurosci. 17:7532–7540. doi:10.1523/jneurosci.17-19-07532.1997.

Kapur J, Stringer JL, Lothman EW. 1989. Evidence that repetitive seizures in the hippocampus cause a lasting reduction of GABAergic inhibition. J. Neurophysiol. 61:417–426. doi:10.1152/jn.1989.61.2.417.

Kasugai M, Akaike K, Imamura S ichi, Matsukubo H, Tojo H, Nakamura M, Tanaka S, Sano A. 2007. Differences in two mice strains on kainic acid-induced amygdalar seizures. Biochem.

Biophys. Res. Commun. 357:1078–1083. doi:10.1016/j.bbrc.2007.04.067.

Kim YS, Choi MY, Lee DH, Jeon BT, Roh GS, Kim HJ, Kang SS, Cho GJ, Choi WS. 2014. Decreased interaction between FoxO3a and Akt correlates with seizure-induced neuronal death. Epilepsy Res. 108:367–378. doi:10.1016/j.eplepsyres.2014.01.003.

Kobau R, Gilliam F, Thurman DJ. 2006. Prevalence of self-reported epilepsy or seizure disorder and its associations with self-reported depression and anxiety: Results from the 2004 Healthstyles Survey. Epilepsia 47:1915–1921. doi:10.1111/j.1528-1167.2006.00612.x.

Kobayashi T, Deak M, Morrice N, Cohen P. 1999. Characterization of the structure and regulation of two novel isoforms of serum- and glucocorticoid-induced protein kinase. Biochem. J. 344 Pt 1:189–97. doi:10.1042/0264-6021:3440189.

Kobow K, Blümcke I. 2014. Epigenetic mechanisms in epilepsy.

Krajewska M, Mai JK, Zapata JM, Ashwell KWS, Schendel SL, Reed JC, Krajewski S. 2002. Dynamics of expression of apoptosis-regulatory proteins Bid, Bcl-2, Bcl-X, Bax and Bak during development of murine nervous system. Cell Death Differ. 9:145–157. doi:10.1038/sj.cdd.4400934.

Kubisch C, Schroeder BC, Friedrich T, Lütjohann B, El-Amraoui A, Marlin S, Petit C, Jentsch TJ. 1999. KCNQ4, a novel potassium channel expressed in sensory outer hair cells, is mutated in dominant deafness. Cell 96:437–446. doi:10.1016/S0092-8674(00)80556-5.

Kyyriäinen J, Bolkvadze T, Koivisto H, Lipponen A, Pérez LO, Ekolle Ndode-Ekane X, Tanila H, Pitkänen A. 2019. Deficiency of urokinase-type plasminogen activator and its receptor affects social behavior and increases seizure susceptibility. Epilepsy Res. 151:67–74. doi:10.1016/j.eplepsyres.2019.02.009.

Lamas JA. 2005. [The development of the concept of neuronal resting potential. Fundamental and clinical aspects]. Rev. Neurol. 41:538–549.

Lambert, Michelle V; Robertson MM. 1999. Depression in epilepsy: Etiology, diagnosis and treatment. Epilepsia 40:21–47. doi:10.3280/PDS2018-003002.

Legriel S, Azoulay E, Resche-Rigon M, Lemiale V, Mourvillier B, Kouatchet A, Troché G, Wolf M, Galliot R, Dessertaine G, et al. 2010. Functional outcome after convulsive status epilepticus. Crit. Care Med. 38:2295–2303. doi:10.1097/CCM.0b013e3181f859a6.

Leite JP, Bortolotto Z, Carvalheiro E. 1990. Spontaneous recurrent seizures in rats: an experimental model of partial epilepsy. Neurosci. Biobehav. Rev. 14:511–7.

Lerche C, Scherer CR, Seebohm G, Derst C, Wei AD, Busch AE, Steinmeyer K. 2000. Molecular cloning and functional expression of KCNQ5, a potassium channel subunit that may contribute

to neuronal M-current diversity. J. Biol. Chem. 275:22395–22400. doi:10.1074/jbc.M002378200.

Lerche H, Jurkat-Rott K, Lehmann-Horn F. 2001. Ion channels and epilepsy. Am. J. Med. Genet. 106:146–159. doi:10.1002/ajmg.1582.

Lerche H, Shah M, Beck H, Noebels J, Johnston D, Vincent A. 2013. Ion channels in genetic and acquired forms of epilepsy. J. Physiol. 591:753–764. doi:10.1113/jphysiol.2012.240606.

Lévesque M, Avoli M, Bernard C. 2016. Animal models of temporal lobe epilepsy following systemic chemoconvulsant administration. J. Neurosci. Methods 260:45–52. doi:10.1016/j.jneumeth.2015.03.009.

Li F, Liu L. 2019. Comparison of kainate-induced seizures, cognitive impairment and hippocampal damage in male and female mice. Life Sci. 232:116621. doi:10.1016/j.lfs.2019.116621.

Liu X, Geng J, Guo H, Zhao H, Ai Y. 2020. Propofol inhibited apoptosis of hippocampal neurons in status epilepticus through miR-15a-5p/NR2B/ERK1/2 pathway. Cell Cycle 19:1000–1011. doi:10.1080/15384101.2020.1743909.

Löscher W. 2002. Animal models of epilepsy for the development of antiepileptogenic and disease-modifying drugs. A comparison of the pharmacology of kindling and post-status epilepticus models of temporal lobe epilepsy. Epilepsy Res. 50:105–123. doi:10.1016/S0920-1211(02)00073-6.

Löscher W. 2012. Strategies for antiepileptogenesis: Antiepileptic drugs versus novel approaches in post-status epilepticus models of temporal love epilepsy. In: Jasper's Basic Mechanisms of the Epilepsies.

Löscher W. 2017. Animal Models of Seizures and Epilepsy: Past, Present, and Future Role for the Discovery of Antiseizure Drugs. Neurochem. Res. 42:1873–1888. doi:10.1007/s11064-017-2222-z.

Löscher W, Schmidt D. 2011. Modern antiepileptic drug development has failed to deliver: Ways out of the current dilemma. Epilepsia 52:657–678. doi:10.1111/j.1528-1167.2011.03024.x.

Lothman EW, Collins RC, Ferrendelli JA. 1981. Kainic acid-induced limbic seizures: electrophysiologic studies. Neurology 31:806–812.

Malik AS, Amin HU. 2017. Designing an EEG Experiment. In: Designing EEG Experiments for Studying the Brain. Elsevier. p. 1–30.

Manville RW, Abbott GW. 2019. Cilantro leaf harbors a potent potassium channel–activating anticonvulsant. FASEB J. 33:11349–11363. doi:10.1096/fj.201900485R.

Marchi N, Fan Q, Ghosh C, Fazio V, Bertolini F, Betto G, Batra A, Carlton E, Najm I, Granata T, et al. 2009. Antagonism of peripheral inflammation reduces the severity of status epilepticus. Neurobiol. Dis. 33:171–181. doi:10.1016/j.nbd.2008.10.002.

Marcuse L V, Fields MC, Yoo J (Jenna). 2016. The normal adult EEG. In: Rowan's Primer of EEG. Elsevier. p. 39–66.

Martin-Batista E, Maglio LE, Armas-Capote N, Hernandez G, de la Rosa DA, Giraldez T. 2021 Feb. SGK1.1 limits brain damage after status epilepticus through M current-dependent and independent mechanisms. Neurobiol. Dis.:105317. doi:10.1016/j.nbd.2021.105317.

Mathern GW, Adelson PD, Cahan LD, Leite JP. 2002. Hippocampal neuron damage in human epilepsy: Meyer's hypothesis revisited. Prog. Brain Res. 135:237–251. doi:10.1016/S0079-6123(02)35023-4.

Mathern GW, Babb TL, Armstrong DL. 1997. Hippocampal sclerosis. In: Engel J, Pedley TA, editors. Epilepsy: a comprehensive textbook. Philadelphia. p. 133–155.

Mathern GW, Cifuentes F, Leite JP, Pretorius JK, Babb TL. 1993. Hippocampal EEG excitability and chronic spontaneous seizures are associated with aberrant synaptic reorganization in the rat intrahippocampal kainate model. Electroencephalogr. Clin. Neurophysiol. 87:326–339. doi:10.1016/0013-4694(93)90186-Y.

Mazzuferi M, Kumar G, Rospo C, Kaminski RM. 2012. Rapid epileptogenesis in the mouse pilocarpine model: video-EEG, pharmacokinetic and histopathological characterization. Exp. Neurol. 238:156–167. doi:10.1016/j.expneurol.2012.08.022.

McCaig C, Ataliotis P, Shtaya A, Omar AS, Green AR, Kind CN, Pereira AC, Naray-Fejes-Toth A, Fejes-Toth G, Yáñez-Muñoz RJ, et al. 2019. Induction of the cell survival kinase Sgk1: A possible novel mechanism for α-phenyl-N-tert-butyl nitrone in experimental stroke. J. Cereb. Blood Flow Metab. 39:1111–1121. doi:10.1177/0271678X17746980.

McCord MC, Lorenzana A, Bloom CS, Chancer ZO, Schauwecker PE. 2008. Effect of age on kainate-induced seizure severity and cell death. Neuroscience 154:1143–1153. doi:10.1016/j.neuroscience.2008.03.082.

McKeon A, Benarroch EE. 2018. Glial fibrillary acid protein. Neurology 90:925–930. doi:10.1212/WNL.0000000000005534.

McKhann GM, Wenzel HJ, Robbins CA, Sosunov AA, Schwartzkroin PA. 2003. Mouse strain differences in kainic acid sensitivity, seizure behavior, mortality, and hippocampal pathology. Neuroscience 122:551–561. doi:10.1016/S0306-4522(03)00562-1.

McLin JP, Steward O. 2006. Comparison of seizure phenotype and neurodegeneration induced

by systemic kainic acid in inbred, outbred, and hybrid mouse strains. Eur. J. Neurosci. 24:2191–2202. doi:10.1111/j.1460-9568.2006.05111.x.

Medvedev A, MacKenzie L, Hiscock JJ, Willoughby JO. 2000. Kainic acid induces distinct types of epileptiform discharge with differential involvement of hippocampus and neocortex. Brain Res. Bull. 52:89–98. doi:10.1016/S0361-9230(00)00239-2.

Meencke HJ, Veith G, Lund S. 1996. Bilateral hippocampal sclerosis and secondary epileptogenesis. Epilepsy Res. Suppl. 12:335–42.

Mello LEAM, Cavalheiro EA, Tan AM, Kupfer WR, Pretorius JK, Babb TL, Finch DM. 1993. Circuit Mechanisms of Seizures in the Pilocarpine Model of Chronic Epilepsy: Cell Loss and Mossy Fiber Sprouting. Epilepsia 34:985–995. doi:10.1111/j.1528-1157.1993.tb02123.x.

Miceli F, Soldovieri MV, Joshi N, Weckhuysen S, Cooper E, Taglialatela M. 2010. KCNQ2-Related Disorders.

Michel MC, Radziszewski P, Falconer C, Marschall-Kehrel D, Blot K. 2012. Unexpected frequent hepatotoxicity of a prescription drug, flupirtine, marketed for about 30 years. Br. J. Clin. Pharmacol. 73:821–825. doi:10.1111/j.1365-2125.2011.04138.x.

Milatovic D, Gupta RC, Dettbarn WD. 2002. Involvement of nitric oxide in kainic acid-induced excitotoxicity in rat brain. Brain Res. 957:330–337. doi:10.1016/S0006-8993(02)03669-7.

Miller MA, Conley Y, Scanlon JM, Ren D, Ilyas Kamboh M, Niyonkuru C, Wagner AK. 2010. APOE genetic associations with seizure development after severe traumatic brain injury. Brain Inj. 24:1468–1477. doi:10.3109/02699052.2010.520299.

Miranda P, Cadaveira-Mosquera A, González-Montelongo R, Villarroel Á, González-Hernández T, Lamas JA, Álvarez de la Rosa D, Giráldez T. 2013. The Neuronal Serum- and Glucocorticoid-Regulated Kinase 1.1 Reduces Neuronal Excitability and Protects against Seizures through Upregulation of the M-Current. J. Neurosci. 33:2684–2696. doi:10.1523/JNEUROSCI.3442-12.2013.

Mishra V, Shuai B, Kodali M, Shetty GA, Hattiangady B, Rao X, Shetty AK. 2015. Resveratrol treatment after status epilepticus restrains neurodegeneration and abnormal neurogenesis with suppression of oxidative stress and inflammation. Sci. Rep. 5:1–19. doi:10.1038/srep17807.

Montagutelli X. 2000. Effect of genetic background on the phenotype of mouse mutations. J. Am. Soc. Nephrol. Soc. 11:S101-5.

Motoyama N, Wang F, Roth KA, Sawa H, Nakayama KI, Nakayama K, Negishi I, Senju S, Zhang Q, Fujii S, et al. 1995. Massive cell death of immature hematopoietic cells and neurons in Bcl-x-deficient mice. Science (80-.). 267:1506–1510. doi:10.1126/science.7878471.

Murphy BM, Engel T, Paucard A, Hatazaki S, Mouri G, Tanaka K, Tuffy LP, Jimenez-Mateos EM, Woods I, Dunleavy M, et al. 2010. Contrasting patterns of Bim induction and neuroprotection in Bim-deficient mice between hippocampus and neocortex after status epilepticus. Cell Death Differ. 17:459–468. doi:10.1038/cdd.2009.134.

Nadler JV, PERRY BW, COTMAN CW. 1978. Intraventricular kainic acid preferentially destroys hippocampal pyramidal cells. Nature 271:676–677. doi:10.1038/271676a0.

Nagao, T; Alonso, A; Avoli M. 1996. Epileptiform activity induced by pilocarpine in the rat hippocampal-entorhinal slice preparation. Neuroscience 72:399–408.

Nappi P, Miceli F, Soldovieri MV, Ambrosino P, Barrese V, Taglialatela M. 2020. Epileptic channelopathies caused by neuronal Kv7 (KCNQ) channel dysfunction. Pflugers Arch. Eur. J. Physiol. 472:881–898. doi:10.1007/s00424-020-02404-2.

do Nascimento AL, dos Santos NF, Campos Pelágio F, Aparecida Teixeira S, de Moraes Ferrari EA, Langone F. 2012. Neuronal degeneration and gliosis time-course in the mouse hippocampal formation after pilocarpine-induced status epilepticus. Brain Res. 1470:98–110. doi:10.1016/j.brainres.2012.06.008.

Nirwan N, Vyas P, Vohora D. 2018. Animal models of status epilepticus and temporal lobe epilepsy: A narrative review. Rev. Neurosci. 29:757–770. doi:10.1515/revneuro-2017-0086.

Noebels J, Avoli M, Rogawski M, Al E. 2012. Jasper's Basic Mechanisms of the Epilepsies [Internet]. 4th Edition. Bethesa (MD): National Center for Biotechnology Information (US). 51. doi:10.1111/j.1528-1167.2010.02793.x.

Novy J, Belluzzo M, Caboclo LO, Catarino CB, Yogarajah M, Martinian L, Peacock JL, Bell GS, Koepp MJ, Thom M, et al. 2013. The lifelong course of chronic epilepsy: the Chalfont experience. Brain 136:3187–3199. doi:10.1093/brain/awt117.

Novy J, Logroscino G, Rossetti AO. 2010. Refractory status epilepticus: A prospective observational study. Epilepsia 51:251–256. doi:10.1111/j.1528-1167.2009.02323.x.

Nuber UA, Kriaucionis S, Roloff TC, Guy J, Selfridge J, Steinhoff C, Schulz R, Lipkowitz B, Ropers HH, Holmes MC, et al. 2005. Up-regulation of glucocorticoid-regulated genes in a mouse model of Rett syndrome. Hum. Mol. Genet. 14:2247–2256. doi:10.1093/hmg/ddi229.

O'Connor L, Strasser A, O'Reilly LA, Hausmann G, Adams JM, Cory S, Huang DCS. 1998. Bim: A novel member of the Bcl-2 family that promotes apoptosis. EMBO J. 17:384–395. doi:10.1093/emboj/17.2.384.

Olesen MS, Bentzen BH, Nielsen JB, Steffensen AB, David J-P, Jabbari J, Jensen HK, Haunsø S, Svendsen JH, Schmitt N. 2012. Mutations in the potassium channel subunit KCNE1 are

associated with early-onset familial atrial fibrillation. BMC Med. Genet. 13:24. doi:10.1186/1471-2350-13-24.

Oliveros JC, Franch M, Tabas-Madrid D, San-León D, Montoliu L, Cubas P, Pazos F. 2016. Breaking-Cas—interactive design of guide RNAs for CRISPR-Cas experiments for ENSEMBL genomes. Nucleic Acids Res. 44:W267–W271. doi:10.1093/nar/gkw407.

Palmada M, Dieter M, Boehmer C, Waldegger S, Lang F. 2004. Serum and glucocorticoid inducible kinases functionally regulate ClC-2 channels. Biochem. Biophys. Res. Commun. 321:1001–1006. doi:10.1016/j.bbrc.2004.07.064.

Parent JM, Elliott RC, Pleasure SJ, Barbaro NM, Lowenstein DH. 2006. Aberrant seizure-induced neurogenesis in experimental temporal lobe epilepsy. Ann. Neurol. 59:81–91. doi:10.1002/ana.20699.

Patel DC, Tewari BP, Chaunsali L, Sontheimer H. 2019. Neuron–glia interactions in the pathophysiology of epilepsy. Nat. Rev. Neurosci. 20:282–297. doi:10.1038/s41583-019-0126-4.

Paternain A V., Herrera MT, Nieto MA, Lerma J. 2000. GluR5 and GluR6 kainate receptor subunits coexist in hippocampal neurons and coassemble to form functional receptors. J. Neurosci. 20:196–205. doi:10.1523/jneurosci.20-01-00196.2000.

Peng A, Qiu X, Lai W, Li W, Zhang L, Zhu X, He S, Duan J, Chen L. 2018. Altered composition of the gut microbiome in patients with drug-resistant epilepsy. Epilepsy Res. 147:102–107. doi:10.1016/j.eplepsyres.2018.09.013.

Pérez-Burgos A, Alamilla J. 2010. El fosfatidilinositol-4,5-bifosfato y sus acciones sobre los canales iónicos. Rev. Biomédica 21:97–107.

Pitkänen, Asla; Schwartzkroin, Philip; Moshé S. 2005. Models of seizures and epilepsy.

Pitkänen A. 2002. Efficacy of current antiepileptics to prevent neurodegeneration in epilepsy models. Epilepsy Res. 50:141–160. doi:10.1016/S0920-1211(02)00076-1.

Pitkänen A. 2004. New pharmacotherapy for epilepsy. IDrugs 7:471–7.

Pitkänen A, Lukasiuk K. 2009. Molecular and cellular basis of epileptogenesis in symptomatic epilepsy. Epilepsy Behav. 14:16–25. doi:10.1016/j.yebeh.2008.09.023.

Pitkänen A, Lukasiuk K, Dudek E, Staley K. 2014. Epileptogenesis. In: Encyclopedia of the Neurological Sciences. Elsevier. p. 196–199.

Plouin, P; Anderson V. 2005. Epileptic syndromes in infancy, childhood and adolescence. 4th ed. Roger, J; Bureau, M; Dravet C, editor.

Potschka H. 2013. Pharmacological treatment strategies: Mechanisms of antiepileptic drugs.

Epileptology 1:31–37. doi:10.1016/j.epilep.2012.11.004.

Putcha G V., Moulder KL, Golden JP, Bouillet P, Adams JA, Strasser A, Johnson EM. 2001. Induction of BIM, a proapoptotic BH3-only BCL-2 family member, is critical for neuronal apoptosis. Neuron 29:615–628. doi:10.1016/S0896-6273(01)00238-0.

Putnam, TJ; Merritt H. 1937. Experimental determination of the anticonvulsant properties of some phenyl derivatives. Science (80-.). 85:525–6.

Racine RJ. 1972. Modification of seizure activity by electrical stimulation. II. Motor seizure. Electroencephalogr. Clin. Neurophysiol. 32:281–294.

Raedt R, Van Dycke A, Van Melkebeke D, De Smedt T, Claeys P, Wyckhuys T, Vonck K, Wadman W, Boon P. 2009. Seizures in the intrahippocampal kainic acid epilepsy model: Characterization using long-term video-EEG monitoring in the rat. Acta Neurol. Scand. 119:293–303. doi:10.1111/j.1600-0404.2008.01108.x.

Ramaswamy S, Nakamura N, Vazquez F, Batt DB, Perera S, Roberts TM, Sellers WR. 1999. Regulation of G1 progression by the PTEN tumor suppressor protein is linked to inhibition of the phosphatidylinositol 3-kinase/Akt pathway. Proc. Natl. Acad. Sci. 96:2110–2115. doi:10.1073/pnas.96.5.2110.

Raspall-Chaure, M; Chin, RFM; Neville, BG; Scott R. 2006. Outcome of convulsive status epilepticus: A review. Lancet Neurol.:769–79. doi:10.1136/adc.2006.107516.

Ravizza T, Gagliardi B, Noé F, Boer K, Aronica E, Vezzani A. 2008. Innate and adaptive immunity during epileptogenesis and spontaneous seizures: Evidence from experimental models and human temporal lobe epilepsy. Neurobiol. Dis. 29:142–160. doi:10.1016/j.nbd.2007.08.012.

Reddy DS, Kuruba R. 2013. Experimental models of status epilepticus and neuronal injury for evaluation of therapeutic interventions. Int. J. Mol. Sci. 14:18284–18318. doi:10.3390/ijms140918284.

Ribak CE, Tran PH, Spigelman I, Okazaki MM, Nadler J V. 2000. Status epilepticus-induced hilar basal dendrites on rodent granule cells contribute to recurrent excitatory circuitry. J. Comp. Neurol. 428:240–253.

Robel S, Buckingham SC, Boni JL, Campbell SL, Danbolt NC, Riedemann T, Sutor B, Sontheimer H. 2015. Reactive astrogliosis causes the development of spontaneous seizures. J. Neurosci. 35:3330–3345. doi:10.1523/JNEUROSCI.1574-14.2015.

Ronen GM, Rosales TO, Connolly M, Anderson VE, Leppert M. 1993. Seizure characteristics in chromosome 20 benign familial neonatal convulsions. Neurology 43:1355–1360.

Rothenberg I, Piccini I, Wrobel E, Stallmeyer B, Müller J, Greber B, Strutz-Seebohm N, Schulze-Bahr E, Schmitt N, Seebohm G. 2016. Structural interplay of KV7.1 and KCNE1 is essential for normal repolarization and is compromised in short QT syndrome 2 (KV7.1-A287T). Hear. Case Reports 2:521–529. doi:10.1016/j.hrcr.2016.08.015.

Roy M, Hom JJ, Sapolsky RM. 2002. HSV-mediated delivery of virally derived anti-apoptotic genes protects the rat hippocampus from damage following excitotoxicity, but not metabolic discruption. Gene Ther. 9:214–219. doi:10.1038/sj.gt.3301642.

Royle SJ, Collins FC, Rupniak HT, Barnes JC, Anderson R. 1999. Behavioural analysis and susceptibility to CNS injury of four inbred strains of mice. Brain Res. 816:337–349. doi:10.1016/S0006-8993(98)01122-6.

Ryan DP, Ptáček LJ. 2010. Episodic neurological channelopathies. Neuron 68:282–292. doi:10.1016/j.neuron.2010.10.008.

Scerrati M, Onofrj M, Pacifici L, Pola P, Ramacci MT, Rossi GF. 1986. Electrocerebral and behavioural analysis of systemic kainic acid-induced epilepsy in the rat. Drugs Exp. Clin. Res. 12:671–80.

Schachter SC. 2002. Vagus nerve stimulation therapy summary. Neurology 24:15–20.

Schauwecker PE. 2000. Seizure-induced neuronal death is associated with induction of c-Jun N-terminal kinase and is dependent on genetic background. Brain Res. 884:116–128. doi:10.1016/S0006-8993(00)02888-2.

Schauwecker PE. 2002. Complications associated with genetic background effects in models of experimental epilepsy. Prog. Brain Res. 135:139–148.

Schauwecker PE, Steward O. 1997. Genetic determinants of susceptibility to excitotoxic cell death: Implications for gene targeting approaches. Proc. Natl. Acad. Sci. U. S. A. 94:4103–4108. doi:10.1073/pnas.94.8.4103.

Scheffer IE, Berkovic S, Capovilla G, Connolly MB, French J, Guilhoto L, Hirsch E, Jain S, Mathern GW, Moshe SL, et al. 2017. DOCUMENTO DE POSICIÓN DE LA ILAE Clasificación de las epilepsias de la ILAE: Documento de posición de la Comisión de Clasificación y Terminología de la ILAE. 58:512–521. doi:10.1111/epi.13709.

Schmidt D. 2012. Is antiepileptogenesis a realistic goal in clinical trials? Concerns and new horizons. Epileptic Disord. 14:105–113.

Schmued LC, Albertson C, Slikker W. 1997. Fluoro-Jade: A novel fluorochrome for the sensitive and reliable histochemical localization of neuronal degeneration. Brain Res. 751:37–46. doi:10.1016/S0006-8993(96)01387-X.

Schoenebeck B, Bader V, Zhu XR, Schmitz B, Lubbert H, Stichel CC. 2005. Sgk1, a cell survival response in neurodegenerative diseases. Mol. Cell. Neurosci. 30:249–264. doi:10.1016/j.mcn.2005.07.017.

Scholl EA, Dudek FE, Ekstrand JJ. 2013. Neuronal degeneration is observed in multiple regions outside the hippocampus after lithium pilocarpine-induced status epilepticus in the immature rat. Neuroscience 252:45–59. doi:10.1016/j.neuroscience.2013.07.045.

Schroeder BC, Hechenberger M, Weinreich F, Kubisch C, Jentsch TJ. 2000. KCNQ5, a Novel Potassium Channel Broadly Expressed in Brain, Mediates M-type Currents. J. Biol. Chem. 275:24089–24095. doi:10.1074/jbc.M003245200.

Schroeder BC, Kubisch C, Stein V, Jentsch TJ. 1998. Moderate loss of function of cyclic-AMP-modulated KCNQ2/KCNQ3 K+ channels causes epilepsy. Nature 396:687–690. doi:10.1038/25367.

Schuetz F, Kumar S, Poronnik P, Adams DJ. 2008. Regulation of the voltage-gated K(+) channels KCNQ2/3 and KCNQ3/5 by serum- and glucocorticoid-regulated kinase-1. Am. J. Physiol. Cell Physiol. 295:C73-80. doi:10.1152/ajpcell.00146.2008.

Schwartzkroin PA. 1986. Hippocampal slices in experimental and human epilepsy. Adv. Neurol. 44:991–1010.

Schwob JE, Fuller T, Price JL, Olney JW. 1980. Widespread patterns of neuronal damage following systemic or intracerebral injections of kainic acid: A histological study. Neuroscience 5:991–1014. doi:10.1016/0306-4522(80)90181-5.

Sculier C, Gaínza-Lein M, Sánchez Fernández I, Loddenkemper T. 2018. Long-term outcomes of status epilepticus: A critical assessment. Epilepsia 59:155–169. doi:10.1111/epi.14515.

Seebohm G, Strutz-Seebohm N, Baltaev R, Korniychuk G, Knirsch M, Engel J, Lang F. 2005. Regulation of KCNQ4 Potassium Channel Prepulse Dependence and Current Amplitude by SGK1 in Xenopus oocytes. Cell. Physiol. Biochem. 16:255–262. doi:10.1159/000089851.

Shah MM, Mistry M, Marsh SJ, Brown DA, Delmas P. 2002. Molecular correlates of the M-current in cultured rat hippocampal neurons. J. Physiol. 544:29–37. doi:10.1113/jphysiol.2002.028571.

Sharma AK, Reams RY, Jordan WH, Miller MA, Thacker HL, Snyder PW. 2007. Mesial temporal lobe epilepsy: Pathogenesis, induced rodent models and lesions. Toxicol. Pathol. 35:984–999. doi:10.1080/01926230701748305.

Sierra Ramos C. 2017. SGK1 como mediador de los efectos deletéreos del receptor de mineralocorticoides. Universidad de la Laguna.

Sillanpää M, Schmidt D. 2006. Natural history of treated childhood-onset epilepsy: Prospective,

long-term population-based study. Brain 129:617–624. doi:10.1093/brain/awh726.

Silver J, Miller JH. 2004. Regeneration beyond the glial scar. Nat. Rev. Neurosci. 5:146–156. doi:10.1038/nrn1326.

Singh NA, Charlier C, Stauffer D, DuPont BR, Leach RJ, Melis R, Ronen GM, Bjerre I, Quattlebaum T, Murphy J V., et al. 1998. A novel potassium channel gene, KCNQ2, is mutated in an inherited epilepsy of newborns. Nat. Genet. 18:25–29. doi:10.1038/ng0198-25.

Singh NA, Westenskow P, Charlier C, Pappas C, Leslie J, Dillon J, Anderson VE, Sanguinetti MC, Leppert MF. 2003. KCNQ2 and KCNQ3 potassium channel genes in benign familial neonatal convulsions: Expansion of the functional and mutation spectrum. Brain 126:2726–2737. doi:10.1093/brain/awg286.

Smolders I, Khan GM, Manil J, Ebinger G, Michotte Y. 1997. NMDA receptor-mediated pilocarpine-induced seizures: Characterization in freely moving rats by microdialysis. Br. J. Pharmacol. 121:1171–1179. doi:10.1038/sj.bjp.0701231.

Snyder PM, Olson DR, Kabra R, Zhou R, Steines JC. 2004. cAMP and serum and glucocorticoid-inducible kinase (SGK) regulate the epithelial Na+ channel through convergent phosphorylation of Nedd4-2. J. Biol. Chem. 279:45753–45758. doi:10.1074/jbc.M407858200.

Sofroniew M V. 2014. Astrogliosis. Cold Spring Harb. Perspect. Biol. 7.

Soldovieri MV, Boutry-Kryza N, Milh M, Doummar D, Heron B, Bourel E, Ambrosino P, Miceli F, De Maria M, Dorison N, et al. 2014. Novel KCNQ2 and KCNQ3 mutations in a large cohort of families with benign neonatal epilepsy: First evidence for an altered channel regulation by syntaxin-1A. Hum. Mutat. 35:356–367. doi:10.1002/humu.22500.

Soldovieri MV, Miceli F, Taglialatela M. 2011. Driving with no brakes: molecular pathophysiology of Kv7 potassium channels. Physiology (Bethesda). 26:365–376. doi:10.1152/physiol.00009.2011.

Song MK, Cui YY, Zhang WW, Zhu L, Lu Y, Chen HZ. 2009. The facilitating effect of systemic administration of Kv7/M channel blocker XE991 on LTP induction in the hippocampal CA1 area independent of muscarinic activation. Neurosci. Lett. 461:25–29. doi:10.1016/j.neulet.2009.05.042.

Sontheimer H. 2015. Diseases of the nervous system. Elsevier Inc.

Sperk G. 1994. Kainic acid seizures in the rat. Prog. Neurobiol. 42:1–32. doi:10.1016/0301-0082(94)90019-1.

Sperk G, Lassmann H, Baran H, Kish SJ, Seitelberger F, Hornykiewicz O. 1983. Kainic acid induced seizures: Neurochemical and histopathological changes. Neuroscience 10:1301–1315.

doi:10.1016/0306-4522(83)90113-6.

Steinlein OK. 2008. Genetics and epilepsy. Dialogues Clin. Neurosci. 10:29–38. doi:10.31887/DCNS.2008.10.1/oksteinlein.

Suh BC, Hille B. 2005. Regulation of ion channels by phosphatidylinositol 4,5-bisphosphate. Curr. Opin. Neurobiol. 15:370–378. doi:10.1016/j.conb.2005.05.005.

Surti TS, Huang L, Jan YN, Jan LY, Cooper EC. 2005. Identification by mass spectrometry and functional characterization of two phosphorylation sites of KCNQ2/KCNQ3 channels. Proc. Natl. Acad. Sci. U. S. A. 102:17828–17833. doi:10.1073/pnas.0509122102.

Surur AS, Bock C, Beirow K, Wurm K, Schulig L, Kindermann MK, Siegmund W, Bednarski PJ, Link A. 2019. Flupirtine and retigabine as templates for ligand-based drug design of K V 7.2/3 activators. Org. Biomol. Chem. 17:4512–4522. doi:10.1039/c9ob00511k.

Tauck D, Nadler J. 1985. Evidence of functional mossy fiber sprouting in hippocampal formation of kainic acid-treated rats. J. Neurosci. 5:1016–1022. doi:10.1523/JNEUROSCI.05-04-01016.1985.

Tellez-Zenteno JF, Patten SB, Jetté N, Williams J, Wiebe S. 2007. Psychiatric comorbidity in epilepsy: A population-based analysis. Epilepsia 48:2336–2344. doi:10.1111/j.1528-1167.2007.01222.x.

Temkin NR. 2009. Preventing and treating posttraumatic seizures: The human experience. Epilepsia 50:10–13. doi:10.1111/j.1528-1167.2008.02005.x.

Terada Y, Kuwana H, Kobayashi T, Okado T, Suzuki N, Yoshimoto T, Hirata Y, Sasaki S. 2008. Aldosterone-Stimulated SGK1 Activity Mediates Profibrotic Signaling in the Mesangium. J. Am. Soc. Nephrol. 19:298–309. doi:10.1681/ASN.2007050531.

Thom M. 2014. Review: Hippocampal sclerosis in epilepsy: A neuropathology review. Neuropathol. Appl. Neurobiol. 40:520–543. doi:10.1111/nan.12150.

Towne AR, Pellock JM, Ko D, DeLorenzo RJ. 1994. Determinants of Mortality in Status Epilepticus. Epilepsia 35:27–34. doi:10.1111/j.1528-1157.1994.tb02908.x.

Trinka E, Cock H, Hesdorffer D, Rossetti AO, Scheffer IE, Shinnar S, Shorvon S, Lowenstein DH. 2015. A definition and classification of status epilepticus - Report of the ILAE Task Force on Classification of Status Epilepticus. Epilepsia 56:1515–1523. doi:10.1111/epi.13121.

Turski WA, Cavalheiro EA, Bortolotto ZA, Mello LM, Schwarz M, Turski L. 1984. Seizures produced by pilocarpine in mice: A behavioral, electroencephalographic and morphological analysis. Brain Res. 321:237–253. doi:10.1016/0006-8993(84)90177-X.

Turski WA, Cavalheiro EA, Schwarz M, Czuczwar SJ, Kleinrok Z, Turski L. 1983. Limbic seizures produced by pilocarpine in rats: Behavioural, electroencephalographic and neuropathological study. Behav. Brain Res. 9:315–335. doi:10.1016/0166-4328(83)90136-5.

Vale FL, Vivas AC, Manwaring J, Schoenberg MR, Benbadis SR. 2015. Temporal lobe epilepsy and cavernous malformations: surgical strategies and long-term outcomes. Acta Neurochir. (Wien). 157:1887–1895. doi:10.1007/s00701-015-2592-4.

Vezzani A, French J, Bartfai T, Baram TZ. 2011. The role of inflammation in epilepsy. Nat. Rev. Neurol. 7:31–40. doi:10.1038/nrneurol.2010.178.

Vincent P, Mulle C. 2009. Kainate receptors in epilepsy and excitotoxicity. Neuroscience 158:309–323. doi:10.1016/j.neuroscience.2008.02.066.

Vismer MS, Forcelli PA, Skopin MD, Gale K, Koubeissi MZ. 2015. The piriform, perirhinal, and entorhinal cortex in seizure generation. Front. Neural Circuits 9:1–14. doi:10.3389/fncir.2015.00027.

Van Vliet EA, Araújo SDC, Redeker S, Van Schaik R, Aronica E, Gorter JA. 2007. Blood-brain barrier leakage may lead to progression of temporal lobe epilepsy. Brain 130:521–534. doi:10.1093/brain/awl318.

Wagner AK, Miller MA, Scanlon J, Ren D, Kochanek PM, Conley YP. 2010. Adenosine A1 receptor gene variants associated with post-traumatic seizures after severe TBI. Epilepsy Res. 90:259–272. doi:10.1016/j.eplepsyres.2010.06.001.

Wang D, Huang Z, Li L, Yuan Y, Xiang L, Wu X, Ni C, Yu W. 2019. Intracarotid cold saline infusion contributes to neuroprotection in MCAO-induced ischemic stroke in rats via serum and glucocorticoid-regulated kinase 1. Mol. Med. Rep. 20:3942–3950. doi:10.3892/mmr.2019.10599.

Wang HS, Pan Z, Shi W, Brown BS, Wymore RS, Cohen IS, Dixon JE, McKinnon D. 1998. KCNQ2 and KCNQ3 potassium channel subunits: Molecular correlates of the M-channel. Science (80-.). 282:1890–1893. doi:10.1126/science.282.5395.1890.

Wang Q, Yu S, Simonyi A, Sun GY, Sun AY. 2005. Kainic acid-mediated excitotoxicity as a model for neurodegeneration. Mol. Neurobiol. 31:3–16. doi:10.1385/mn:31:1-3:003.

Webster MK, Goya L, Ge Y, Maiyar AC, Firestone GL. 1993. Characterization of sgk, a novel member of the serine/threonine protein kinase gene family which is transcriptionally induced by glucocorticoids and serum. Mol. Cell. Biol. 13:2031–2040. doi:10.1128/MCB.13.4.2031.

Wesch D, Miranda P, Afonso-Oramas D, Althaus M, Castro-Hernández J, Dominguez J, Morty RE, Clauss W, González-Hernández T, Alvarez De la Rosa D, et al. 2010. The neuronal-specific SGK1 . 1 kinase regulates δ -epithelial Na+ channel independently of PY motifs and couples it

to phospholipase C signaling. Am. J. Cell Physiol. 299:779–790. doi:10.1152/ajpcell.00184.2010.

West AE, Chen WG, Dalva MB, Dolmetsch RE, Kornhauser JM, Shaywitz AJ, Takasu MA, Tao X, Greenberg ME. 2001. Calcium regulation of neuronal gene expression. Proc. Natl. Acad. Sci. 98:11024–11031. doi:10.1073/pnas.191352298.

White HS, Löscher W. 2014. Searching for the Ideal Antiepileptogenic Agent in Experimental Models: Single Treatment Versus Combinatorial Treatment Strategies. Neurotherapeutics 11:373–384. doi:10.1007/s13311-013-0250-1.

Wickenden AD, Roeloffs R, McNaughton-Smith G, Rigdon GC. 2004. KCNQ potassium channels: Drug targets for the treatment pf epilepsy and pain. Expert Opin. Ther. Pat. 14:457–469. doi:10.1517/13543776.14.4.457.

Wickenden AD, Zou A, Wagoner PK, Jegla T. 2001. Characterization of KCNQ5/Q3 potassium channels expressed in mammalian cells. Br. J. Pharmacol. 132:381–384. doi:10.1038/sj.bjp.0703861.

Wiebe S, Blume WT, Girvin JP, Eliasziw M. 2001. A randomized, controlled trial of surgery for temporal-lobe epilepsy. N. Engl. J. Med. 345:311–318. doi:10.1056/NEJM200108023450501.

Wieser HG. 2004. Mesial temporal lobe epilepsy with hippocampal sclerosis: Report of the commission on Neurosurgery. Epilepsia 45:695–714.

Willoughby JO, Mackenzie L, Medvedev A, Hiscock JJ. 1997. Fos induction following systemic kainic acid: Early expression in hippocampus and later widespread expression correlated with seizure. Neuroscience 77:379–392. doi:10.1016/S0306-4522(96)00462-9.

World Health Organization. 2019. Epilepsy. Key facts. [accessed 2021 Mar 15]. https://www.who.int/news-room/fact-sheets/detail/epilepsy.

Wulff H, Castle NA, Pardo LA. 2009. Voltage-gated potassium channels as therapeutic targets. Nat. Rev. Drug Discov. 8:982–1001. doi:10.1038/nrd2983.

Wyllie AH, Kerr JFR, Currie AR. 1980. Cell Death: The Significance of Apoptosis.

Xiong Q, Sun H, Zhang Y, Nan F, Li M. 2008. Combinatorial augmentation of voltage-gated KCNQ potassium channels by chemical openers. Proc. Natl. Acad. Sci. 105:3128–3133. doi:10.1073/pnas.0712256105.

Yasuda CL, Tedeschi H, Oliveira ELP, Ribas GC, Costa ALC, Cardoso TAMO, Montenegro MA, Guerreiro CAM, Guerreiro MM, Li LM, et al. 2006. Comparison of short-term outcome between surgical and clinical treatment in temporal lobe epilepsy: A prospective study. Seizure 15:35–40. doi:10.1016/j.seizure.2005.10.005.

Youle RJ, Strasser A. 2008. The BCL-2 protein family: Opposing activities that mediate cell death. Nat. Rev. Mol. Cell Biol. 9:47–59. doi:10.1038/nrm2308.

Zaczek R, Chorvat RJ, Saye JA, Pierdomenico ME, Maciag CM, Logue AR, Fisher BN, Rominger DH, Earl RA. 1998. Two new potent neurotransmitter release enhancers, 10, 10-bis(4-pyridinylmethyl)-9(10H)-anthracenone and 10,10-bis(2-fluoro-4- pyridinylmethyl)-9(10H)-anthracenone: Comparison to linopirdine. J. Pharmacol. Exp. Ther. 285:724–730.

Zanuzzi CN, Nishida F, Sisti MS, Barbeito CG, Portiansky EL. 2019. Reactivity of microglia and astrocytes after an excitotoxic injury induced by kainic acid in the rat spinal cord. Tissue Cell 56:31–40. doi:10.1016/j.tice.2018.11.007.

Zhang W, Qian C yun, Li SQ. 2014. Protective effect of SGK1 in rat hippocampal neurons subjected to ischemia reperfusion. Cell. Physiol. Biochem. 34:299–312. doi:10.1159/000363000.

Zhang XM, Mao XJ, Zhang HL, Zheng XY, Pham T, Adem A, Winblad B, Mix E, Zhu J. 2012. Overexpression of apolipoprotein E4 increases kainic-acid-induced hippocampal neurodegeneration. Exp. Neurol. 233:323–332. doi:10.1016/j.expneurol.2011.10.024.